APPLICATION OF ACOUSTIC IMPEDANCE INVERSION OF E-SAND RESERVOIR ON DULANG UNIT FIELD

PUTERI NURLINA BINTI MOKHTAR

MSc. PETROLEUM GEOSCIENCE
UNIVERSITI TEKNOLOGI PETRONAS
JANUARY 2006

STATUS OF THESIS

Title of thesis	Application of Acoustic Impedance Inversion of E-sand Reservoir on Dulang Unit Field.

I PUTERI NURLINA BINTI MOKHTAR hereby allow my thesis to be placed at the Information Resources Center (IRC) of Universiti Teknologi PETRONAS (UTP) with the following conditions:

1. The thesis becomes the property of UTP
2. The IRC of UTP may make copies of the thesis for academic purposes only.
3. This thesis is classified as

√	Confidential
	Non-confidential

Reason:
As instructed by Petronas Carigali Sdn Bhd (PCSB) and Petronas Research Sdn Bhd (PRSB).

Endorsed by

Petronas Carigali Sdn Bhd,
Level 16, Tower 2, Petronas Twin Tower,
Kuala Lumpur City Centre,
50088, Kuala Lumpur.

Date: 21st January 2008

Petronas Research Sdn Bhd,
Lot 3288 & 3289,
Off Jalan Ayer Itam,
Kawasan Institusi Bangi,
43000, Kajang.

Date: 21st January 2008

APPROVAL

UNIVERSITI TEKNOLOGY PETRONAS

Approval by supervisor (s)

The undersigned certify that they have read, and recommend to The Postgraduate Studies Programme for acceptance, a thesis entitled "**Application of Acoustic Impedance Inversion of E-sand Reservoir on Dulang Unit Field**" submitted by **Puteri Nurlina binti Mokhtar** for the fulfillment of the requirements for the degree of MSc Petroleum Geoscience.

Date : 21st January 2008

Signature :

Main Supervisor : M Firdaus B A Halim

Date : 21st January 2008

Co-Supervisor 1 : M K Sen Gupta

Co-Supervisor 2 : Shaidin B Arshad

UNIVERSITI TEKNOLOGI PETRONAS

Application of Acoustic Impedance Inversion of E-sand Reservoir on Dulang Unit Field

By

Puteri Nurlina Binti Mokhtar

A THESIS

SUBMITTED TO THE POSTGRADUATE STUDIES PROGRAMME

AS A REQUIREMENT FOR THE DEGREE OF MSC. PETROLEUM GEOSCIENCE

IN PETROLEUM GEOSCIENCE

BANDAR SERI ISKANDAR

PERAK

JANUARY, 2008

DECLARATION

I hereby declare that the thesis is based on my original work except for quotations and citations which have been duly acknowledged. I also declare that it has not been previously or currently submitted for any other degree at UTP or other institutions.

Signature: 

Name : Puteri Nurlina Binti Mokhtar

Date : 21st January 2008

ACKNOWLEDGEMENT

Firstly I would like to thank my supervisors M Firdaus A Halim and M K Sengupta for their support during the completion of my thesis. I would also like to thank to all the Geophysical Team in Petronas Research Sdn Bhd (PRSB) especially to Shaidin B Arshad, Nor Azhar B Ibrahim, Salbiah Isa and M Faizal B Abd Rahim for discussion and their input. Not forget to Nik M Nazrane for IT support on preparing computer with big and double screen and also installation of Hampson Russell software. Next, also thanks to Amar Ghaziah, for being kindness for lending me his computer. Thank you to all staff in PRSB who is involves making this thesis successfully.

Secondly, my acknowledgement to IFP's lecturer who are give all their support and being so patient in helping and teaching us when their in Malaysia. Merci beaucoup! Next, thank you to all UTP's lecturer especially AP Wan Ismail for his capability in managing this first batch MSc Programme.

To my entire colleague, who are always helping me to complete all the chapters and this thesis, thank you very much. Special thank you, to Ummi Farah, Azwa Jannah, Harminzar, Hamzah, Faizal and Wong Eng Yao for all your support and uncomplaining in helping me to understand the concepts especially in Geology. I love you all.

Lastly, to my husband Mohamad Rizuan who so understand and always behind me for a year especially in taking care of my beloved son, and not forget to Mama, Papa and my family too. With your blessing, Alhamdulillah, I have completed my thesis and a degree of MSc Petroleum Geoscience.

Thank you.

ABSTRACT

An acoustic impedance inversion study as conducted over the Dulang Field. The seismic data acquired in Dulang Field, represents a 3D data volume containing sand reservoirs in interbedded sand and shale formations at different depths. The most important formation in this field is the E-group formation, which consists of stacked reservoirs. The objective of this study is to look at the extension of the E-sand reservoirs. Inversion study is the preferred method to delimit the extent of E-group focusing on the E7, E14, E23 and E34 sand reservoirs. The main steps of the Dulang inversion study are initial seismic well ties, velocity-impedance model and acoustic impedance inversion. Feasibility rock physics study need to be done using well logs to differentiate between hydrocarbons. Gas sand, oil sand and wet sand can be differentiated using cross plot between Impedance and Gamma Ray or any other logs. Cross plotting was done on three vertical wells DLG 01, DLG 02 and DLG 04. Estimating the wavelet that will be used to invert seismic data is an important step in seismic inversion. Wavelet extraction is central to all seismic inversion techniques. Statistical method was chosen to extract the wavelet. Finally, a model based acoustic impedance inversion method was tested on a seismic line and an analysis of hydrocarbons was done on the inverted volume. In the results shows a clear extension of sand reservoirs in each sand package over DLG 01, DLG 02 and DLG 04 wells.

TABLE OF CONTENTS

LIST OF TABLES

LIST OF FIGURES

CHAPTER 1
INTRODUCTION

1.1 INTRODUCTION

An acoustic impedance inversion study as conducted over the Dulang Field. The main steps of the Dulang inversion study are Initial seismic well ties, velocity-impedance model and acoustic impedance inversion.

The scope of work for this study includes well and seismic data loading, wavelet extraction using statistical method or using well data, well-seismic correlation, velocity and initial impedance model building and 2D acoustic impedance inversion of seismic line passing through selected producer/injector wells. There are 135 wells interpreted in the Dulang Area. Dulang Field is divided into three units, Western area, Unit Area and Eastern Area. For this study, we will focus in the Dulang Unit Area and only three vertical wells were used in the well data analysis and for the inversion process and it shown in Figure 1.1.

1.2 GEOLOGIC OVERVIEW

Dulang field is located in the west central portion of Malay Basin about 130km from Terengganu Crude Oil Terminal (TCOT) with average water depth of 76m. This field was discovered in 1981 by EPMI. It is divided into three major areas, the Unit Area, Western Area and Eastern Area. Today, the field produces from four platforms, three within the Dulang Unit and one in Dulang West. First production was on 15 March 1991 and the highest production was in October 1994 about 54Mstb/d. The Group-D and Group-E reservoir age is middle to upper Miocene. The reservoirs are labeled in Figure 1.2. In Upper Miocene, compressional tectonics formed the anticlinal traps and resulted in wrench faulting. This deformation becomes younger from North to South.

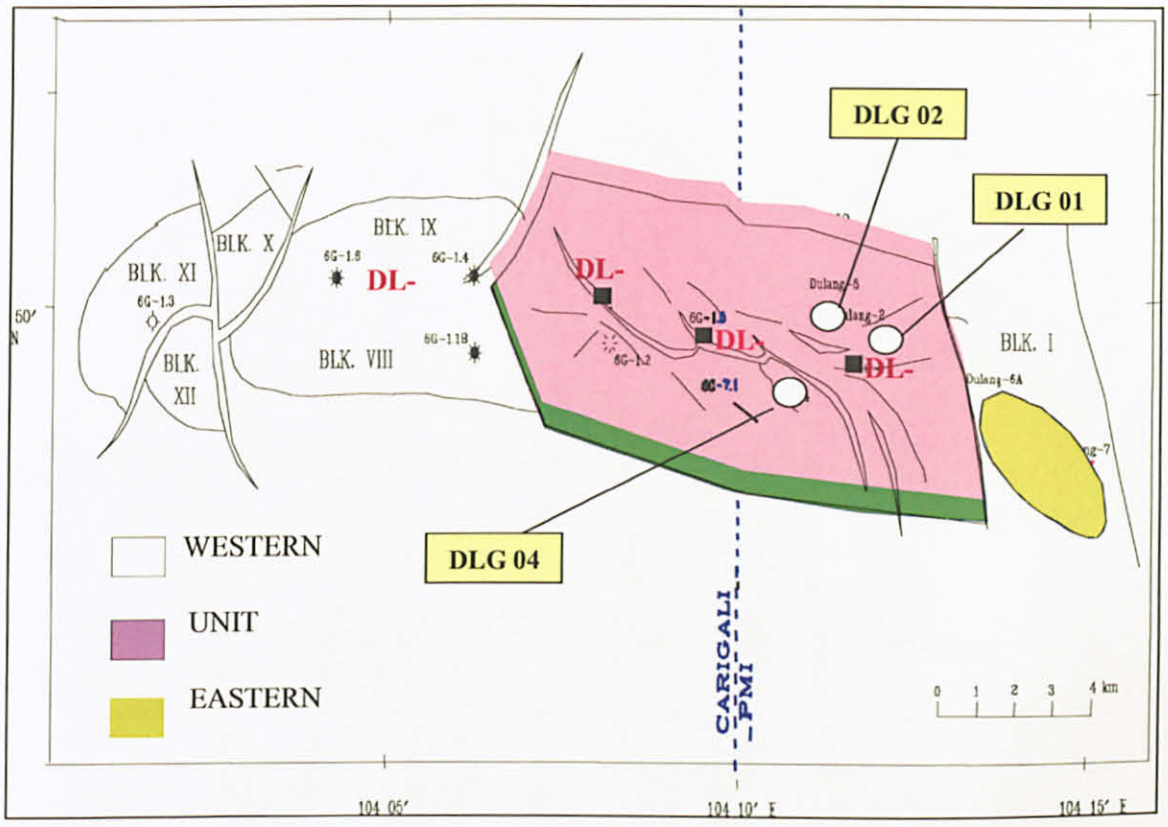

Figure 1.1: Three major areas in Dulang Field

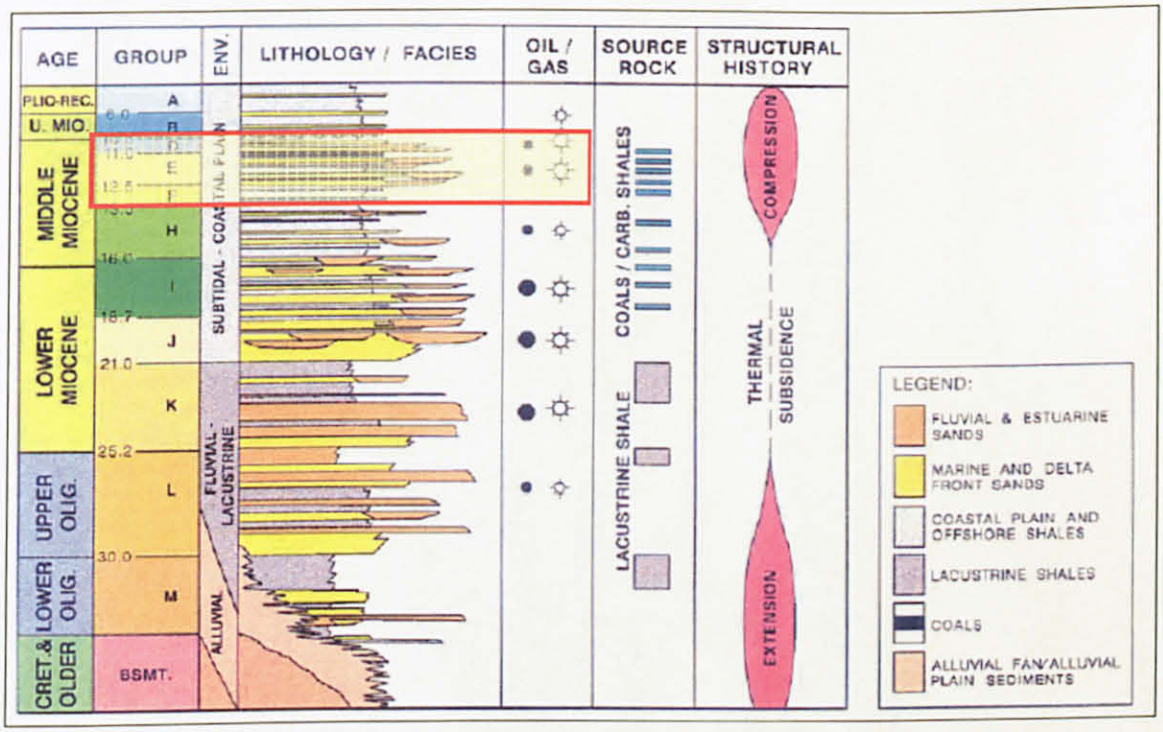

Figure 1.2: Hydrocarbon occurrence and structural history of the Malay Basin (EPIC, 1984)

Structural setting for Dulang Field is consists of anticline with 25 x 3.5km and it is plunging to the westward. It is highly faulted field which have three major fault sets that are, NW-SE to NNW-SSE with throws of few meters to more than 100 meters, NE-SW as antithetic component of first fault set and E-W which is smaller and discontinuous fault with throws of 5-20 meters. Oil field almost located in northernmost of Malay Basin.

Six environment of depositional were interpreted and it consists of shoreface with sharp-base sand and blocky log signature and it can be characterize by high-energy environment. Another environmental of depositional that were interpreted before, are active channel fill, proximal and distal mouth bar, bayfill and swamp which are presence of autochthonous coal and its associated paleosol. These thin layers are important as correlative surfaces, depositional boundaries and flow barriers.

Figure 1.3 shows a model of depositional of Dulang field. It likely located on a coastal plain with shoreface interpretation and the most marine-influenced unit is E14 sand reservoir, while younger or older sequences show an increasingly fluvial imprint. E01 sand unit shows thick sand encased in shale which may be an incised valley fill and it is topped by SME coal. Followed by the Group-D that is LD1-LD3 units which have marine influence. Lower-D series probably marks the beginning of a transgression with a possible maximum flooding surface above the SME coal. If we looked in Figure 1.4, E14 sand reservoir is a sequence boundary while overlying E14 sand is transgressive sand followed by highstand deposits of E1213 and younger units. Above the E14 sand, channelized features become more frequent upwards with amalgamated sand and later with thinner sand or single-body sands.

An example of log from DLG 01 showing the sequences of Group-D and Group-E reservoir which is Group-D consists of LD1, LD2 and LD3 whereas in Group-E are E1, E2, E6, E7, E8, E1011, E1213, E14 E2022, E23, E32, E34, E36, E40, E42, E47, E48, E50 and E51. This is stacked of reservoir in Dulang Field (Appendix 1 to 3). Only four reservoirs namely, E7, E14, E23 and E34 were used for all the process and analysis.

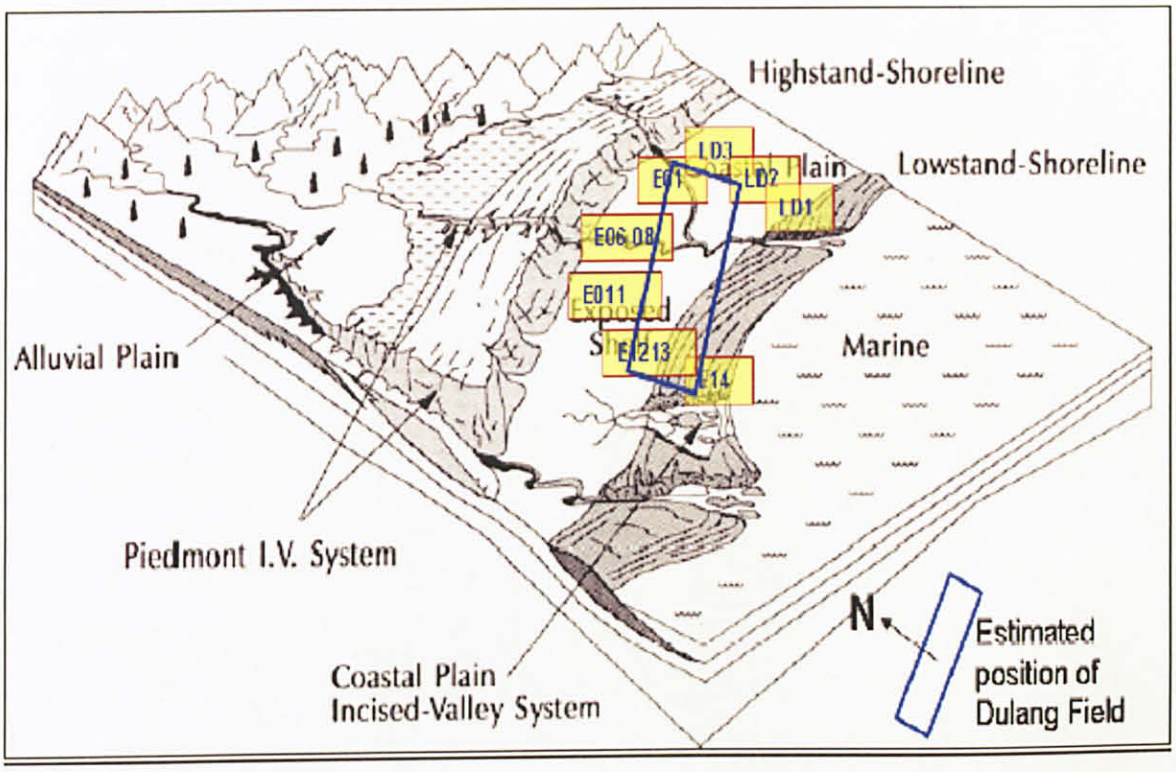

Figure 1.3: Depositional Model of Dulang Field

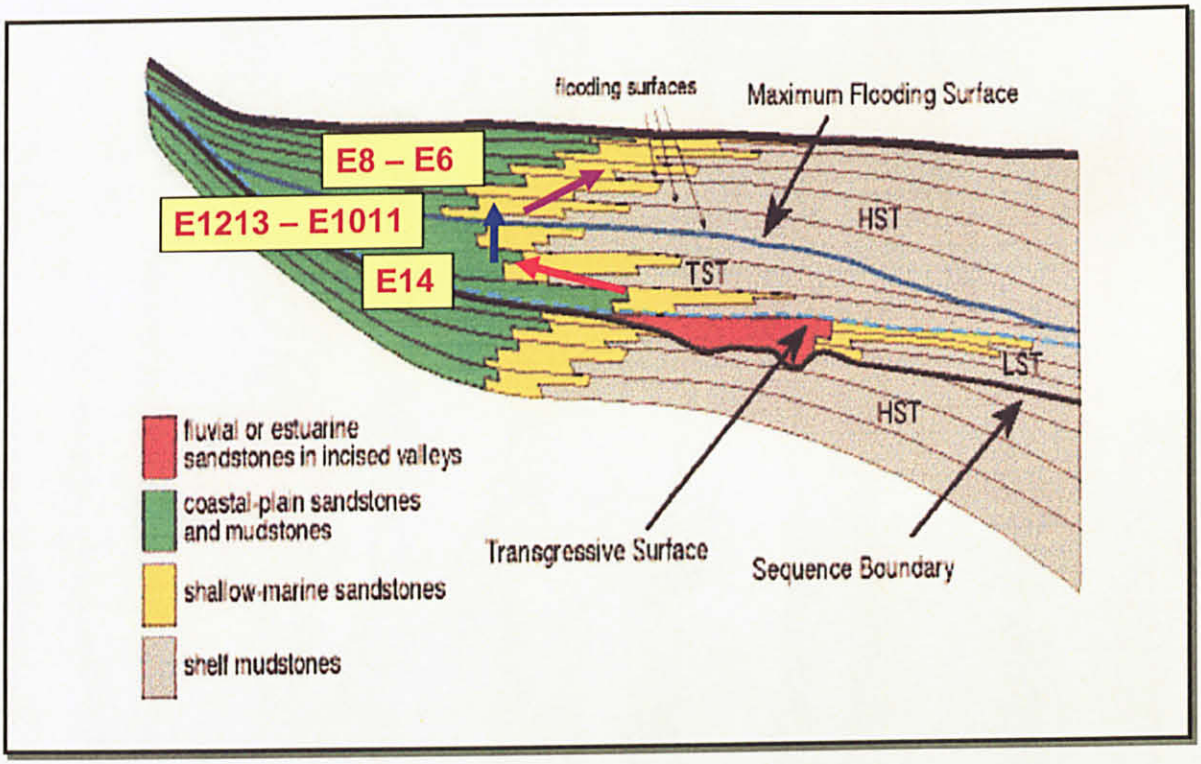

Figure 1.4: Sequence stratigraphic model of Dulang field

1.3 RESEARCH OBJECTIVE

The objective for this study is to look at the extension of E-sand reservoir in Dulang Unit Area by using the impedance inversion method. Only four sand package that are E7, E14, E23 and E34 reservoir will used in all the analysis for this study. The result of inversion later will show the continuity and the extension of four sand reservoirs in Dulang Unit Area. The impedance is a layer property, so the changes in impedance will relate to the property changes within a reservoir. The use of impedance inversion is expected to differentiate sand-shale classes.

The remainder of this study is divided into six additional chapters. In Chapter 2, an analysis of the well log data is presented. This analysis is important since the seismic inversion links the seismic data with the well data. By using the well data, the relationship between the rock properties related to P-Impedance is calibrated.

Chapter 3 will discuss on wavelet extraction that used two methods to get the best wavelet. The theory of inversion method used in this study is discussed in Chapter 4 that is the Model Based Inversion method. Chapter 5 addresses the impedance result of inversion method. A concern about reservoir thickness is discussed, because the thickness is below the seismic resolution. Finally, the summary, conclusion and recommendations are discussed in Chapter 6.

1.4 DATA

The data used in this study consist of well data and 3D seismic data. 135 wells drilled in this Dulang Area. However, we will use only three of them that are vertical well and it is useful in the well data analysis and in the inversion process. Wells DLG 01 and DLG 02 are nearby to each other, in the same block but DLG 04 is in a different block, and separated by a fault. Wells DLG 01 and DLG 02 are in N3 block whereas DLG 04 is in S3 block.

1.4.1 Well data

Three wells containing both bulk density and P-wave sonic logs were used in the well data analysis and inversion process. The wells are DLG 01, DLG 02 and DLG 04. All vertical wells drilled during the 1980's while the 3D seismic data was in year 2002. In the inversion process, the sonic and density logs were used to estimate the wavelet and to build the low-frequency model. In the well data analysis, investigation of the relationships between the rock properties such as porosity, velocity, density, acoustic impedance, volume of clay, water saturation and gamma ray was done.

From all the logs, we need to identify the lithology such as coal, sand and shale. Well completion reports for each well were used to help in interpreting all the logs. From the interpretation, we can classify into five classes that are coal, gas sand, oil sand, wet sand and shale.

1.4.2 Seismic Data

The 3D seismic volume for Dulang Area is in year 2002 and Western Geco carried out the acquisition whereas for processing by CGGAP Sdn Bhd. DLG 01 well crosses the Inline of 2082 and for the Xline of 3300. Meanwhile for DLG 02, Inline is 2066 and Xline is 3200 and lastly for DLG 04 the Inline is 2007 and for the Xline is 3162. Approximately 350 surface km^2 of prime 3D seismic streamer data were shot with the following parameters:

Table 1.1: Acquisition parameters for seismic survey

Survey	Dulang 3D
Location	Offshore Terengganu
Survey carried out by	Western Geco
Total number of sail lines	123
Number of traces per shotpoint	6 x 288 channels, 6 x 144 channels
Bin size	12.50m x 18.75m
Stacking Fold	48 fold and 24 fold

SOURCES	
Type of energy source	Bolt Longlife airgun array
Shot point interval	18.75 meters flip-flop
Number of sources	2 x 2098 cubic inches flip-flop
Source pressure	2000 psi
Source depth	4 +- 1 meters
Source separation	37.50 meters
RECEIVERS	
Number pf cables	6
Nominal cable interval	75 meters
Cable length	3600 meters and 1800 meters
Number of groups	288 channels and 144 channels
Group interval	12.50 meters
Cable depth	5 +- 1 meters

Table 1.2: Processing flow for seismic survey

DESIGNATURE USING GHOSTED FARFIELD SIGNATURE
Output zerophase

Q COMPENSATION PHASE AND AMPLITUDE
Phase Q = 125 and amplitude 10Db

TAU P FILTERING
An inner mute was applied in Tau P domain to attenuate linear noise

TAU P DECONVOLUTION
Operator Length : 150ms
Window : 200 – 2150ms, 1820ms – 3500ms
White Noise : 0.5%
Gap : 20ms

TAU P REVERSE TRANSFORM OUTPUT EVERY ALTERNATE TRACE
Alternate trace drop changes the trace spacing from 12.5m to 25m

FIRST PASS VELOCITY ANALYSIS 1km x 1km velocity grid

SHOTS AND RECEIVERS AMPLITUDE CORRECTION

HIGH RESOLUTION PARABOLIC RADON DEMULTIPLE
Time of application : 500ms – 6000ms
Noise rejection : 25%
Thresholds between primaries and multiples : 140ms (lines with 288 channels per streamer)

Thresholds between primaries and multiples : 80ms (lines with 144 channels per streamer)
Lower limit for scanning parabolas : -200ms
Upper limit for scanning parabolas : 2000ms
Incremental between parabolas : 20ms

SORT TO 48 OFFSET PLANES

STATITC BINNING AND 3D MISSING TRACE RESTORATION
Creates missing traces in f-xy domain from existing traces

TRACE INTERPOLATION
From bin size 12.5m x 18.75m to 12.5m x 12.5m
SECOND PASS VELOCITY ANALYSIS 0.5km x 0.5km velocity grid

TRACE EQUALIZATION WITH 3000ms OPERATOR LENGTH, 50% WINDOW OVERLAP

3D KIRCHHOFF PRE STACK TIME MIGRATION
Dip : 75 degrees
Aperture : 4000m
Velocity : 5 points smoothed 2nd pass velocity

AUTOMATIC THIRD PASS VELOCITY ANALYSIS

NMO CORRECTION AND MUTE
Outer mute following 35 degrees and inner mute following 5 degrees on the isoangle gather

Outer mute:

Time (s)	2	195	305	490	795	1100	1500	2005	2470	3025
Offset (m)	495	556	652	766	1010	1236	1628	2264	2882	3923

Inner mute:

Time (s)	1700	1895	2100	6000
Offset (m)	115	652	840	930

FULL FOLD STACK
Stack 48 fold

K-NOTCH FILTER
To remove acquisition foot print

3D FXY DENOISED

TIME VARIANT FILTER

Time (s)	0-2	2-3	3-6
Frequency (Hz)	6-100	5-90	4-80

MULTI WINDOW TRACE EQUALIZATION
Operator length 1000ms without any overlapping

ACOUSTIC IMPEDANCE

CHAPTER 2
WELL DATA ANALYSIS

2.1 INTRODUCTION

The acoustic impedance is the product of sonic velocity and density, which can be obtained indirectly by inverting the P-wave seismic data. The impedance inversion integrates the seismic and the well log data. Therefore, the understanding of the reservoir properties related to the impedance by using the well log is needed.

This chapter studies the reservoir properties such as velocity, density, porosity and gamma ray derived from well log data. Relationships between those properties and Impedance are investigated as well. Understanding of rock properties is one of the essentials in ensuring the success of direct hydrocarbon detection, reservoir characterization and recovery monitoring by seismic methods. The relationships among rock trends and properties are helpful in providing the link between the seismic and the hydrocarbon accumulations, reservoir characters and physical properties.

Some feasibility investigations need to be carried out. We can differentiate hydrocarbon (fluids) such as gas sand, oil sand and wet sand by performing a well log cross plot analysis between Impedance ((m/s)*(g/cc)) versus Gamma Ray (API) or any other logs. Gamma Ray was used in this study to look at the discrimination between them. We need to find a trend for five classes at each well located in the Dulang Unit area. The wells used in this research are DLG 01, DLG 02 and DLG 04 and the five classes are coal, gas sand, oil sand, wet sand and shale.

2.2 ANALYSIS OF WELL DATA

Analysis of well data is derived from three wells in this study that have sonic and density logs. The location of those wells: DLG 01, DLG 02 and DLG 04 are shown in Figure 2.1. The depth of the E-sand reservoir for each wells are summarized below in the table of 2.1. Appendix 4 shows the arbitary line from the 3D seismic volume that is seismic line start from DLG 04 to DLG 02 and end at DLG 01.

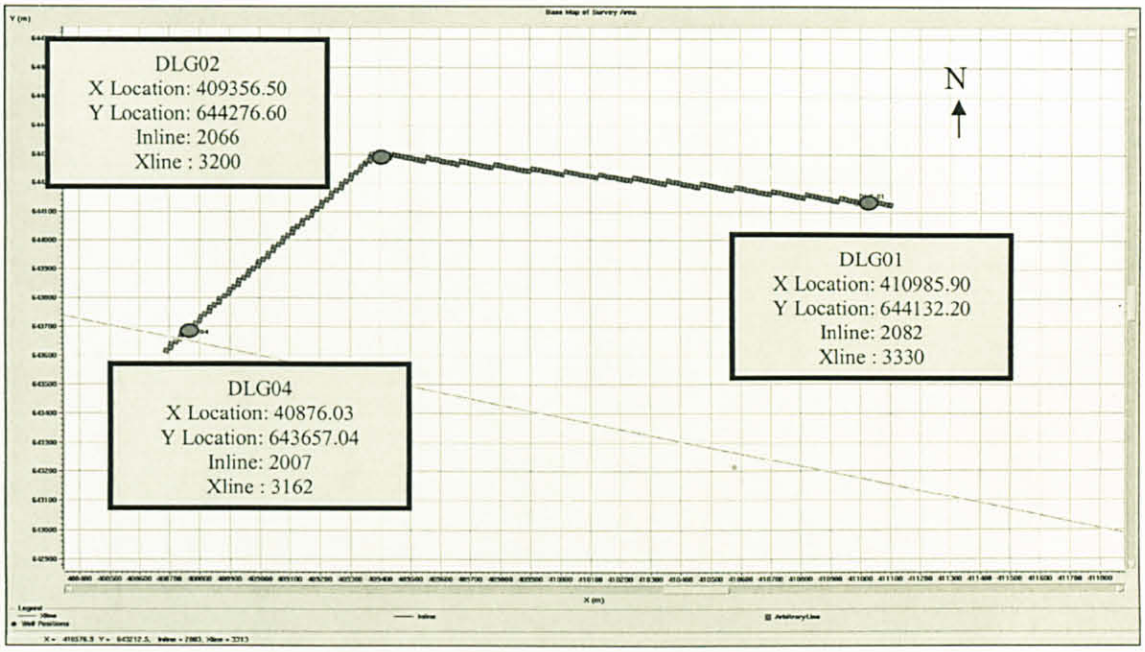

Figure 2.1: Base map of the survey for DLG 01, DLG 02 and DLG 04 wells. Red dot is the location of the wells with X& Y location. The black line is the arbitary seismic lines that start from DLG 04 to DLG 02 and end of DLG01.

According to Table 2.1, E7, E14, E23 and E34 are stacked reservoirs, which contain gas, oil or water. E7 sand reservoir is the shallowest sand reservoir with depth of 1173m in DLG 01, 1152m in DLG 02 and 1154m in DLG 04. E34 sand reservoir is the deepest reservoir with depth of 1313m in DLG 01, 1295m in DLG 02 and 1309m in DLG 04. All depth value is markers for top of sand in each reservoir.

Table 2.1: Approximately depth for each reservoir in all the three wells

Reservoirs	DLG 01 TVD (m) from surface	DLG 02 TVD (m) from surface	DLG 04 TVD (m) from surface
E7	1173	1152	1154
E14	1226	1204	1222
E23	1268	1248	1262
E34	1313	1295	1309

2.3 FEASIBILITY CROSS PLOT

Cross plot technique is a very useful and powerful method in providing information whether the hydrocarbon reservoir could be mapped out from seismic data. It can also help the geoscientists to decide on work flow to proceed; for example; to choose whether elastic or acoustic impedance inversion techniques. Here, cross plotting was done on well log data of DLG 01, DLG 02 and DLG 04 using e-Log that is one of the applications in Hampson-Russell software. It is an important method to separate the five classes that have been discussed before by using log data such as Acoustic Impedance, Gamma Ray (GR), Water saturation (Sw), Volume of Clay (VCL), Porosity, etc.

For example, if we plot Impedance versus Gamma Ray and use Water Saturation as a Color Attribute we can say that if Sw=1, is it shale and coal. To differentiate between shale and coal, we need to look at the value of the impedance. Shale class have a big different through impedance, which is much higher than coal. Same goes to sand and shale which is shale still having a high impedance compare to sand class. Acoustic Impedance log comes from Sonic Log*Density Log. This process can be computed using 'Math' process in e-Log. Figure 2.2a shows some examples using e-Log for cross plot the Gamma ray and Impedance derived from log data.

For DLG 01, value of Gamma Ray for sand is 52.5 to 75.00 API. This value comes from DLG 01's log (see Appendix 1 with cut off Gamma Ray is 75.00 API).

After we classify the classes of coal (black dot), sand (yellow dot) and shale (green dot), we plot it with Impedance versus Depth to look at the trend of each class through depth, and it shows in Figure 2.2b.

At certain depth, the sand will overlap with the shale or in other words, sand and shale have same impedance values. An example is shown in the red box in Figure 2.2b. It may due to the quality of the sand, because of impurities of shale in the sand so that the impedance will become higher and will overlap the shale class. This result will effect in the next process which is to separate hydrocarbon in sand reservoir. It will discuss next when we go into detail analysis on the sand reservoir only. The same case happen in DLG 02 and DLG 04 cross plot that shown in Figure 2.3b and Figure 2.4b.

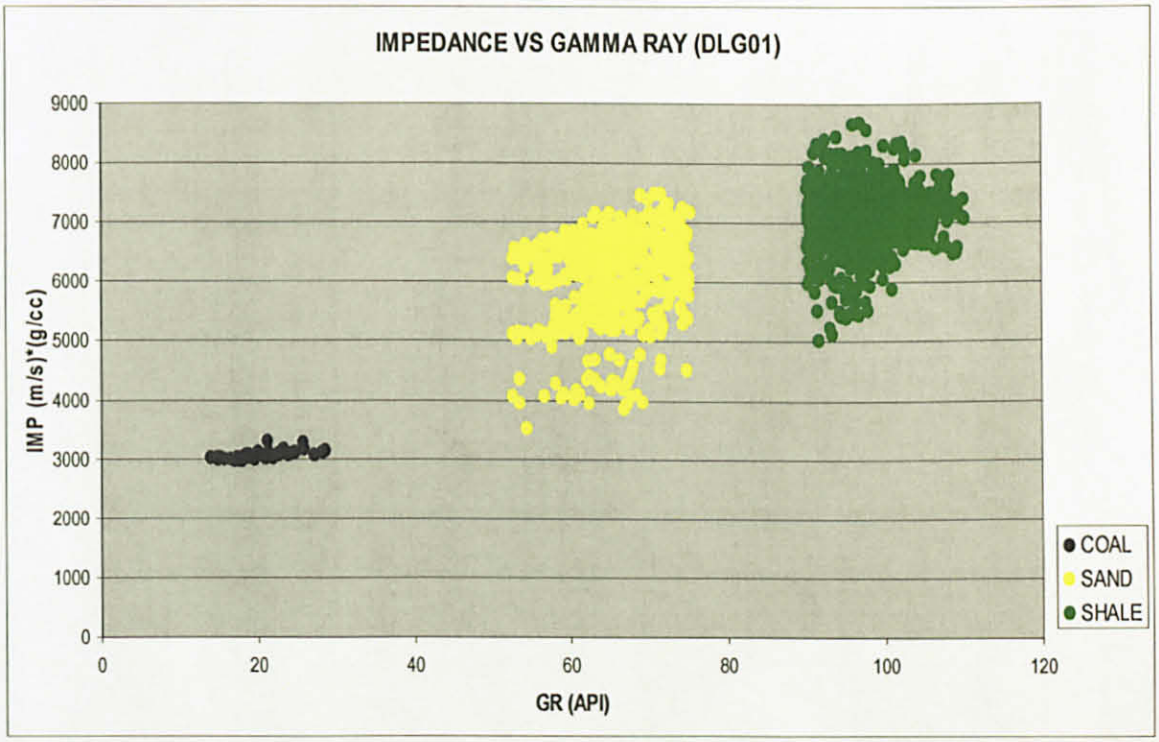

Figure 2.2a: Cross plot between Gamma Ray versus Impedance in DLG 01

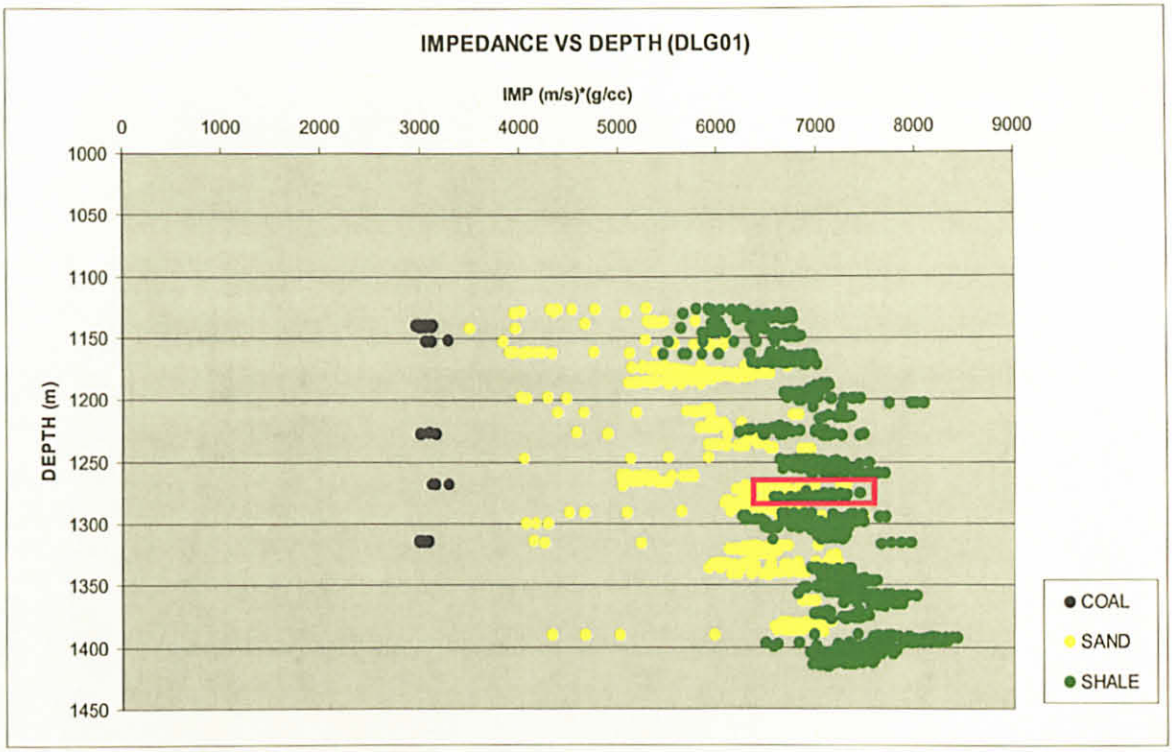

Figure 2.2b: Cross plot between Impedance versus Depth at DLG 01. Red box shows at certain depth sand and shale class are overlapping each other.

For Figure 2.3a, the value of Gamma Ray for sand is 45.00 to 67.50 API (see Appendix 2 with cut off Gamma Ray is 75.00 API) and used this value for sand, which have certain impedance and plotted it through depth. It shows in Figure 2.3b, the data taken from DLG 02 within the reservoir column. Finally, for the DLG 04, the value of Gamma Ray is 52.50 to 75.00 API (see Appendix 3 with cut off Gamma Ray is 90.00 API), the same process was done and the result shows in Figure 2.4b.

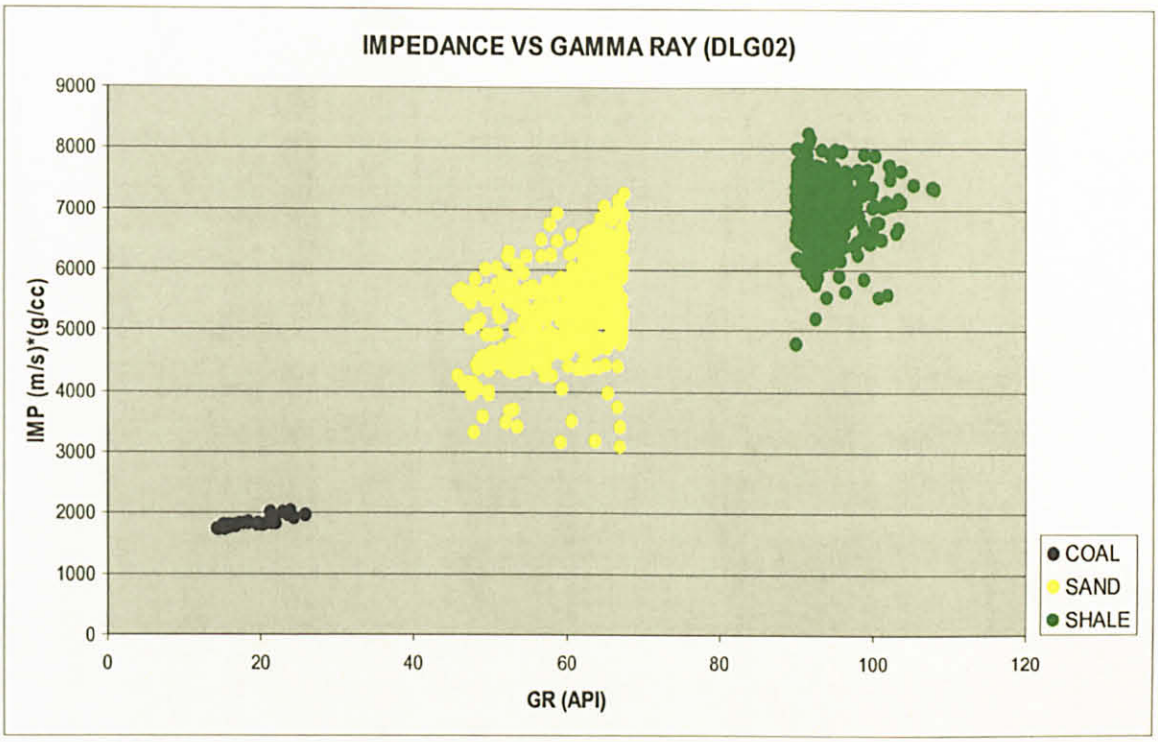

Figure 2.3a: Cross plot between Gamma Ray versus Impedance in DLG 02

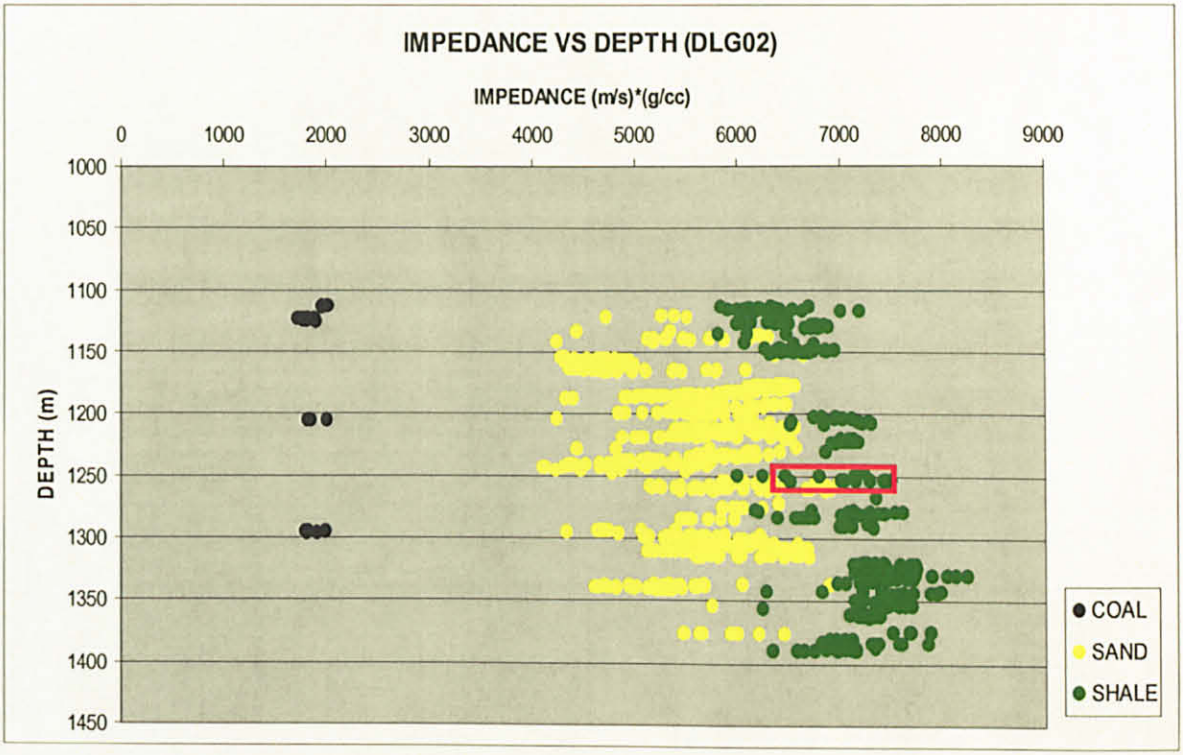

Figure 2.3b: Cross plot between Impedance versus Depth at DLG 02. Red box shows at certain depth sand and shale class are overlapping each other.

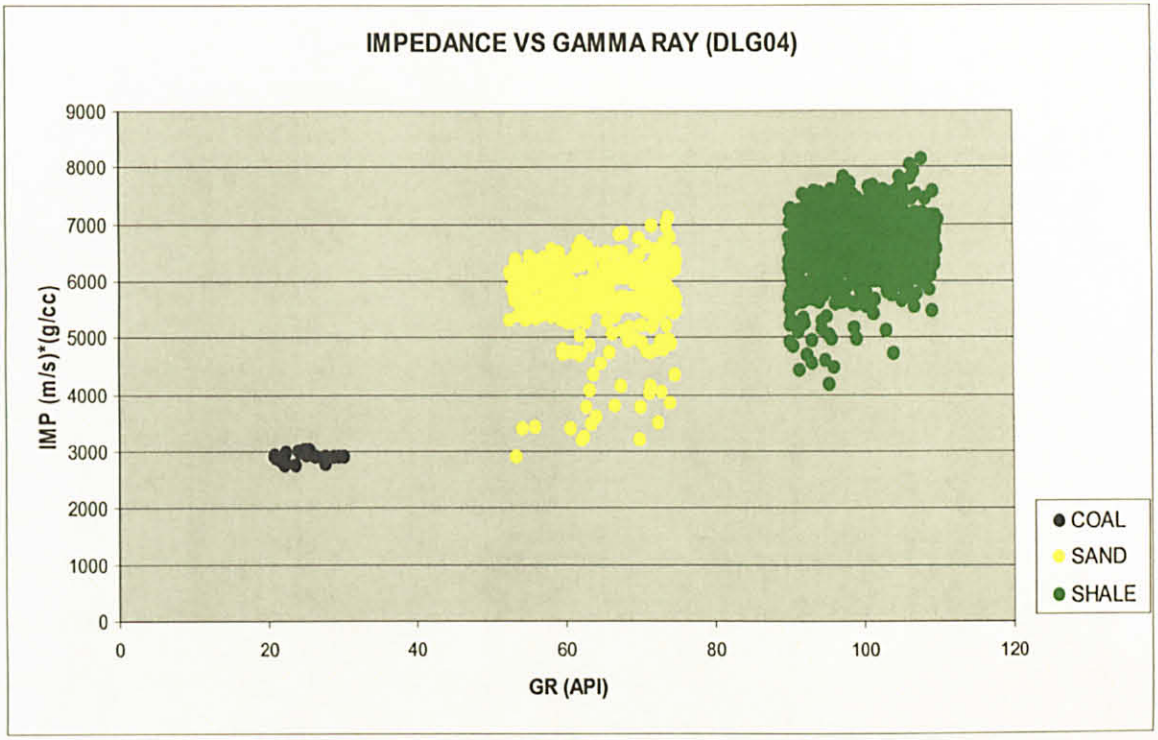

Figure 2.4a: Cross plot between Gamma Ray versus Impedance in DLG 04

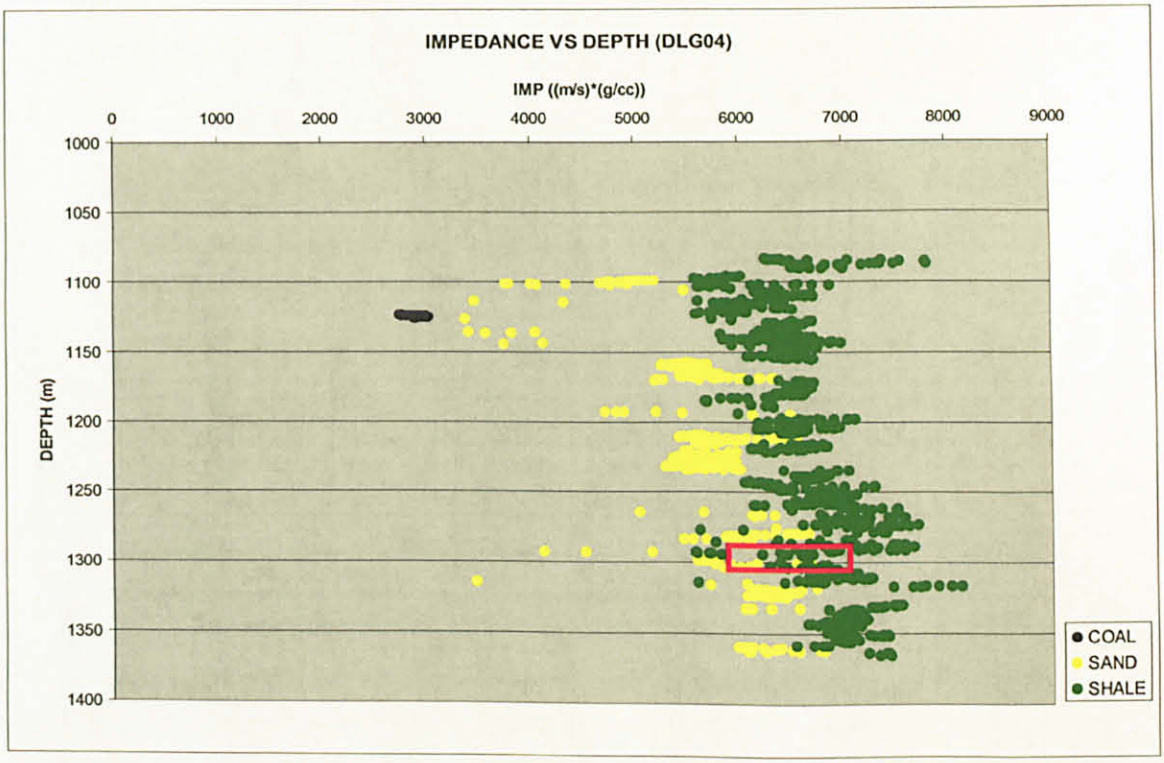

Figure 2.4b: Cross plot between Impedance versus Depth at DLG 04. Red box shows at certain depth sand and shale class are overlapping each other.

If we plotted all the three wells together, it will show the Dulang trend for each class that are coal, gas sand, oil sand, wet sand and shale. See Figure 2.5. Coal and gas sand sample data coming from all the three wells, but oil sand and wet sand coming from DLG 01 and DLG 04 wells. Meanwhile shale class taken from DLG 01 and DLG 02 wells.

Figure 2.5 shows, all the classes can be separate but not exactly at a certain depth and the sand will overlap with the shale. For example at 1340m of depth, we can see the sand and shale overlapping each other. It may due to the quality of the sand that is having more shale and it will falls under same impedance with the shale. Dirty sand will become denser due to the quantity of shale and at the end, the impedance will also become higher and will overlap with the shale class. Another example is on wet sand and shale class, it is overlapping and it so difficult to separate them. This trend can be summarized in a simple way as shown in Figure 2.6.

We can summarized the cross plot in a conclusion through Figure 2.6, where is coal have a lowest impedance that is below 3000 ((m/s)*(g/cc)), followed by gas sand, oil sand and wet sand which falls in 3500 to 7000 ((m/s)*(g/cc)). Shale class has highest impedance that is greater than 7000 ((m/s)*(g/cc)). There was overlapped of sand and shale between wet sand and shale that is have same value of impedance.

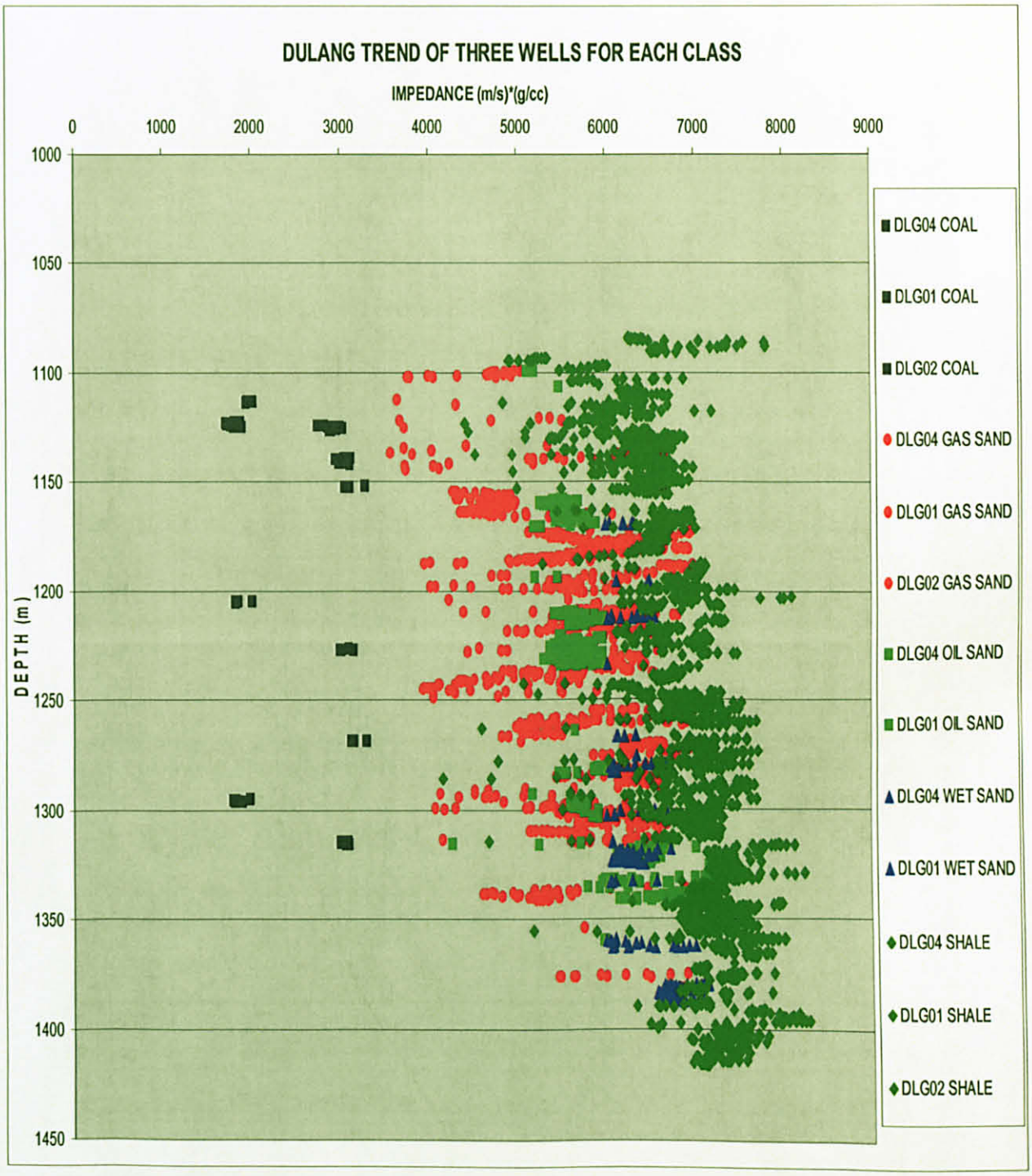

Figure 2.5: Dulang trend of three wells for each class. We can summarized that black dot is coal class, red dot is gas sand class, light green is oil sand class, blue dot is wet sand class and dark green is shale class.

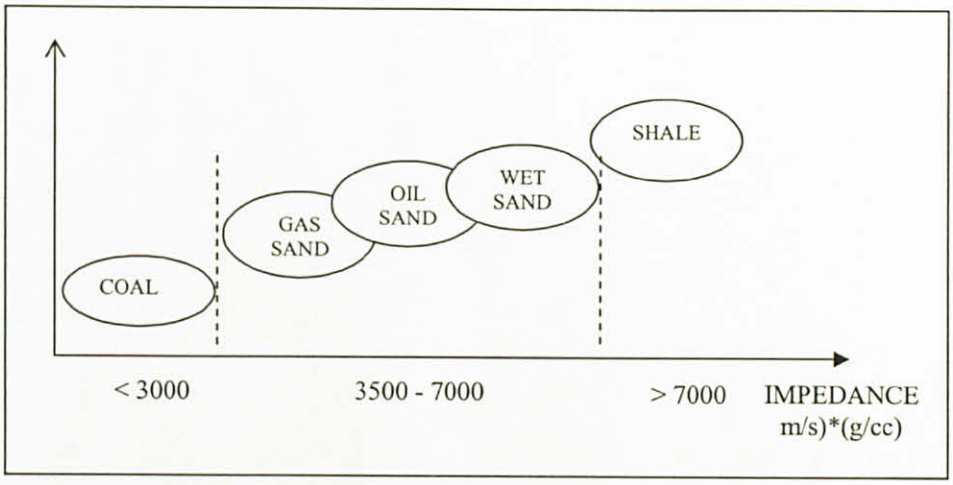

Figure 2.6: Classification of three major classes that are coal, sand and shale. The value of the impedance is valid according to the depth (m). The real example will show below when we focusing on the sand class only which is consist of gas, oil or water.

After we look at the major classes, now we go more detail on sand class only. We have tried to discriminate hydrocarbon between gas, oil and wet sand in wells DLG 01, DLG 02 and DLG 04. Figure 2.7 to 2.9 shows the results from each wells using e-Log for cross plot of the Impedance versus Depth for E-sand reservoirs that are E7, E14, E23 and E34 which is from shallower to deeper sand. We go with one single class of sand reservoir and comparing with all the three wells. To make a comparison, certain depth was taken within the range of depth that is occurred in all the three wells for each the reservoir. For example, E7 sand reservoir range between 1152m to 1173m (refer Table 2.1), and within that depth we will try to get the same sample for three wells and that is in 1160m of depth. Same goes to the E14, E23 and E34 sand reservoir. Conclusion is made in Table 2.2.

Figure 2.7, 2.8, and 2.9 shows the entire E-sand reservoirs at a same depth. From the graph, we know that E7 sand reservoir is in shallow depth, followed by E14 sand, E23 sand and E34 sand. From Dulang Full Field Review, E7 sand at DLG 01 is a gas reservoir with value of impedance approximately around 5700 to 6200 ((m/s)*(g/cc)) which is higher than E7 at DLG 02 and DLG 04. E14 sand reservoir at DLG 01 is also gas reservoir and have value of impedance is around 6000 to 6600 ((m/s)*(g/cc)), next reservoir is E23 but this is water and lastly E34 is oil sand reservoir with value of impedance is 5400 to 6667 ((m/s)*(g/cc)).

Overall if we looked at the value of the impedance for the E7 and E14 gas sand, we can say that they are in the same class with value of impedance is around 5700 to 6600 ((m/s)*(g/cc)). It is overlapping with the E34 oil sand reservoir because the E34 oil sand starts at 5400 ((m/s)*(g/cc)). E7 and E14 sand is under one reservoir but the E34 sand is another reservoir which contains oil but have a same range of impedance with E7 and E14 gas sand reservoir that is in the shallow depth. If we look at the density and the sonic logs for each sand that are E7, E14 and E34 it is not much difference. But if we look at the volume of clay log, E34 sand is much cleaner than E7 and E14 sand and this is the reason why we have gas reservoir with high impedance and the oil sand reservoir will fall in the same range of impedance of gas sand. See appendix 5. It becomes much difficult to separate them together.

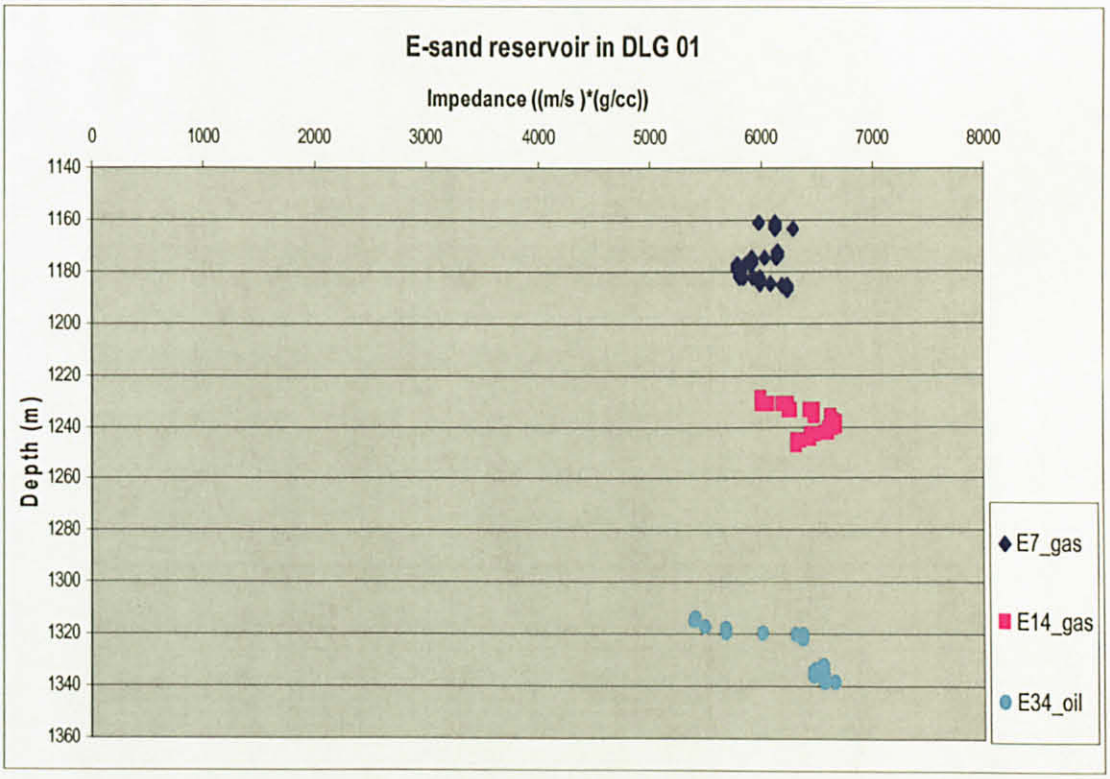

Figure 2.7: Cross plot Impedance versus Depth for E-sand reservoir in DLG01

At DLG 02 well shows in Figure 2.8, E7 sand reservoir is classified as a gas reservoir, which have value of impedance is around 4400 to 5700 ((m/s)*(g/cc)). Followed by E14 and E23 sand reservoir also as a gas reservoir with impedance is 5848 to 5882 ((m/s)*(g/cc)) for E14 sand and 5590 to 6790 ((m/s)*(g/cc)) for E23 sand reservoir. E34 oil sand reservoir with 5100 to 6300 ((m/s)*(g/cc)) is the deepest

reservoir in all the three wells. We can conclude the gas sand reservoir will have a value of impedance is around 4400 to 6790 ((m/s)*(g/cc)).

The same problem occur in DLG 02, which is gas sand have a higher impedance than oil sand and also the same reason that is due to the quality of each sand. E34 oil sand has lower impedance, which is cleaner than other sand reservoirs (see Appendix 6). It also may due to the thin layer of coal beds is E34 sand reservoir. We know that the coal impedance will have the lowest impedance if we compare to other class like sand and shale. So with presence of coal layer, the impedance will fall into low impedance due to the slightly difference in density of the coal. This is another reason that we can justify why the oil sand have a low impedance compare to the gas sand. It is not following the simple diagram that has been shown before (Figure 2.6) where we can see in that figure, gas, oil and wet sand was overlapping each other.

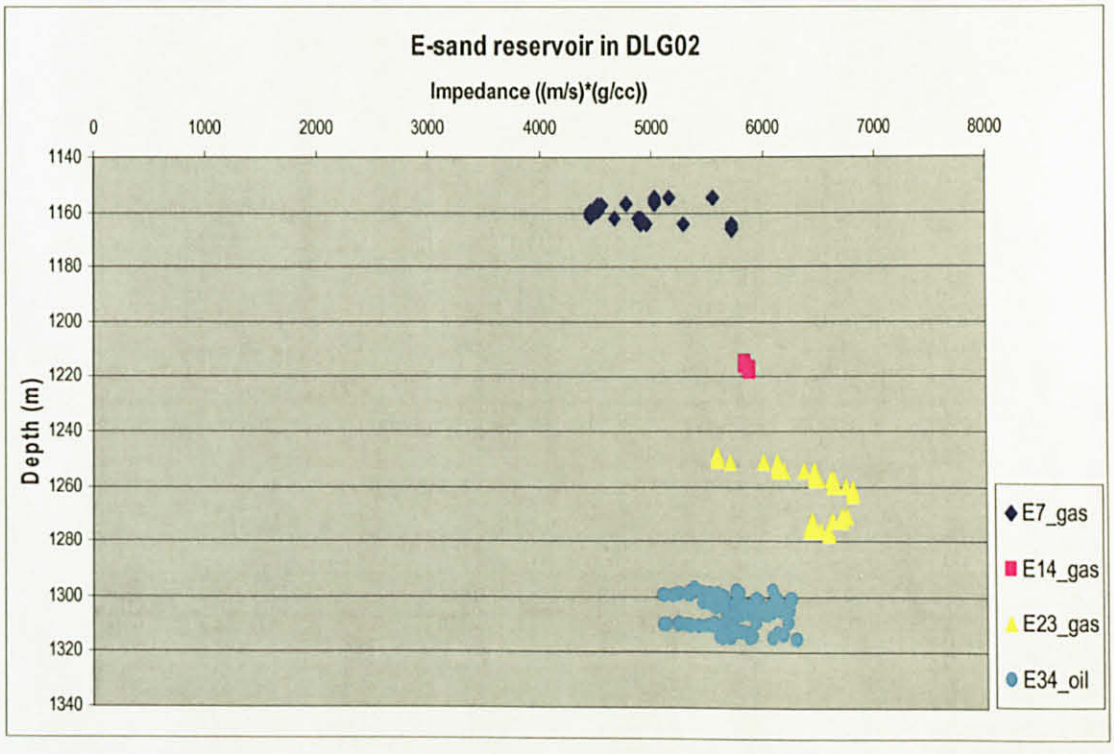

Figure 2.8 Cross plot Impedance versus Depth for E-sand reservoir in DLG02

In DLG 04 well (Figure 2.9), which is the entire reservoir, is in oil sand starting from E7 to E34 reservoir. E7 oil sand have impedance around 4700 to 5700 ((m/s)*(g/cc)), followed by E14 oil sand with 5300 to 6000 ((m/s)*(g/cc)), next is E23

with 5100 to 6400 ((m/s)*(g/cc)) and E34 is 5900 to 6700 ((m/s)*(g/cc)). So we can conclude that the value of impedance for oil sand in DLG 04 is around 4700 to 6700 ((m/s)*(g/cc)). Here we do not have any problem to differentiate the classes because there was only one class in DLG 04 well which is oil sand. See Table 2.2 for the summarized of all E-sand reservoirs in each well.

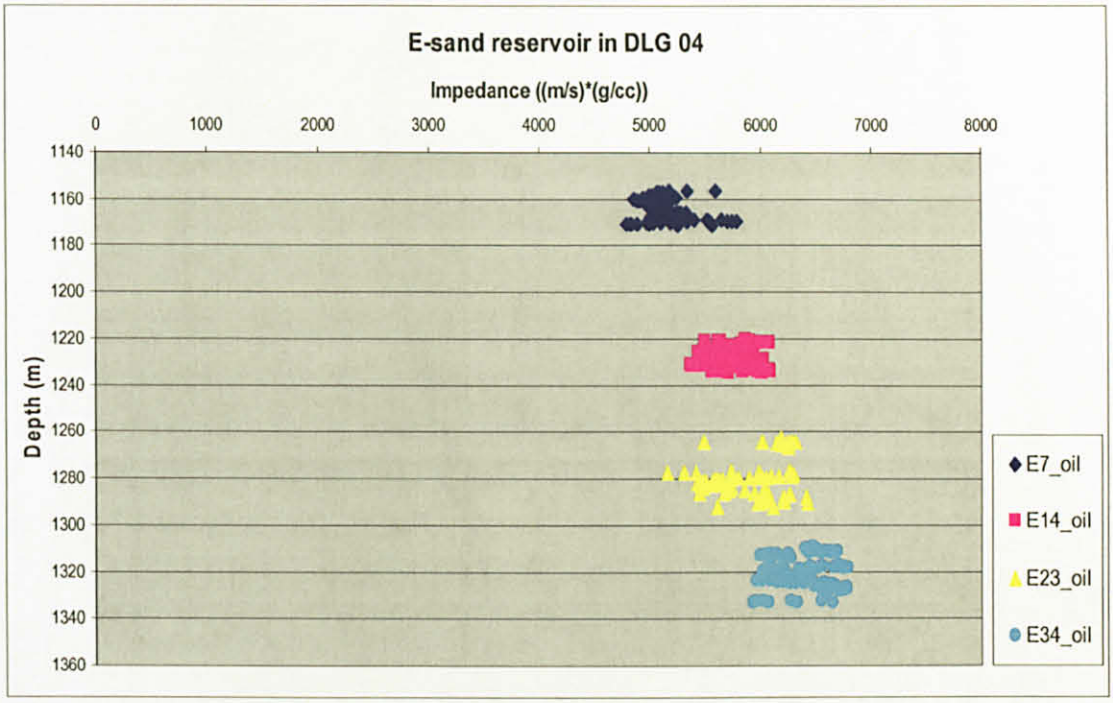

Figure 2.9: Cross plot Impedance versus Depth for E-sand reservoir in DLG04

Table 2.2: Summarized of all E-sand reservoir in three wells at a certain depth

Depth (m)	Impedance ((m/s)*(g/cc)) at DLG01	Impedance ((m/s)*(g/cc)) at DLG02	Impedance ((m/s)*(g/cc)) at DLG04
1160	5700-6200 E7 – GAS SAND	4400-5700 E7 – GAS SAND	4700-5700 E7 – OIL SAND
1230	6000-6600 E14 – GAS SAND	5848-5882 E14 – GAS SAND	5300-6000 E14 – OIL SAND
1278	- E23 - water	5590-6790 E23 –GAS SAND	5100-6400 E23 – OIL SAND
1310	5400-6667 E34 – OIL SAND	5110-6300 E34 – OIL SAND	5900-6700 E34 – OIL SAND

In Table 2.2, it summarized the entire reservoir at a certain depth with the hydrocarbon information and the value of the impedance. To follow what was explained in Figure 2.6, we have tried to plot the entire reservoirs at each well together to look at the trend for sand-shale relationship and the result is shown in Figure 2.10.

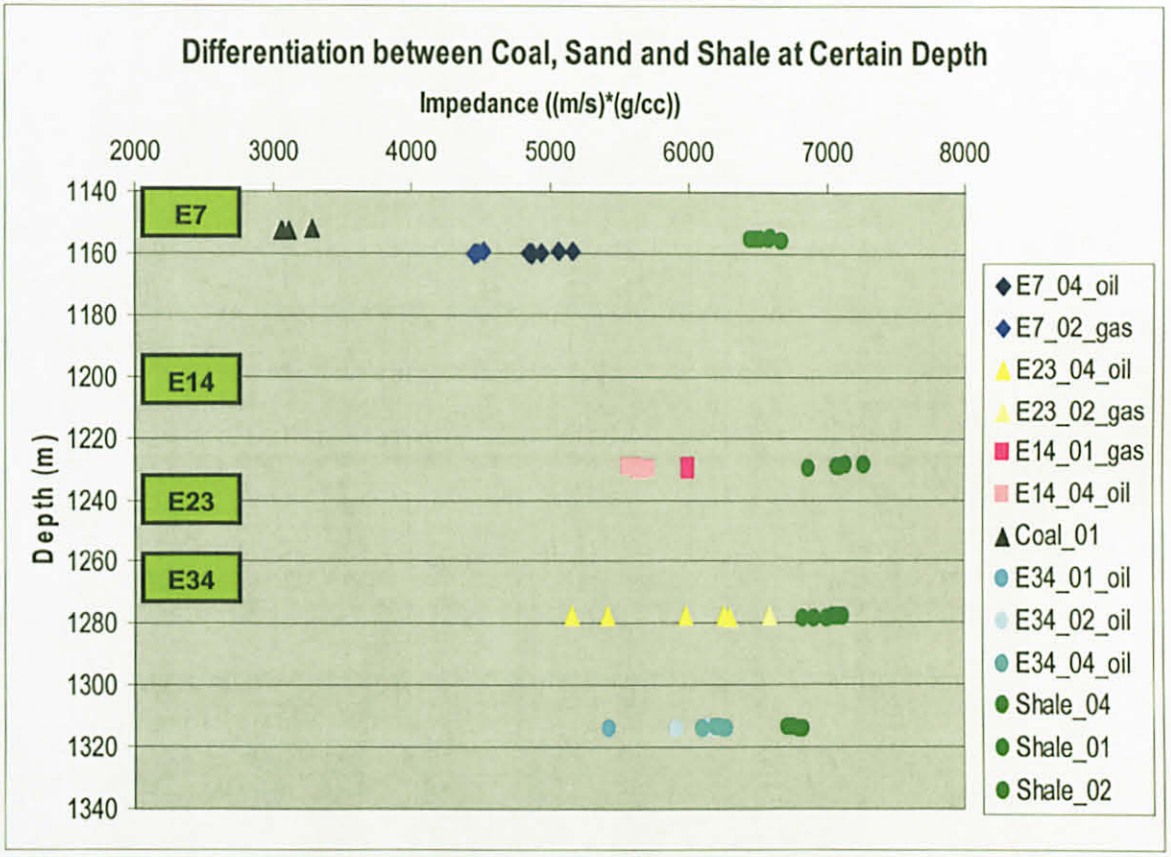

Figure 2.10: Differentiation of coal, sand and shale at certain depth

If we looked at 1160m of depth which is sample of coal in DLG 01, gas sand in DLG 02, oil sand in DLG 04 and shale in DLG 04, it clearly have been separated each other. Coal has the lowest impedance but the depth of coal is not exactly at 1160m, so we have take sample from the nearest depth that is 1152m, followed by gas sand then oil sand and the highest impedance is shale. It is follows the diagram that have been shown in the Figure 2.6. Unfortunately, at the depth of 1230m for E14 sand reservoir and at 1278m for E23 sand reservoir, it is not follow as the diagram. It becomes inverted, which is the gas sand reservoir has higher impedance than the oil sand reservoir. This is again due to the quality of the sand, which was discussed before. This result also proves the depositional environment of E14 that was

influenced by a marine condition. For E34 oil sand reservoir, this is clean reservoir with value of volume of clay is approximately 25%. It means that 25% of shale is within the sand reservoir where else the other is the sand. We can say that if we have value of volume of clay is below than 50% is clean sand and if it greater than 50% it is bad quality or dirty sand.

Appendix 5 to 7 shows a new log for DLG 01, DLG 02 and DLG 04 wells. One process was done to those logs that is filter of high cut frequency which have values from 75Hz to 100Hz. High cut filter was done to the density and sonic log only. This frequency is follows the seismic band frequency and my reason doing this are to have a better interpretation of well when we compare to the seismic resolution. After filtering, both are in the same resolution and the logs will become smoother log than the original one. This filter process can be done in e-Log's application. This new density and sonic logs will also give an impact to the impedance log. It also becomes smoother, and when we are interpreting the result, it will become easier because it has same resolution as the seismic itself. This will explain later in Chapter 5.

2.4 SUMMARY

In developing the regional rock seismic properties trends, log data from three wells DLG 01, DLG 02 and DLG 04 in the Dulang Unit area was used. Each of the wells has a density and sonic logs are useful to create an impedance logs. Dulang trend for each class that are the major class consists of coal, sand and shale have been derived by plotting all the three wells together in one graph. From that graph, we can conclude that coal has lowest impedance, than followed by sand class and the highest impedance is the shale class. In some case, sand and shale will overlapping each other and it is due to the quality of the sand, which is clean sand or dirty sand. Generally, the rock properties are behaving in a systematic fashion as the rocks undergoing compaction deeper into the earth. P-wave velocity, P-impedance and density, are getting higher with depth. It is possible to segregate between shale, wet sand, and hydrocarbon sands but differentiate between the hydrocarbon sands itself are rather difficult. If we look at the previously mentioned figures, we would notice that the oil and gas sands clustered close to each other making segregation impossible.

CHAPTER 3
WAVELET ESTIMATION

3.1 INTRODUCTION

Wavelet estimation is central to all seismic inversion techniques. Estimating the wavelet that will be used to invert seismic data is an important step in seismic inversion. In inversion schemes, seismic trace can be viewed as the convolution of an unknown wavelet with an unknown earth impulse response. Therefore, wavelet estimation itself is an inversion problem, which yields non-unique solution. The presence of noise makes this problem even more complicated. The wavelet is a function of the source signature, filtering and scattering in the earth, and the processing that was applied to the data. The wavelet can vary from trace to trace and vary in time within a single trace, so the wavelet extraction process can yield a large set of wavelets. In practice, a single wavelet is used for an entire survey to reduce the variability of the wavelet. The wavelet is usually estimated from a band-limited seismic window that includes the zone of interest and a continuous reflector with high amplitude, in order to achieve a higher signal to noise ratio.

There are two way to extract the wavelet that is statistical method and using well data. If the impedance log is not available, a wavelet estimated will use a statistical method. In this method, the earth reflectivity spectrum is assumed to be white, random and stationery (Brown et al., 1996). If the impedance (sonic and density logs) logs exist, it will extract using well data and then it may reduce the non-uniqueness in the wavelet estimation. A representative reflectivity sequence is assumed to be easily predicted from the well log, and the noise in the seismic data is assumed to be low amplitude random, and uncorrelated with the other components (Hampson and Galbraith, 1981).

In this approach, no assumption has to be made about the phase. The problem with this approach is that the result is very sensitive to the tie between the well log and the seismic data. The adjustment between synthetic trace and the real seismic data will change the phase and amplitude spectrum of the wavelet. The quality of well log also will affect the accuracy of wavelet estimation.

In Hampson Russell's software, STRATA are another application build in, it has provided extraction wavelet using statistical method, using well data and we can create Ricker wavelet too. In this study, a lot of test needs to be done to get the best wavelet. First method, we used statistical and look at their result, after that we used well data and will decide which wavelet have a better result to be used in correlation process between well and seismic data and also used in inversion process later.

3.2 EXTRACTION WAVELET USING STATISTICAL METHOD

The wavelet estimation methods depend critically on the availability of data. Then wavelet amplitude spectrum can be computed from the amplitude spectrum of recorded seismic data. The basic assumption of this method is that the auto-correlation and the amplitude spectrum of the seismic trace are similar to those of the seismic wavelet (Yilmaz, 2001). The phase spectrum is usually assumed as zero or constant phase. Zero phased seismic data has been used for a practical seismic interpretation purposes. However, real seismic wavelets can differ substantially from the assumed theoretical zero or minimum phase wavelets (Brown et al., 1996). In reality, the seismic data can contain mixed phase (Ziolkowski et al., 1998).

In statistical method where is no wells that lie on seismic, the wavelet estimation workflow is relatively simple. We will take two windows for designing the wavelet as options to extract the wavelet. First options, wavelet taken from water bottom reflection and in this study water bottom is at 100ms with a continuity of a hard kick from the seabed reflection. Looking at the data it seems like zero phase because it shows low impedance to high impedance that means it from soft to hard material (seabed) and it will give positive impedance and appear as a peak. Typically, a wavelet has most of its energy in the middle and tapers off to zero at both ends. The selection of wavelet is within the good data zone, which has a strong peak and continuous reflector, shown in Figure 3.1.

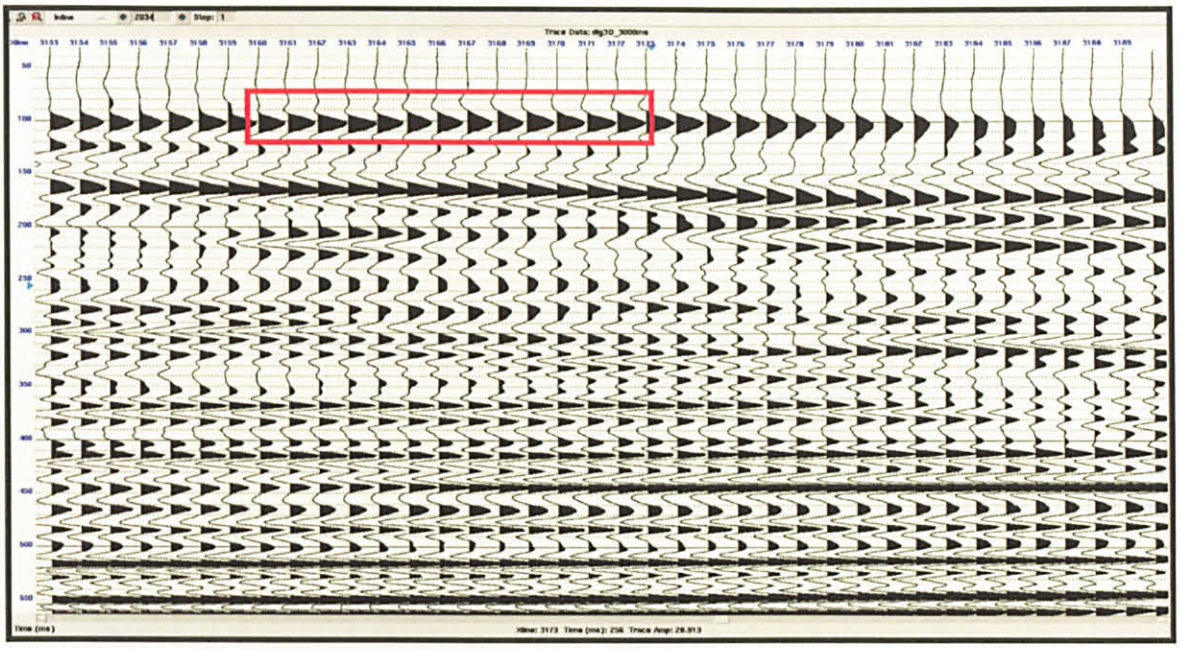

Figure 3.1: Example of water bottom extraction is in red box for wavelet extraction at time 80ms to 140ms.

Parameters that have been used to extract the wavelet from water bottom are taken from time 80ms to 140ms (example shown in Figure 3.1), Xline from 3161 to 3179 and for Inline is from 2034 to 2034 and for the wavelet length is 100ms. From water bottom wavelet, we can get stable and clean wavelet due to the first reflection that from water column to hard rock, which is seabed and the result is shown in Figure 3.2.

In Figure 3.2, left diagram is the wavelet of water bottom reflection and it is in zero phase and for the spectrum for seismic frequency that is in right diagram. This is one option to extract the wavelet from seismic and looking at the wavelet it seems like it is stable with zero phase data and symmetrical side lobe. With statistical method also, it does not have information about phase.

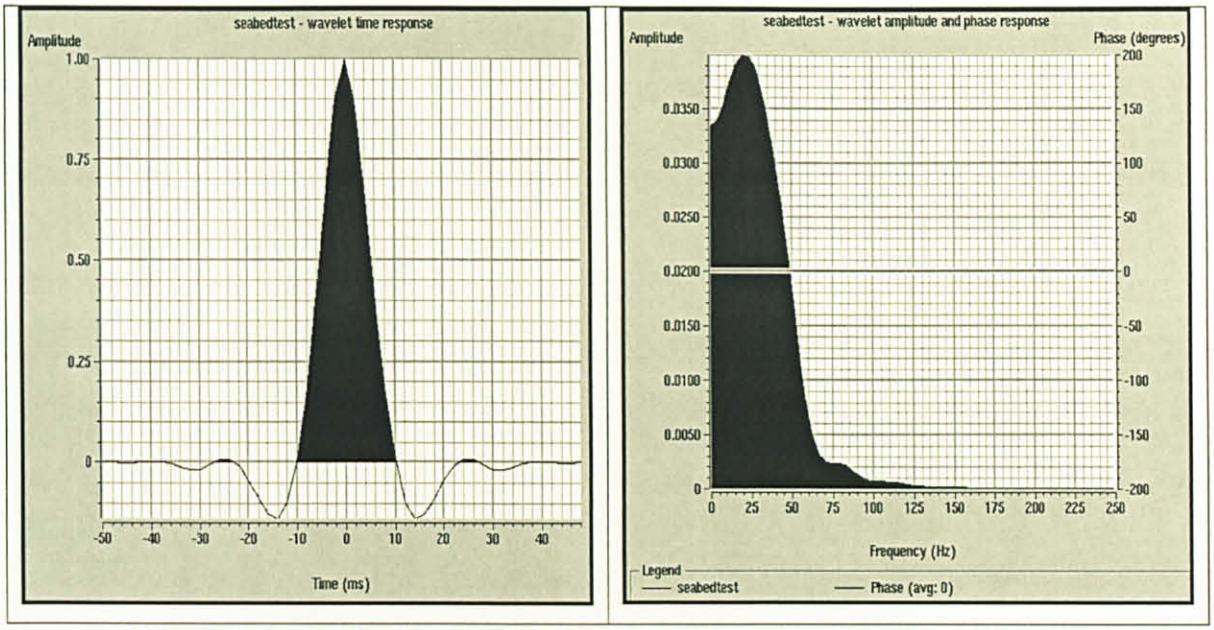

Figure 3.2: Result of wavelet and spectrum from water bottom extraction

Second options, we have taken the window within the reservoir that is about 1200ms to 1600ms. Three windows or time gate that is 300ms, 500ms and 1000ms have been test to design the wavelet. For wavelet length, we have test with three lengths that is 100ms, 150ms and 200ms and the result is in Figure 3.3. This test has been done to all the wells (near by DLG 01, DLG 02 and DLG 04) to look at the lateral variations within the reservoir. Wavelet extraction near by DLG 01 and DLG 02 are similar but in DLG 04 it different. As we know, DLG 01 and DLG 02 wells is in a same block where else DLG 04 well is in another block. Each of these blocks is separated by fault and they are not having a same depositional environment. That why wavelet near by DLG 04 well is not similar with others wavelet like in DLG 01 and DLG 02.

After discussion, we decide to take wavelet at near by DLG 01 well within the reservoir with time gate 1000ms and wavelet length is 100ms. Looking at the wavelet it have symmetrical side lobe compare to the wavelet at the near by DLG 02 well, it have a lots of bounce. We ignore the wavelet that has been extracted using statistical at near DLG 02 and DLG 04. Therefore, we left with one wavelet that is statistical method near DLG 01 well and need to compare with other method that is wavelet extraction using well data.

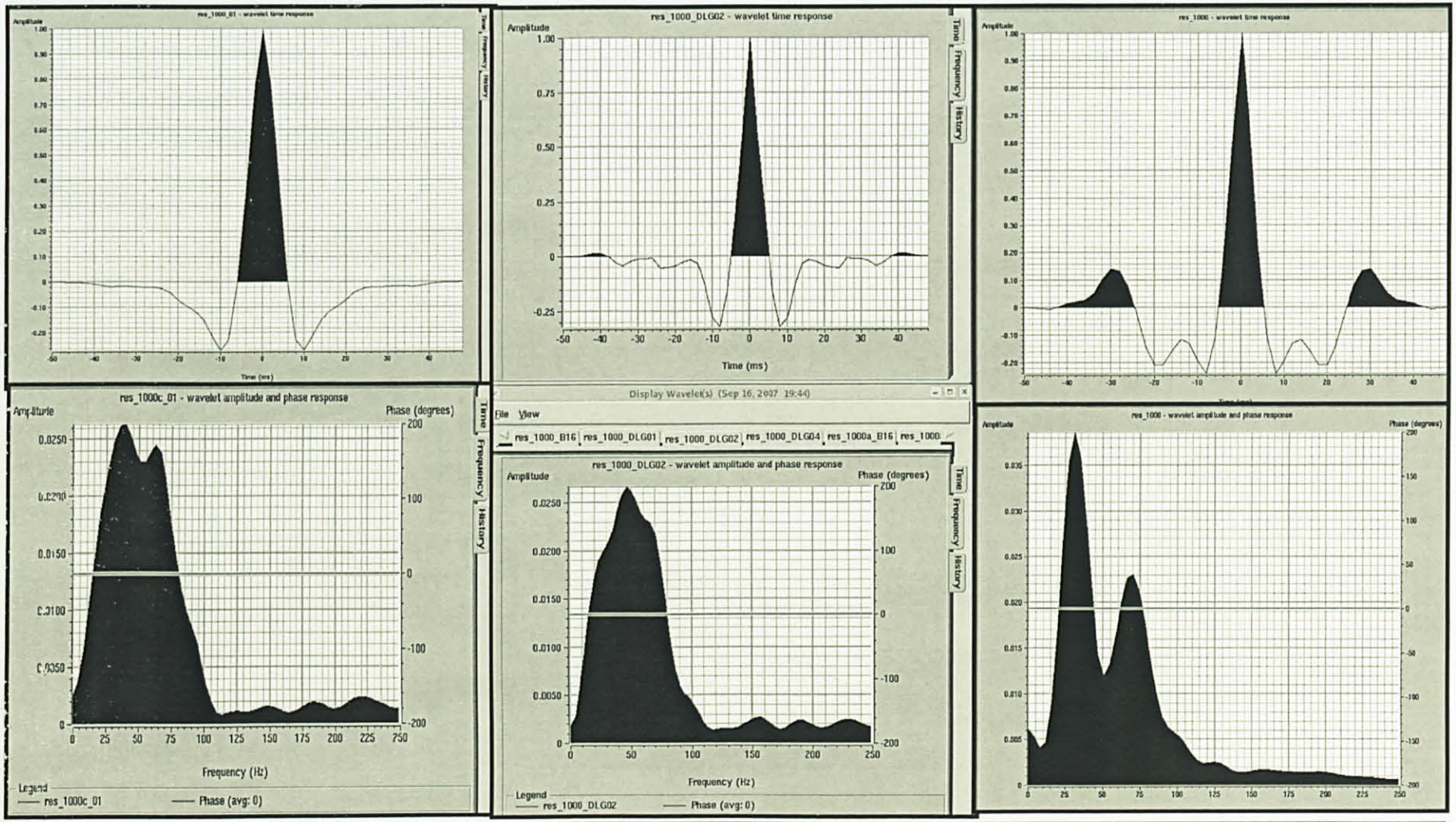

DLG 01	DLG 02	DLG 04

Figure 3.3: Result of near by DLG 01 well with time gate of 1000ms started from 1350 ms to 2350ms and 100ms for wavelet length

3.3 EXTRACTION WAVELET USING WELL DATA

After done with the first method that is statistical, we move to second method that is extraction using well data. DLG 01, DLG 02 and DLG 04 wells have been used to extract the wavelet. The result shows in Figure 3.4 and the data taken from DLG 01, DLG 02 and DLG 04 with 100ms of wavelet length. With this method, the information of phase is given for each well that we can see as a red line in the spectrum below.

For wavelet extraction using well data, it is estimated from three wells with sonic and density logs come from well DLG 01, DLG 02 and DLG 04. During the wavelet estimation, the logs are stretched or squeezed to obtain a good tie between the well data and the recorded seismic trace. It will estimate the wavelet that gives the optimum match between the seismic and the impedance log. For DLG 01 the time window is taken at 1100ms to 1600ms, DLG 02 is 1200ms to 1600ms, DLG 04 is 1100ms to 1600ms, and for the wavelet length is the same that is 100ms.

Looking at the result, for the lateral variation from DLG 01 to DLG 02 and to DLG 04, DLG 01 and DLG 02 have a similar wavelet but different with DLG 04. Same reason when we extract wavelet using well data that is due to the different blocks which is DLG 01 and DLG 02 is nearby each other and in N3 block but DLG 04 is it obviously is in the different block that is S3 block. DLG 04 wavelet shows minimum phase where else the other wells in zero phase. A DLG 01 and DLG 02 show the wavelet is in zero phase but is in a reversed polarity which means at the zero time is appear as a trough. Extraction wavelet using well data it consist of geological and phase information and it shown in the spectrum of the wavelet which shown in Figure 3.4 (in the lower part). By looking at the result of DLG 04, the wavelet is different with others, it may due to the complexity of the geology and interference coming from the layer itself. Therefore, we are not getting a right wavelet.

Further analysis need to be done at DLG 04 and the important thing is the quality of all the logs needs to be taken into account. For example, the logs need to be edited due to invasion or wash out or any spike appearing in the logs. In this study, edited logs are not in my scope of work, we just take the original logs to make an

analysis. We have simplified the workflow of the wavelet estimation using statistical method and using well data, it shown in Figure 3.5.

3.4 SUMMARY

After analysis and discussion, statistical method is being used for the next process that is in building a synthetic seismogram and used it in building the model for the inversion process. In practice, extraction using well data need to be used but seems like the logs is not edited and the result from the well is not in a good wavelet. We decided to take the result using statistical method that is within the reservoir window with the time gate of 1000ms and 100ms for the wavelet of length at near by DLG 01 well. In Appendix 11a, 11b and 11c, is shows the sensitivity of wavelet for DLG 01 well using the different statistical method. In Appendix 11a, it using statistically estimated wavelet near the DLG 01 well, meanwhile for Appendix 11b it using wavelet near DLG 02 well and in Appendix 11c, using wavelet near DLG 04 well. When we make a comparison among each other, there is no drastic change by looking at the inversion result. It only a small difference between them.

It goes to Appendix 12a-c and 13a-c. At the end, we still choose the same result that is extract wavelet using statistical method with 1000ms time gate and 100ms of wavelet length within the reservoir not from the water bottom window. Therefore, this wavelet will be used in well seismic correlation as well as in the inversion process that will discuss in next chapter.

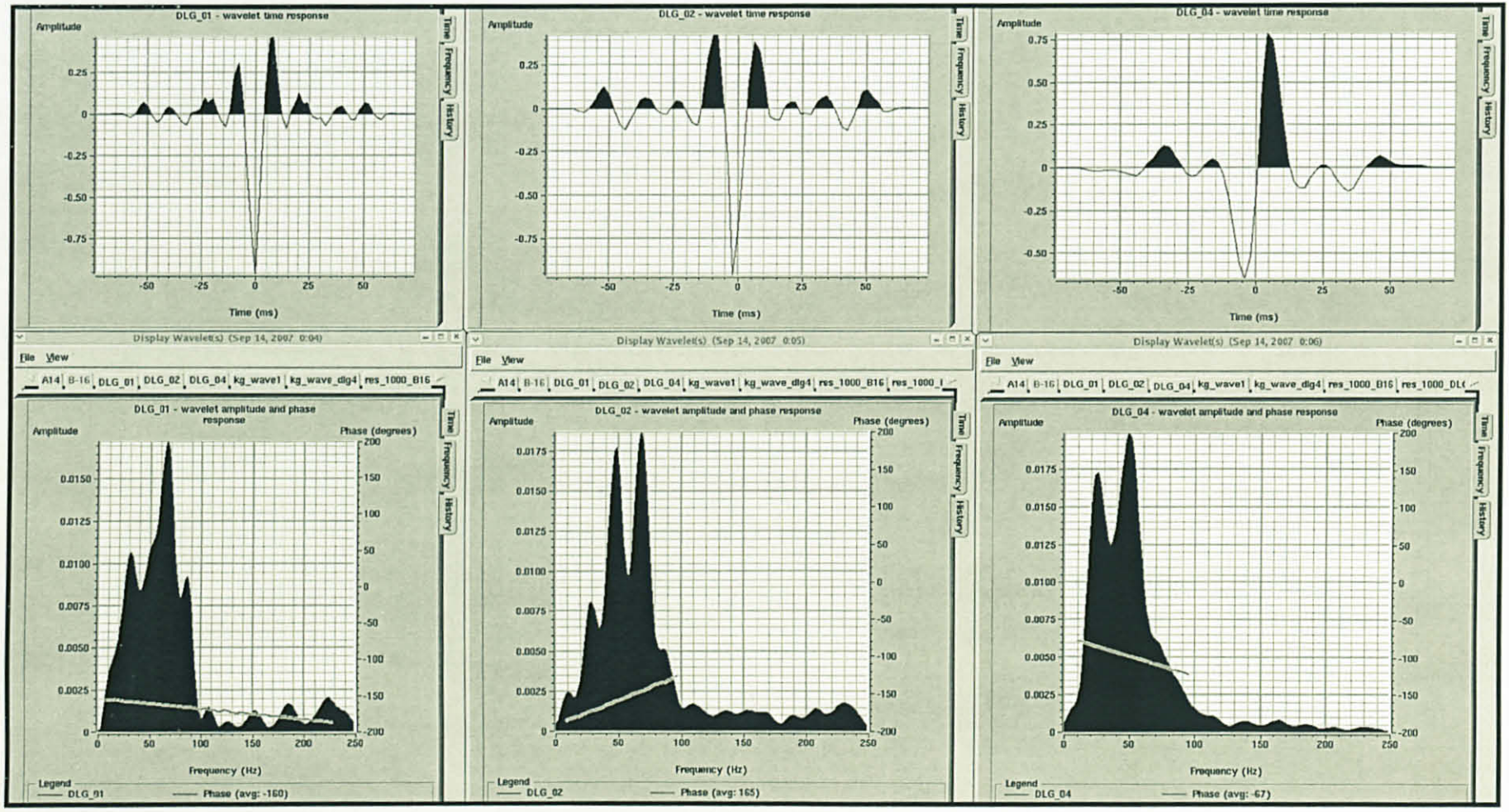

DLG 01	DLG 02	DLG 04

Figure 3.4: Wavelet extraction at DLG 01, DLG 02 and DLG 04 wells within the certain reservoir window

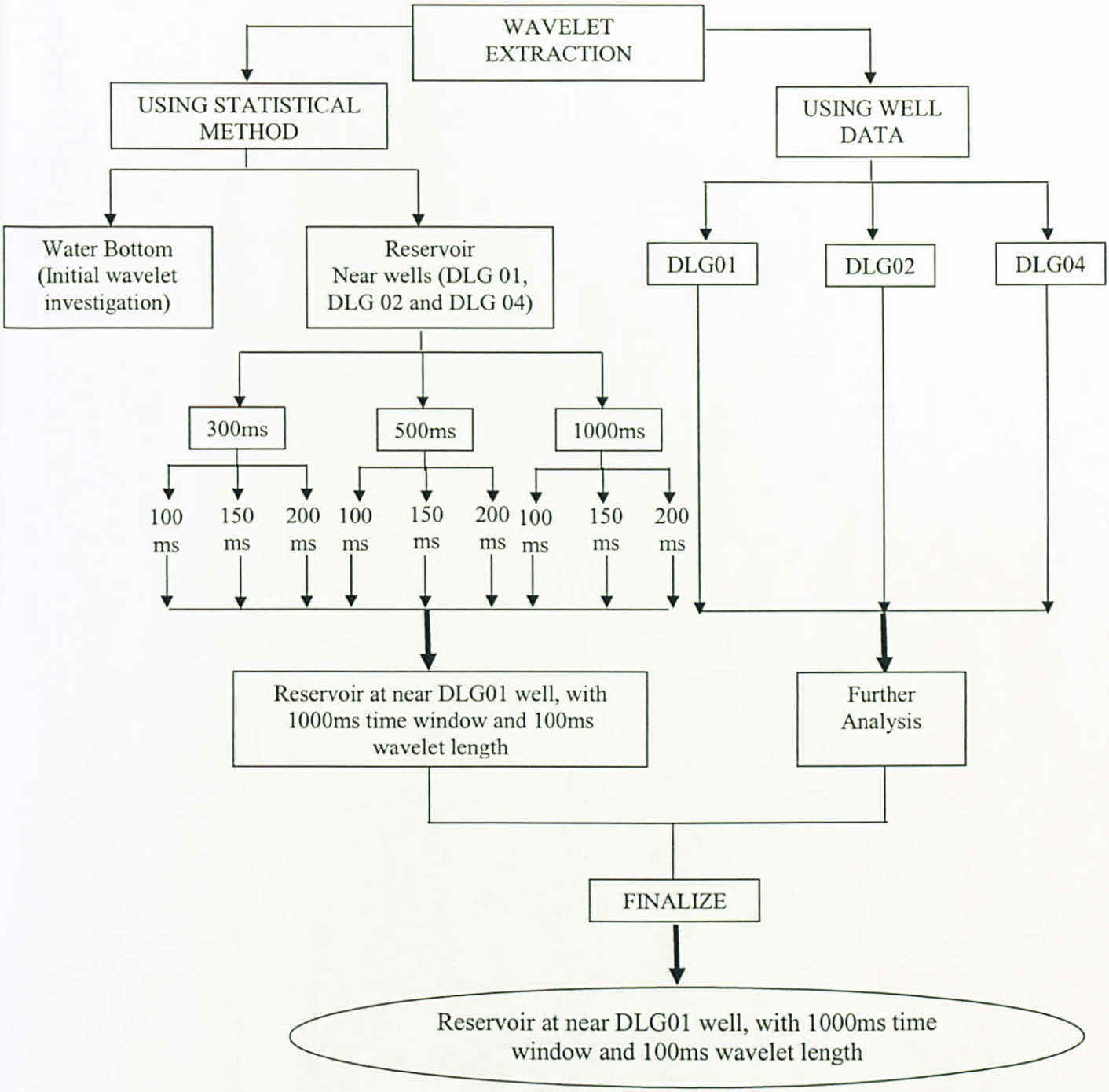

Figure 3.5: Workflow of wavelet extraction

CHAPTER 4
INVERSION THEORY

4.1 INTRODUCTION

Geophysical data are decoded in terms of subsurface geology in two ways that are direct way, known as forward method and an indirect way, known as inverse method. In the forward method, the model parameters of the subsurface geology are estimated from geophysical observations with the help of matching previously drawn curves, e.g. synthetic seismogram of seismic method, etc. On the other hand, the inverse method a model of the subsurface is assumed.

A theoretical geophysical response for various models until there is a minimum difference between computed and compared with the observed response. This process is repeated for various models until there is a minimum difference between computed and observed response. The first question that arises in the inversion problem is to determine whether the proposed models that satisfy the observed data. This is known as the nonuniqueness of a solution of the geophysical inverse problem and it could be because of this three reasons. First is inherent nonuniqueness, then due to uncertainty in the data and parameterization and last one is a combination of both inherent nonuniqueness and uncertainty of data. Other factors, such as signal to noise ratio of the seismic data, the wavelet, and well log data quality, need to be taken into account in order to control the performance of the inversion methods.

Inversion can be defined as a procedure for obtaining models, which adequately describe a data set. Seismic data are inverted to recover the acoustic impedance profile for each seismic trace. The impedance profile relates to the layer properties of the reservoir, density and velocity. The inversion method used to invert seismic data in this study is model-based inversion using the Hampson-Russell inversion package (STRATA). It is used to estimate the reservoir property between

wells and enables to determine petrophysical anomalies and lateral variations within the reservoir layers. This chapter introduces the theory of model based inversion method.

4.2 INVERSION METHOD

Seismic inversion techniques can be classified into two groups: deterministic methods and that are generate a single acoustic impedance model and stochastic methods that result in multiple equally probable models. The deterministic inversion approaches are normally cheaper in terms of computational time and storage. However, the vertical resolution remains constrained by the seismic bandwidth. Therefore, deterministic inversion mainly is useful for deriving general trends and highlighting large features in exploratory stage. Stochastic inversion uses stochastic methods (i.e. random variation of parameters) to create data with vertical resolution that is superior to the conventional data. Figure 4.1 shows diagram on seismic inversion methods.

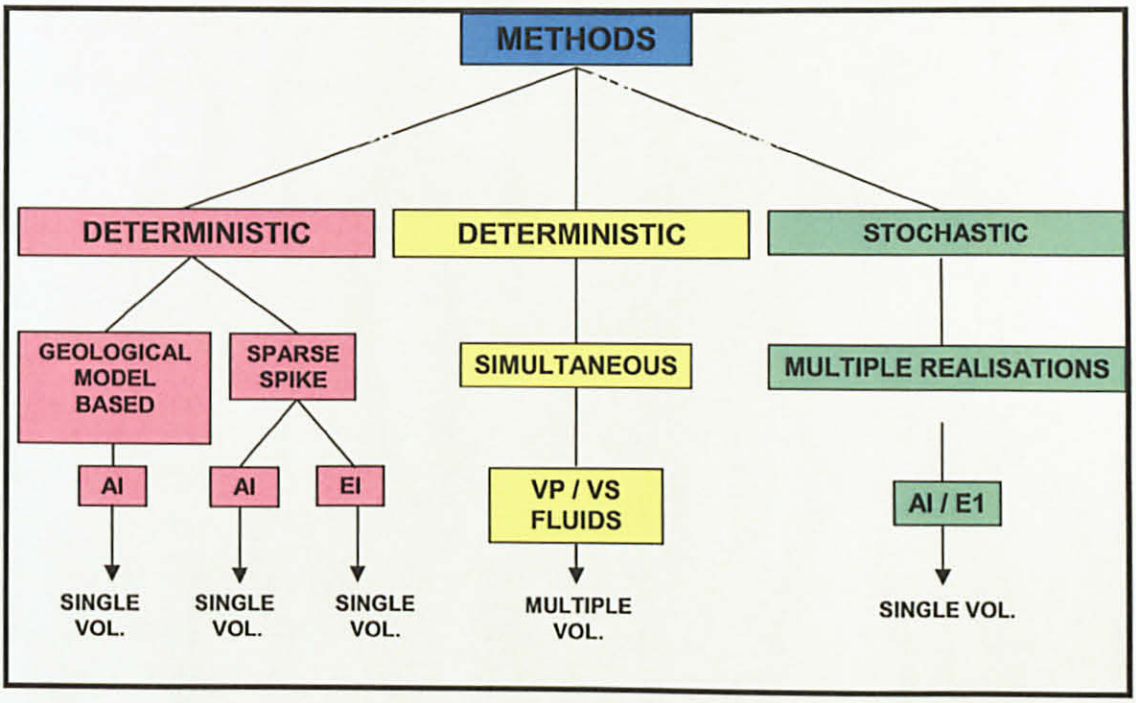

Figure 4.1: Seismic inversion methods

In STRATA software, it provides two way of inversion that is in Post-stack Inversion or in Pre-stack Inversion. For this study, post-stack inversion has been used. The seismic trace can be characterized by convolution of the 1-D earths' reflectivity with a seismic wavelet and the addition of a random noise component as shown in equation 4.1.

$$s(t) = w(t) * r(t) + noise \tag{4.1}$$

where $s(t)$ is the recorded seismic trace

$w(t)$ is the wavelet

$r(t)$ is the reflectivity series

The reflectivity series is computed for a given seismic trace by assuming a seismic wavelet. The seismic wavelet can vary for each trace and is critical to the processing steps applied to the data. Seismic reflectivity changes are caused by changes in acoustic impedance (Z) due to geologic lithofacies boundaries, where acoustic impedance (Z) is defined as the product of density (ρ) and velocity (v). Converting P-wave acoustic impedance to reflectivity involves dividing the difference in the acoustic impedance by the summation of the acoustic impedance. For normal incidence case, the reflectivity at the boundary between two homogeneous layers is given by

$$R = \frac{Z_{i+1} - Z_i}{Z_{i+1} + Z_i} = \frac{\rho_{i+1} V_{i+1} - \rho_i V_i}{\rho_{i+1} V_{i+1} + \rho_i V_i} \tag{4.2}$$

where the subscript i refer to the layer number. The obtained seismic trace will be converted to the acoustic impedance by eliminating the wavelet effect.

In general, r(t) is broadband, but the wavelet is band-limited with typical frequency 10-60Hz. Therefore, the seismic data does not contain the information outside this band, and consequently the low and high-frequency about the acoustic impedance is missing (Oldenburg et al., 1983). The incomplete spectrum causes the underdetermined problem, and therefore the result has no unique solution. However,

this is a fairly ad-hoc procedure, and a more recent approach to inversion is called model-based inversion (Russell and Hampson, 1991).

In model-based inversion it will start with a low-frequency model of the P-impedance and then perturb this model until obtain a good fit between the seismic data and a synthetic trace computed by applying equations (4.1) and (4.2). Model-based inversion uses the assumption that it has extracted a good estimate of the seismic wavelet. Any impedance inversion method can result in one or more solutions of the reflectivity series that produce more than one impedance profile that matches the recorded traces.

4.3 LOW FREQUENCY MODEL

The lack of unambiguous low spatial frequency trends is an important issue in the seismic inversion approach. As mentioned previously, the seismic trace resulting from the convolution does not have the low-frequency information (below 10Hz). The error in the low-frequency trend is related to the non-uniqueness problem in seismic inversion that could produce many possible solutions (Oldenburg et al., 1983). In order to restrict possible solutions, a priori low-frequency information is added. Including low-frequency information gives a more realistic geological model (Oldenburg et al., 1983). For P-wave stacked seismic data, Russell and Lindseth (1982) showed examples of the loss of geological information in inverted seismic sections that was present in the low-frequency component of the sonic log.

Low-frequency information is added to the process and can be derived from the velocity data, for example by using stacking velocities, or well log information (Oldenburg et al., 1983). In this study, the low-frequency model is built by using the sonic and density logs. The impedance logs are interpolated and extrapolated through the area of the survey guided by interpreted horizons and they also provide the trend information (Francis, 1987). The horizons that are utilized in interpolating the well information correspond to the tops of the formation identified in the well log. The horizons that are interpreted for the low-frequency model are LD1, SME Coal, E6,

E14, E23, E34 and E47.

There are three different interpolation methods available in the STRATA inversion package. They are inverse distance weighted, triangulation and kriging methods. The choice of the interpolation method is based primary on the well distribution. The description of those interpolation methods is explained below:

- Inverse distance weighted: The weights are maximum at its well position, then decrease with distance, and are exactly zero at the other well positions.
- Triangulation: Only well logs for connected triangles contribute to the interpolation (Lancaster and Salkauskas, 1986).
- Kriging: Use a simple linear variogram to calculate the weight of interpolated points on the unknown location.

From the well locations in the survey, two of three wells that are close to each other that is DLG 01 and DLG 02 which is they are in the same block, where else DLG 04 is in another block. Due to well distributed, We used the inverse distance weighted method for data interpolation between the well locations. The values from a particular well are distributed throughout the area with some weighted value. The inverse distance well is producing the smooth interpolation where else the triangulation and kriging gives a result of poor continuity.

4.4 MODEL BASED INVERSION

In this study, the geological model-based has been used. It was based on the horizons that define the top and the base of the reservoir. The well data in the model were then added The model-based inversion method in the STRATA program (Hampson-Russell Inc) is based on a generalized linear inversion method (GLI), described by Cooke, 1981; Cooke and Schneider, 1983. The objective of this technique is to obtain the impedance profile as a function of time that produces the seismic data within some error. The synthetic trace is generated using convolution model as described before. This techniques is also known as model perturbation since

it updates the model parameters, in the case the impedance profile, until it generates output with the least error in the least-squares sense. The GLI technique should be conceptually familiar to most seismic interpreters.

We shall consider the case of building a geologic model first and comparing the model to our seismic data. We shall then used the results of this comparison between real and modeled data to iteratively update the model such a way as to better match the seismic data. The basic idea of this approach is shown in Figure 4.2.

Assumptions used in this method are:

- 1D earth consists of a series of number layer.
- As earth is characterized by a "blocky" impedance profile. The average size of a block is generally larger than the sample rate of the input data.
- The wavelet is assumed to be known.

Notice that this method is intuitively very appealing since it avoids the direct inversion of the seismic data itself. On the other hand, it may be possible to come up with a model that matches the data very well, but is incorrect. (This can be seen easily by noting that there are infinitely many velocity/depth pairs that will result in the same time value). This is referred to as the problem of nonuniqueness. (From Brian Russell).

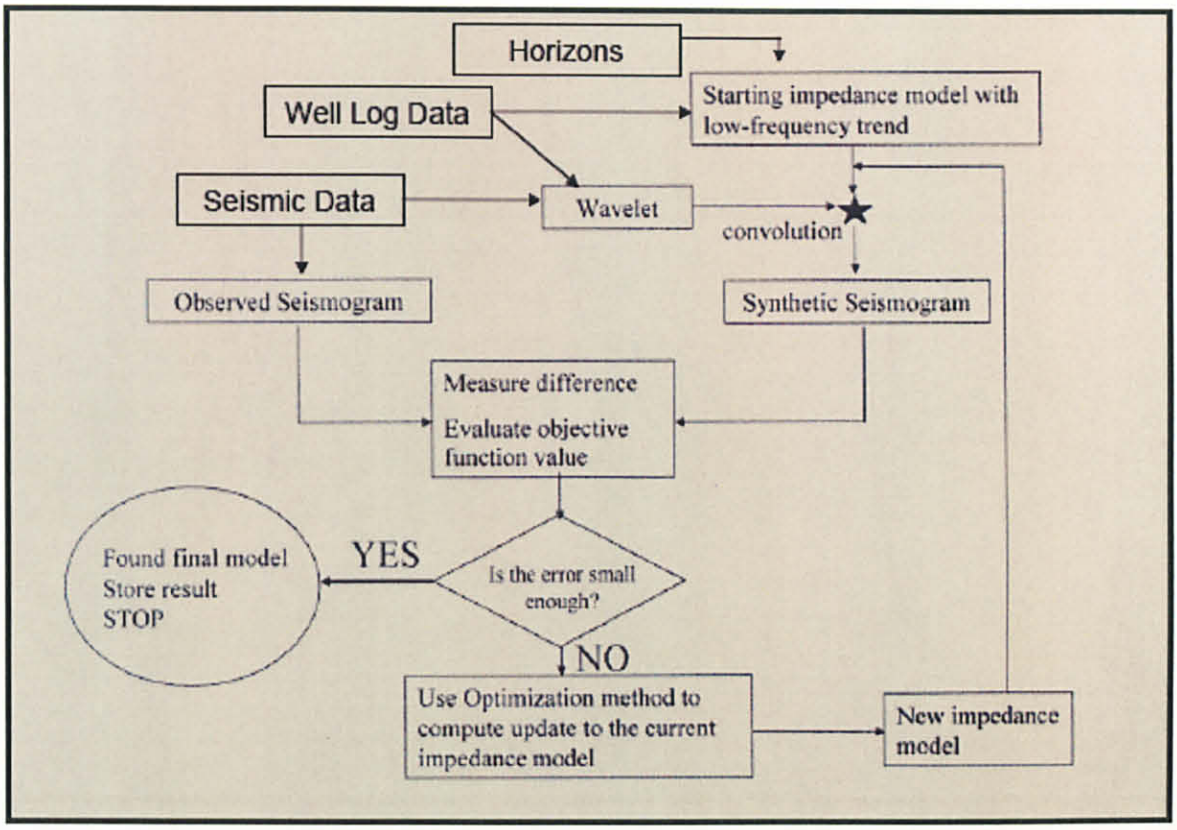

Figure 4.2: A workflow for a model based inversion (modified by Russell, 1998)

CHAPTER 5
RESULTS OF SEISMIC DATA INVERSION

5.1 INTRODUCTION

This chapter presents the inversion of P-wave seismic data using model based inversion method. The important aspect in seismic inversion is wavelet estimation that has been discussed before. The correlation between synthetic data generated from the impedance logs and seismic data is discussed here. This correlation is done carefully, since the tying process affects the amplitude and phase of the wavelet. Some example on correlation at well has been shown in this chapter.

The impedance result from the model based inversion is also discussed in this chapter. The inverted model is compared with the impedance model. In impedance model, it will show continuity of impedance where else when we see the inverted volume it will mix with other layer or the layer will discontinuous. Before we invert the model into the real inversion volume, inversion analysis needs to be done to justify the parameter such as iterative, scaler adjustment and so on to make the inversion successful. All the results of this study will show and discussed here.

5.2 WELL – SEISMIC CORRELATION

Seismic data today, particularly 3-D, contain a great amount of information and can yield maps of considerable accuracy. All seismic information, however, is relative, so to give it the greatest possible accuracy we must calibrate it to the local geology. Since seismic data respond to the acoustic properties of rocks, the geology needs to be expressed in some comparable form. Thus sonic (acoustic) logs and density logs from wells have become the established form of subsurface information used for making seismic ties.

Both a sonic log and a density log, they are multiplied together point-by-point to give an acoustic impedance log. This is converted from depth to time using some velocity function. By subtracting one acoustic impedance value from another progressively down the log, now in time, we obtain acoustic impedance contrasts, which are a direct expression of seismic reflectivity. This is a series of spikes, which implies very high frequency content; this is, of course, what we expect, because the information came directly from well logs measured down a borehole only centimeter from the rock under study.

Where else, seismic data have lower frequency content because the energy has traveled from the surface and back again. Because of this lower frequency content, the seismic energy pulse is rather broad. Some estimate of the shape of this pulse, or wavelet, is then made, and each spike on the reflectivity log is given this broader shape. The superimposition of the resulting many wavelets provides the synthetic seismic trace, or synthetic seismogram. This is compared to the real seismic trace at the well location and a match is made.

Because of velocity error, some relative sliding up and down may be necessary to help the match. In this way, we need to transfer some geological identity onto the seismic section. Although this is a time-honored approach, the similarity between the synthetic seismogram and the seismic trace is often poor - leaving considerable uncertainty as to how to make the match. The causes of these dissimilarities and difficulties are not simple, example is explained below:-

1. The seismic wavelet used to construct the synthetic seismogram may be wrong. It needs to be close to the same as the actual wavelet in seismic data in terms of:

- Polarity.
- Phase.
- and Frequency content.

We assume the data is zero phase - and perhaps it is not. A zero phase (symmetrical) wavelet was used in the when we extract the wavelet using statistical or well techniques. This is what we always hope to be the correct wavelet.

2. Well logging errors and variable borehole conditions (washouts, mud cake, etc.) may mean that the logs are not measuring the properties of the unaltered rock away from the borehole as intended

3. Seismic data and well log data measure the properties of very different sized rock volumes because of their different resolution. A single well log value will be measuring the property of about 10 m^3 of rock. A single seismic value will be measuring the property of about 100,000 m^3 of rock.

4. There may be significant positioning errors of either the well or the seismic data. Surveying on land, navigation at sea and well deviation are all subject to error. Many old wells have been found to be seriously missed located.

5. Amplitude-Variation-with-Offset (AVO) effects in the data before stacking may mean that the stacked output trace that we are trying to tie has amplitudes that are fundamentally wrong.

6. Well logs data is in different time with seismic data for example in this study, the logs are in year 1980's and the seismic is in year 2002. It may cause not to have a good correlation (shown in Table 5.1) of maximum correlation.

All of above dissimilarities and difficulties affects the seismic trace; it should be used for the well tying exercise. Below shows, an example of DLG 01 log in correlation window in Figure 5.1, and in the Table 5.1 will shows the maximum correlation for all the wells that are DLG 01, DLG 02 and DLG 04. DLG 02 and DLG 04 logs correlation is in Figure 5.2 and 5.3.

Table 5.1: Maximum correlation for three wells

Wells	Cross correlation window	Maximum Correlation
DLG 01	1270ms to 1550ms	0.475
DLG 02	1250ms to 1550ms	0.385
DLG 04	1175ms to 1440ms	0.530

Figure 5.1 displays the seismic data for the survey around well DLG 01 and the synthetic data generated using an individual wavelet, which is wavelet extraction using statistical method at near by DLG 01 (Chapter 3). In Figure 5.1, the left diagram show the correlation window that marked with the yellow line start at 1270 ms and end at 1550ms. On the right diagram is the result after the correlation process done. From the correlation window, E6 and E14 top marker is not tie with the seismic data.

Synthetic is in blue trace which is extracted from the logs and the seismic data is in black color of trace. We can see E6 and E14 cannot match with the horizon in the correlation result. It is difficult to tie them due to the fault occurring within that reservoir. The reflector at E6 has broader central lobe that cannot be modeled by synthetic. Note that the same trace scaling is used for the seismic data and synthetic traces in Figure 5.1. By looking at the result, the horizon interpretation is picked at the trough sign. It will follow the continuity of trough but at the certain point at the fault it becomes difficult to pick, for example at E14 marker. This horizon interpretation is being done before by other people. Only two of the horizon doesn't match with the logs that are E6 and E14 marker. The rest is in a good tie between log and the horizon with maximum of correlation of 0.475. This correlation is between logs data in year 1980's and seismic data is in year 2002. Therefore, the correlation is below than 0.5 because the data is not in same year or mix match between the data.

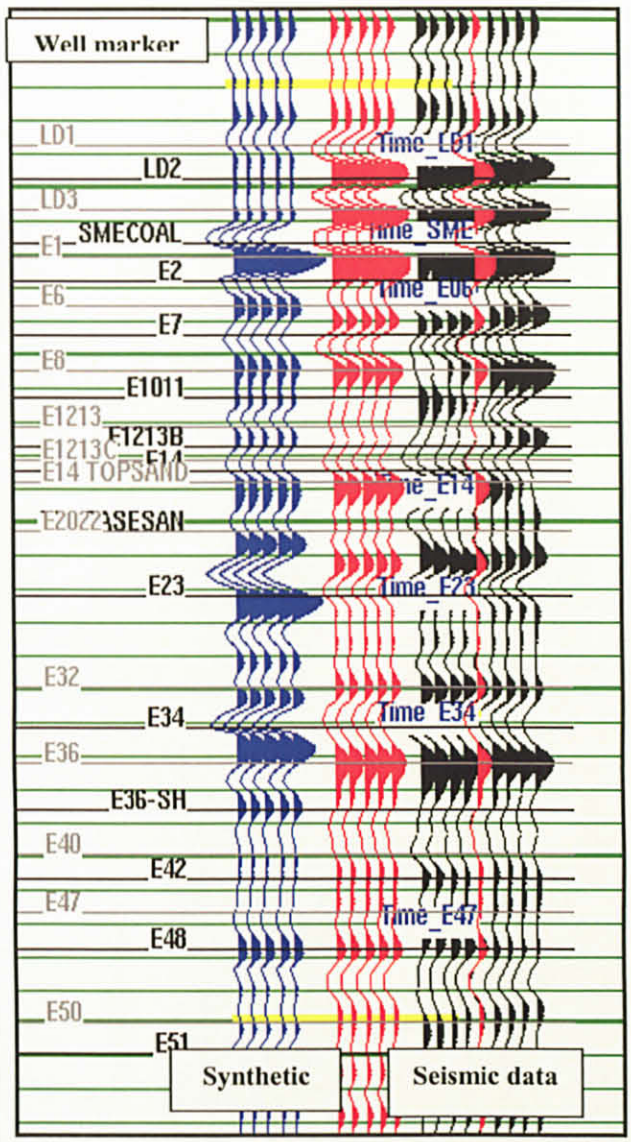

Correlation window

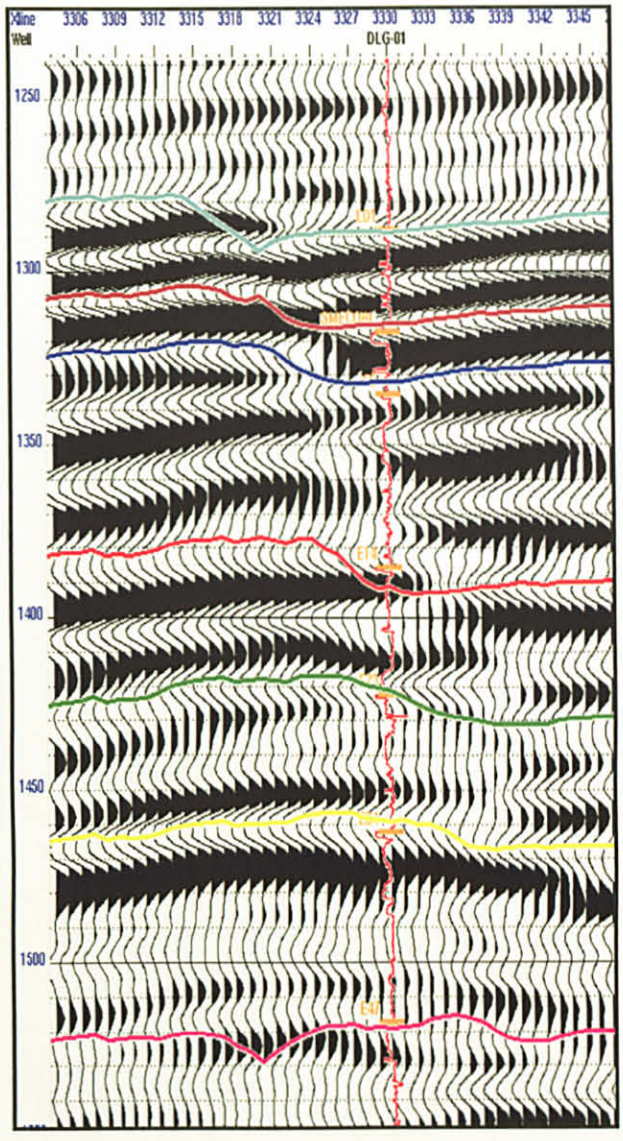

Correlation result at Inline of 2082

Figure 5.1: Correlation of P-wave seismic data with the synthetic data for well DLG 01 using wavelet that have been decide before (See Chapter 3). The same trace scaling is used for the synthetic and seismic traces.

In Figure 5.2, it shows the correlation around well DLG 02. Same as Figure 5.1, the left diagram is correlation window with start of window is 1250ms to 1550ms and the right diagram is the result of the correlation at DLG 02 with maximum of correlation is 0.385. A DLG 02 log is in Inline 2066 with strong continuous reflector and all the logs are good tie with the horizon except at E47 which is much higher than the horizon. It is used wavelet from statistical method which same as in DLG 01.

Same goes to DLG 04 well, the correlation is shown in Figure 5.3 with maximum of correlation is 0.53 and the cross correlation window start at 1175ms and end at 1440ms.

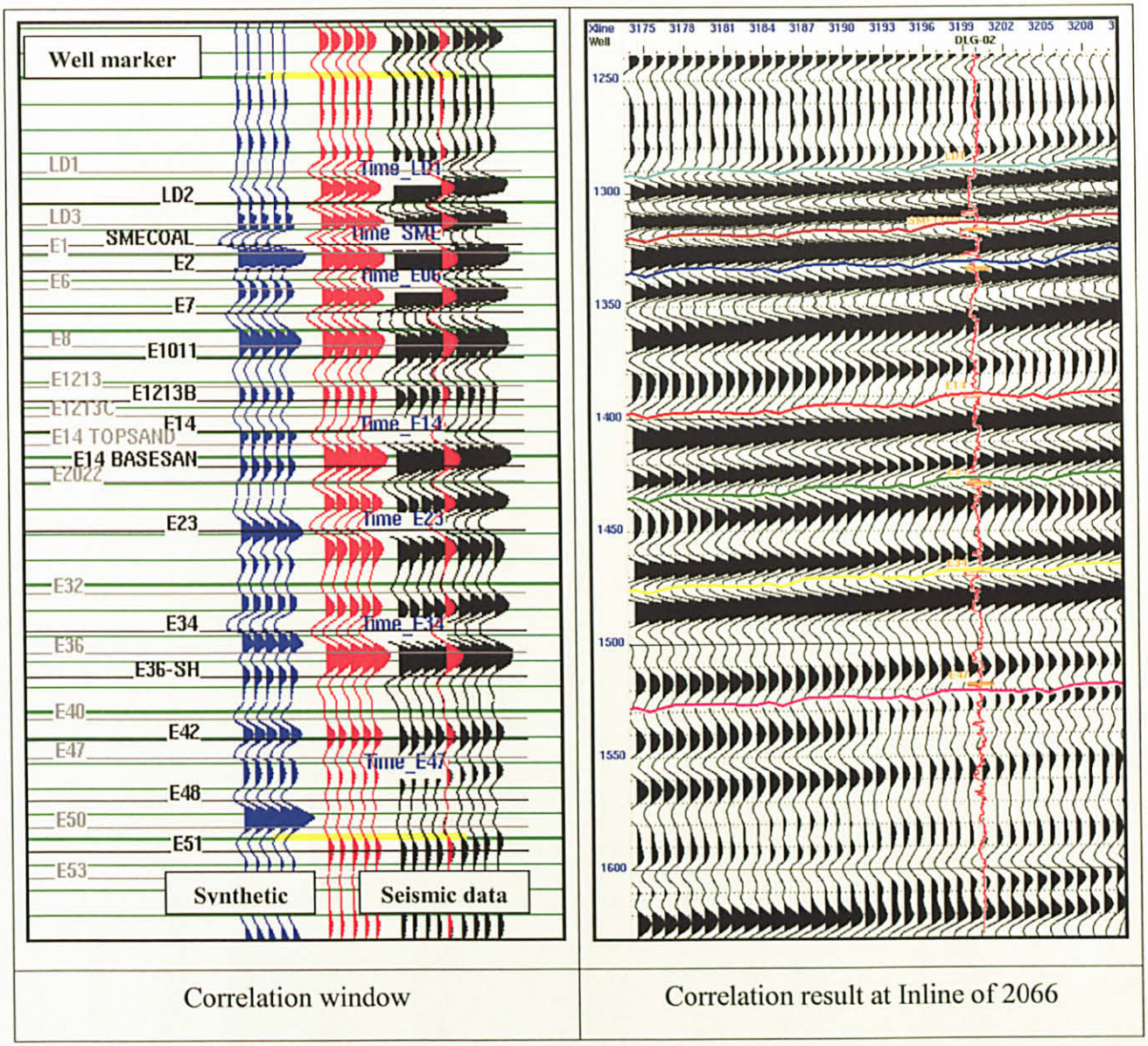

Correlation window | Correlation result at Inline of 2066

Figure 5.2: Correlation of P-wave seismic data with the synthetic data for well DLG 02 using wavelet that have been decide before (See Chapter 3). The same trace scaling is used for the synthetic and seismic traces.

In Figure 5.3, in the correlation result which is in Inline of 2007 (right diagram) we can see at LD1 it is not in a good tie due to present of fault. If we look at the E6 horizon interpretation, it seems like it so difficult to pick the continuous trough and also difficult to make it tie together with the marker from the well. This is the best

correlation that We can get using the same wavelet as before that is using statistical method at near by DLG 01. The result of well-seismic correlation is below than 50% and it may due to mix match between the logs which are in year 1980's and the seismic is in 2002.

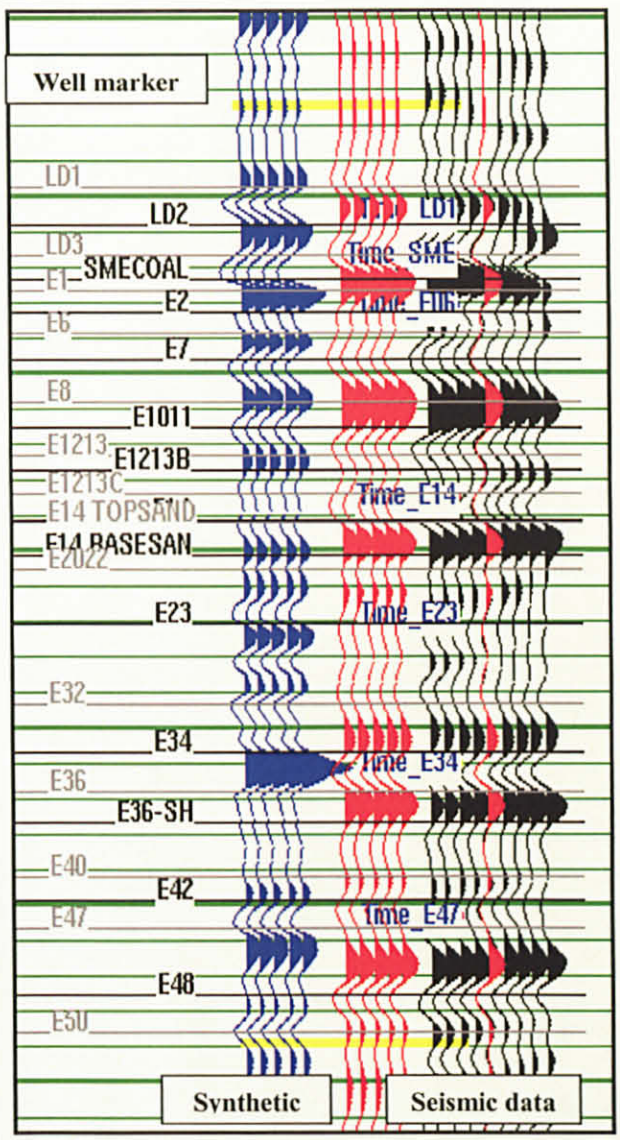

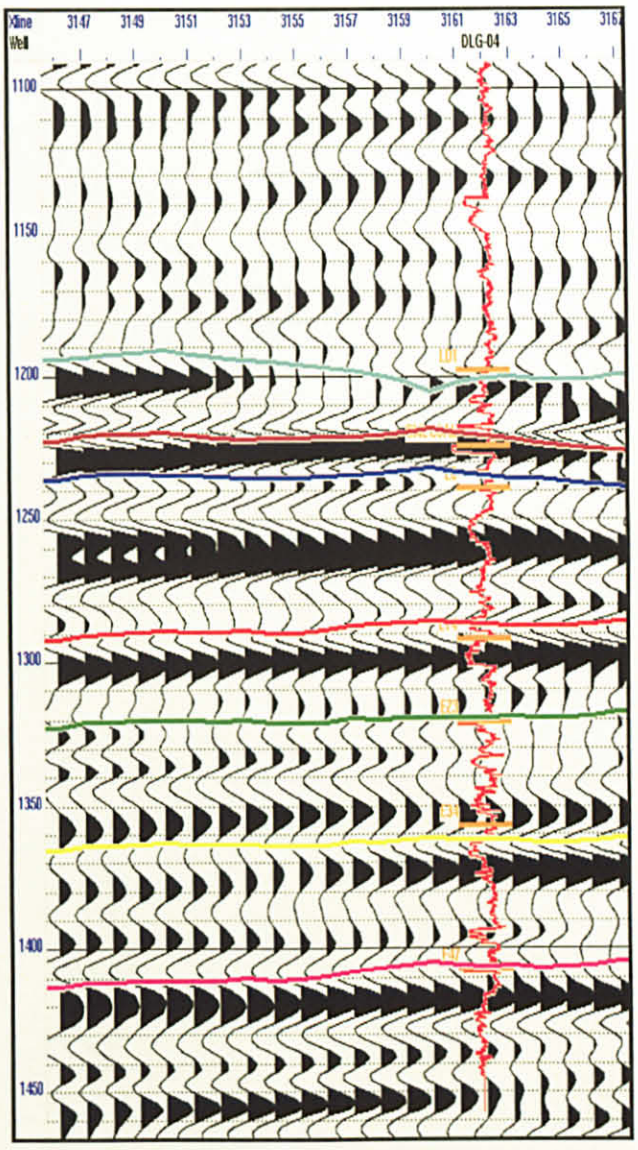

Correlation window

Correlation result at Inline of 2007

Figure 5.3: Correlation of P-wave seismic data with the synthetic data for well DLG 04 using wavelet that have been decide before (See Chapter 3). The same trace scaling is used for the synthetic and seismic traces.

5.3 MODEL BASED INVERSION RESULTS

The inversion method used in this study is the model-based inversion using the Hampson-Russell software package. The theory of this method is discussed in Chapter 4. Model-based inversion is based of the initial model. An initial model is generated from the P-impedance well logs that are interpolated and extrapolated guided by the horizon interpretation. The model is also used as low-frequency information that is added is found in Chapter 4.3. Figure 5.5 shows the example of the impedance section used as an initial model with the available impedance logs.

Now that the model has been built, we are ready to invert the seismic data. This will actually be done in two stages. First we run an analysis at the well locations to optimize the parameters. Then we run the entire volume with the parameters chosen in the first step. We need to select the correct parameters and this analysis is being done to see how well the analysis inversion succeeded or to compare different parameters before performing the actual inversion. Examples on the parameters are wavelet which will be used in the inversion, as well as the time range to invert. Also we need to justify which wells we wish to use in the analysis, by default all are used that are DLG 01, DLG 02 and DLG 04.

Figure 5.4 shows the inversion analysis display and it shows the results of applying the model based inversion at a single well location. Example in Figure 5.4 is at DLG 01 well with the left panel of this display shows an overlay of three impedance curves: the original impedance in blue, the initial guess model in black and the final inversion result in red. The second panel shows the synthetic traces calculated from this inversion result compared with the input seismic trace with correlation of 0.93. The third panel shows the Error, which is the difference between the two previous sets of traces and the error is 0.44.

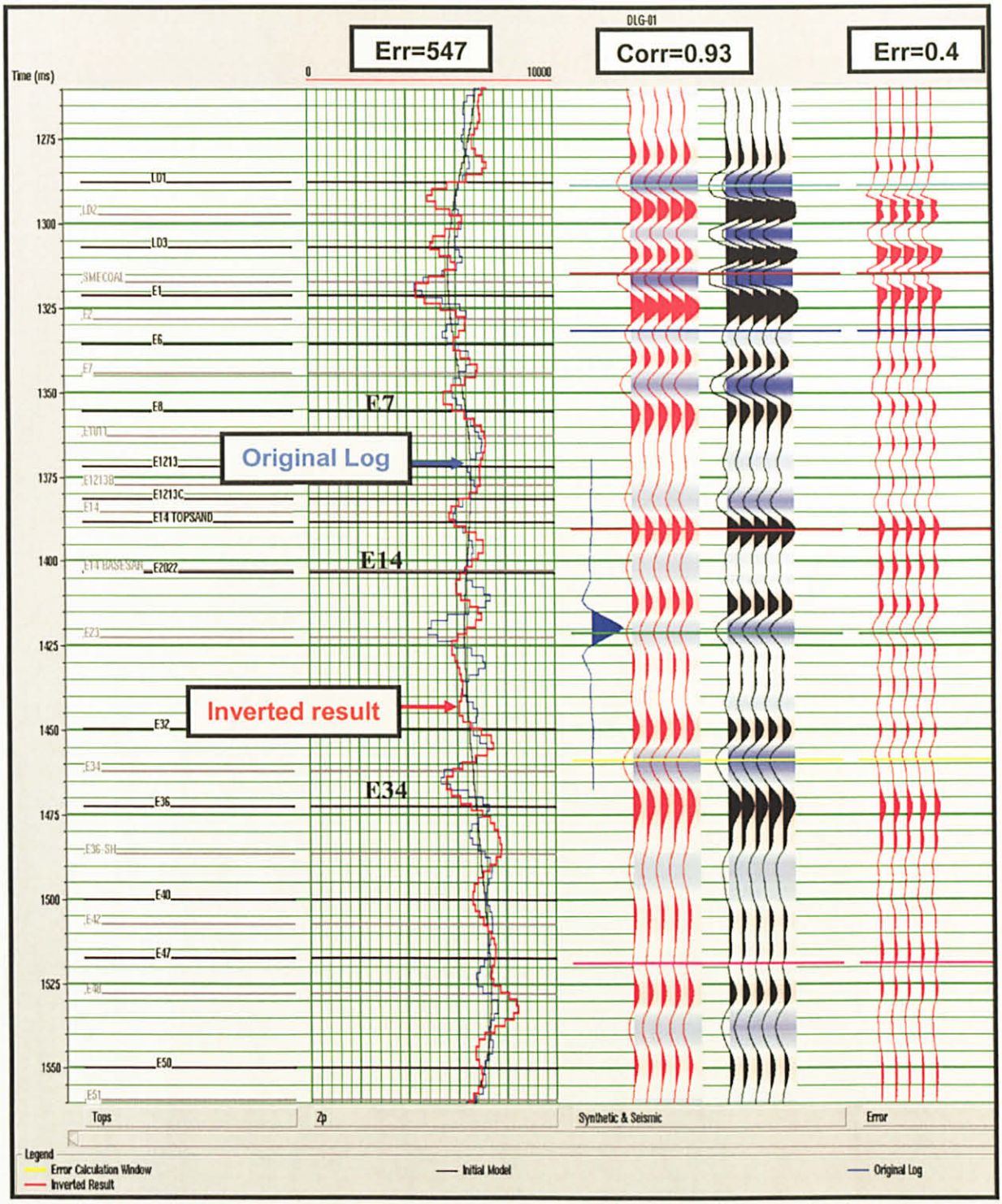

Figure 5.4: An example of analysis of post-stack inversion at DLG 01.

By zooming in on the zone of interest (E7, E14 and E34), we can see a very good correspondence between the real and inverted traces. Finally, the main Model

Based Inversion Window, which is still visible, allows us to interactively modify any of the default inversion parameters and see the new inversion result instantly. For example, we can change the Scaler Option, which is control how the seismic data is scaled to be the right amplitude for inversion. By default, STRATA calculate a single global scaler, which optimizes the fit between the inversion traces and the actual logs. For this data set, the default parameters are excellent, so we will continue to the next section without modifying them.

Another parameter we need to take into account is the iteration, because the model based itself will iteratively update the model such a way as to better match the seismic data. This is done using number of iterations of 20 for the model-based inversion menu (Figure 5.4). So I have run with different of number of iterations that is with 20, 30 and 10 and with different wavelet. The values of error (ERROR) between the inverted volume and the original logs and the correlation (CORR) between the synthetic trace and the seismic trace for a certain wavelet are summarized in table 5.2.

Table 5.2: Inversion Analysis Plot for DLG 01, DLG 02 and DLG 04 wells using different wavelet extraction

Wavelet :	**Statistical (1000ms time window)** DLG01 - 1250ms to 2250ms		
Iteration 10	**DLG01**	**DLG02**	**DLG04**
ERROR	555.184	785.462	516.840
CORR	0.932	0.960	0.971
Iteration 20			
ERROR	**547.667**	**784.652**	**546.518**
CORR	**0.934**	**0.966**	**0.973**
Iteration 30			
ERROR	586.406	791.968	561.927
CORR	0.937	0.970	0.972
Wavelet :	**Statistical (1000ms time window)** DLG04 - 1180ms to 2180ms		
Iteration 10	**DLG01**	**DLG02**	**DLG04**
ERROR	489.877	749.920	501.275
CORR	0.808	0.915	0.945

Wavelet :	**Statistical (1000ms time window)** DLG02 - 1250ms to 2250ms		
Iteration 10	**DLG01**	**DLG02**	**DLG04**
ERROR	551.060	784.011	542.676
CORR	0.923	0.952	0.960
Iteration 20			
ERROR	549.331	779.921	543.111
CORR	0.923	0.961	0.963
Iteration 30			
ERROR	540.767	780.455	530.617
CORR	0.925	0.966	0.967
Wavelet :	**Extraction from Well** DLG01 - 1275ms to 1520ms		
Iteration 10	**DLG01**	**DLG02**	**DLG04**
ERROR	591.868	881.626	765.830
CORR	0.887	0.917	0.920

Iteration 20			
ERROR	482.542	761.249	549.882
CORR	0.832	0.915	0.971
Iteration 30			
ERROR	467.497	797.920	563.412
CORR	0.869	0.945	0.977
Wavelet :	**Extraction from Well** DLG02 - 1200ms to 1400ms		
Iteration 10	**DLG01**	**DLG02**	**DLG04**
ERROR	592.887	858.702	701.600
CORR	0.834	0.895	0.840
Iteration 20			
ERROR	578.718	870.030	711.133
CORR	0.859	0.918	0.875
Iteration 30			
ERROR	585.327	899.432	745.932
CORR	0.876	0.940	0.888

Iteration 20			
ERROR	599.133	903.495	770.861
CORR	0.902	0.936	0.942
Iteration 30			
ERROR	634.566	936.645	764.025
CORR	0.920	0.954	0.953
Wavelet :	**Extraction from Well** DLG04 - 1200ms to 1410ms		
Iteration 10	**DLG01**	**DLG02**	**DLG04**
ERROR	570.596	872.213	630.388
CORR	0.839	0.887	0.965
Iteration 20			
ERROR	569.492	858.078	630.631
CORR	0.855	0.899	0.967
Iteration 30			
ERROR	546.317	884.886	649.771
CORR	0.876	0.925	0.968

The result shown in Table 5.2, with ERROR (between the inverted log and the well log) is 547.667 for DLG 01, 784.652 for DLG 02 and 546.518 for DLG 04 is the minimum or the lowest error that we can get from 20 iterations (refer to yellow box in Table 5.2). Where else with other iterations that are 10 and 30 they have a high value of ERROR, which is why we choose 20 iterations to run the model. Meanwhile, for the correlation between synthetic trace that have been extracted from the inversion result and seismic trace it shows that with 20 iterations it has highest correlation when we compare with other iterations (refer to yellow box in Table 5.2). If we are using other wavelet for example using statistical method near DLG 04 well it shows the error between the inverted log and impedance from well is lower than using the wavelet taken near DLG 01. However, when we looking at the correlation between synthetic trace and the seismic trace it show low correlation compare to the previous result. At the end, still iteration with 20 and using statistically estimated wavelet near the DLG 01 well give the best result among others.

5.4 ACOUSTIC IMPEDANCE INVERSION RESULTS

In previous section, we have done two important things: we have determined that the default inversion parameters are satisfactory, and we have allowed the program to calculate an optimum scaler at well locations. Now we will apply the same parameters throughout the entire three 2D lines that were cross DLG 01, DLG 02 and DLG 04 wells.

In Figure 5.6, shows the result of inverted volume of P-impedance from the model-based inversion result through the impedance wells at DLG 01 using statistically estimated wavelet near the DLG 01 well. This result is showing the inversion result at inline of 2082 and DLG 01 well is crosses that line. By looking at this result, we have a massive sand body from E6 horizon (blue line) until E34 (yellow line) with shale as the permeability barrier in that thick sand body. We still can see the extension or the continuity of sand bodies (E7, E14, and E34) in the faulted block through the whole line

When we compare the inversion result with the impedance log that is coming from DLG 01 well, it looks like is not in a good tie (black circle in Figure 5.6). However, when we see at the bottom of the log, the well and seismic is well tie. We can make a conclusion that it may due to the relative check shot correction.

Looking at the impedance, blue color has a low impedance range from 0 to 5000 ((m/s)*(g/cc)), green and yellow represent sand body which is in a middle impedance range from 5000 to 7000 ((m/s)*(g/cc)) and red color represent shale with high impedance range from 7000 ((m/s)*(g/cc)) onwards. However, when we compare to the cross plot result, some of the sand body will have low impedance that is around 4400 ((m/s)*(g/cc)) that is in DLG 02 well for E7 sand body. It happens also to the shale which, it have a same impedance with sand bodies. This cross plot result will be use when we comparing the inversion result and it will discuss after this. Below shows the inversion result on the 2082 inline.

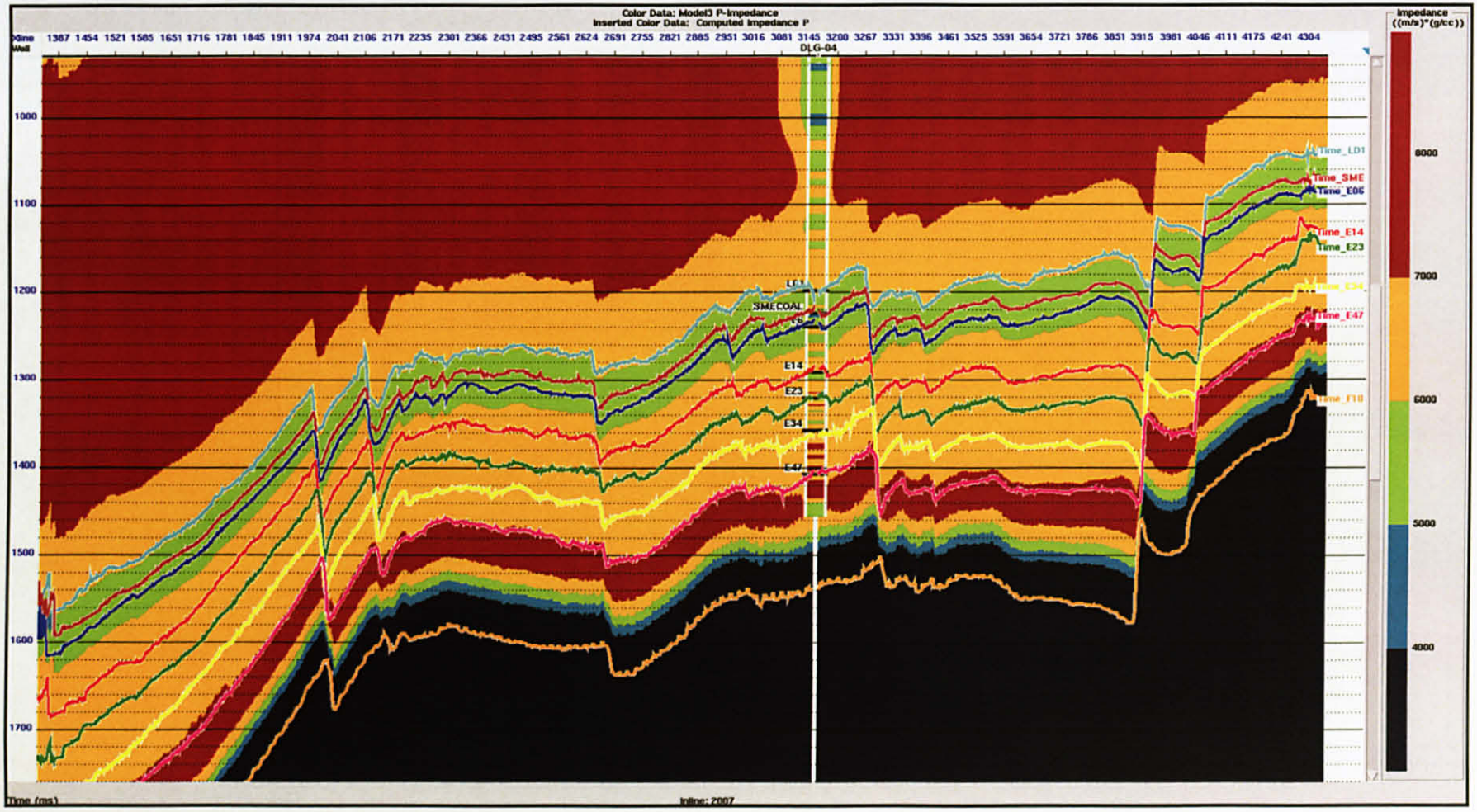

Figure 5.5: Impedance model interpolation and extrapolation from impedance logs used as an initial model and low-frequency model.

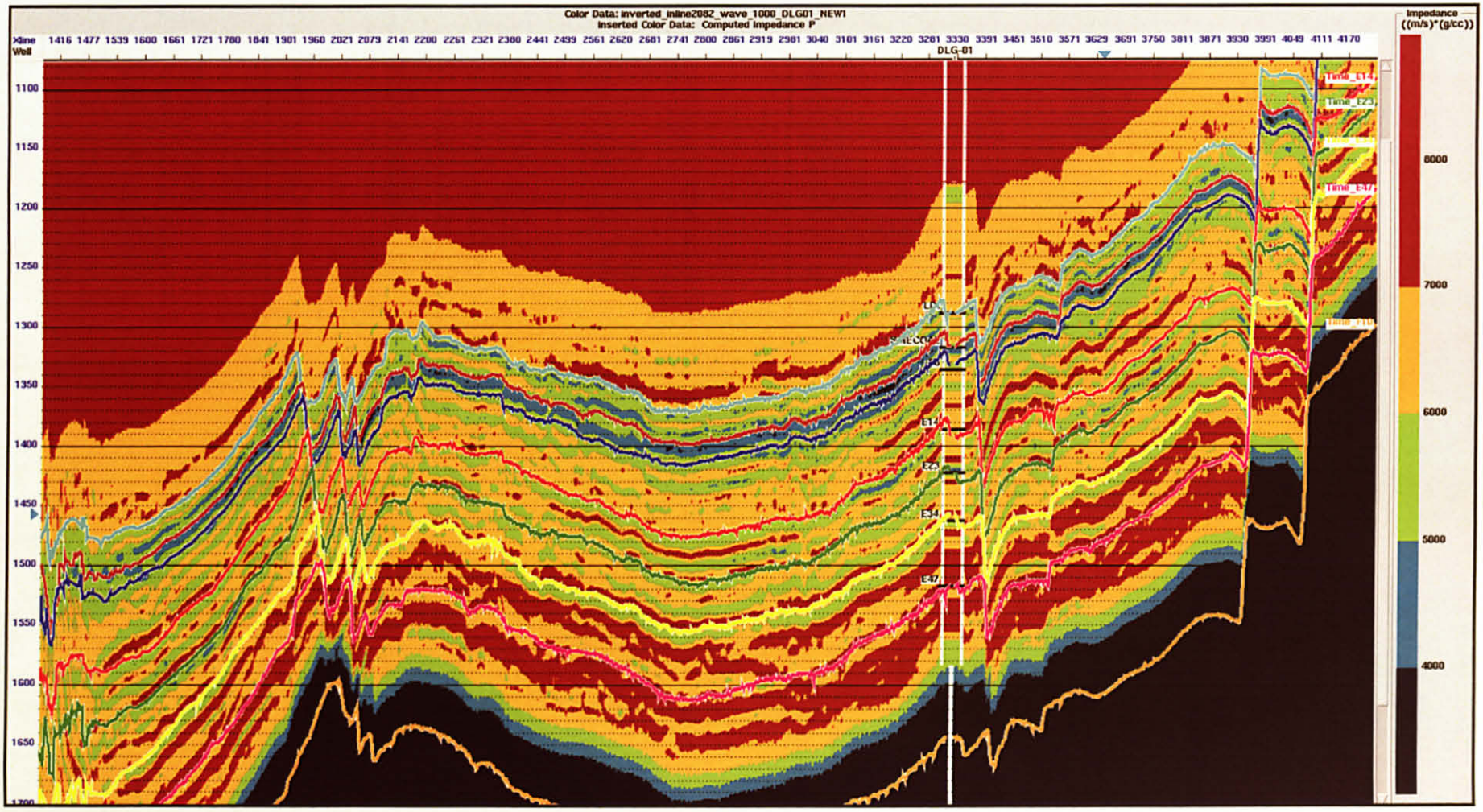

Figure 5.6: Inverted volume of P-impedance from the model-based inversion result through the impedance wells at DLG 01 using statistically estimated wavelet near the DLG 01 well

In Figure 5.7, it shows the inversion result but we are focusing on the zone of interest that is at E-group sand that is in a left diagram. On your right diagram, is the cross plot result that has been discussed before in Chapter 2.

The inversion result is coming from the seismic data and the cross plot result is coming from the well log. Therefore, we can compare the inversion result with the cross plot result. The log has been filtered with high cut frequency from 75Hz to 100Hz, to make an interpretation become easier. It has been done because to make the log is same frequency with the seismic inversion result.

Looking at E7 sand from the cross plot result is 5700 to 6200 impedance and it falls in the green and yellow color for the inversion impedance. However, the result for inversion is in green color impedance that range from 5000 to 6000, so it does not agree with each other and it may due to well to seismic correlation. It obviously does not tie in the shale layer that is below E7 sand and it goes to E14 sand reservoir.

For E14 sand reservoir, it has impedance from cross plot at 6000 to 6600 and it falls under yellow color for the inversion impedance. The impedance from log is following the cross plot but the inversion result shows is low impedance that is in green color that range from 5000 to 6000. It may due to well and seismic correlation is not good here. Next, we move to E34 sand reservoir, which is in cross plot with range of 5400 to 6667 impedance and inversion result will falls under green and yellow color. The inversion result is following the cross plot result because we can see the continuity of green color is break by the yellow color, so their in mix color but still in sand reservoir.

We can make a conclusion for DLG 01 inversion result is that when we have mix impedance between gas and oil sand from cross plot, of course in the inversion result also it will become mix. It is difficult to separate them because the quality of sand that have been discussed before in Chapter 2. In addition, when the well to seismic correlation is not in a good tie it will affect the inversion result.

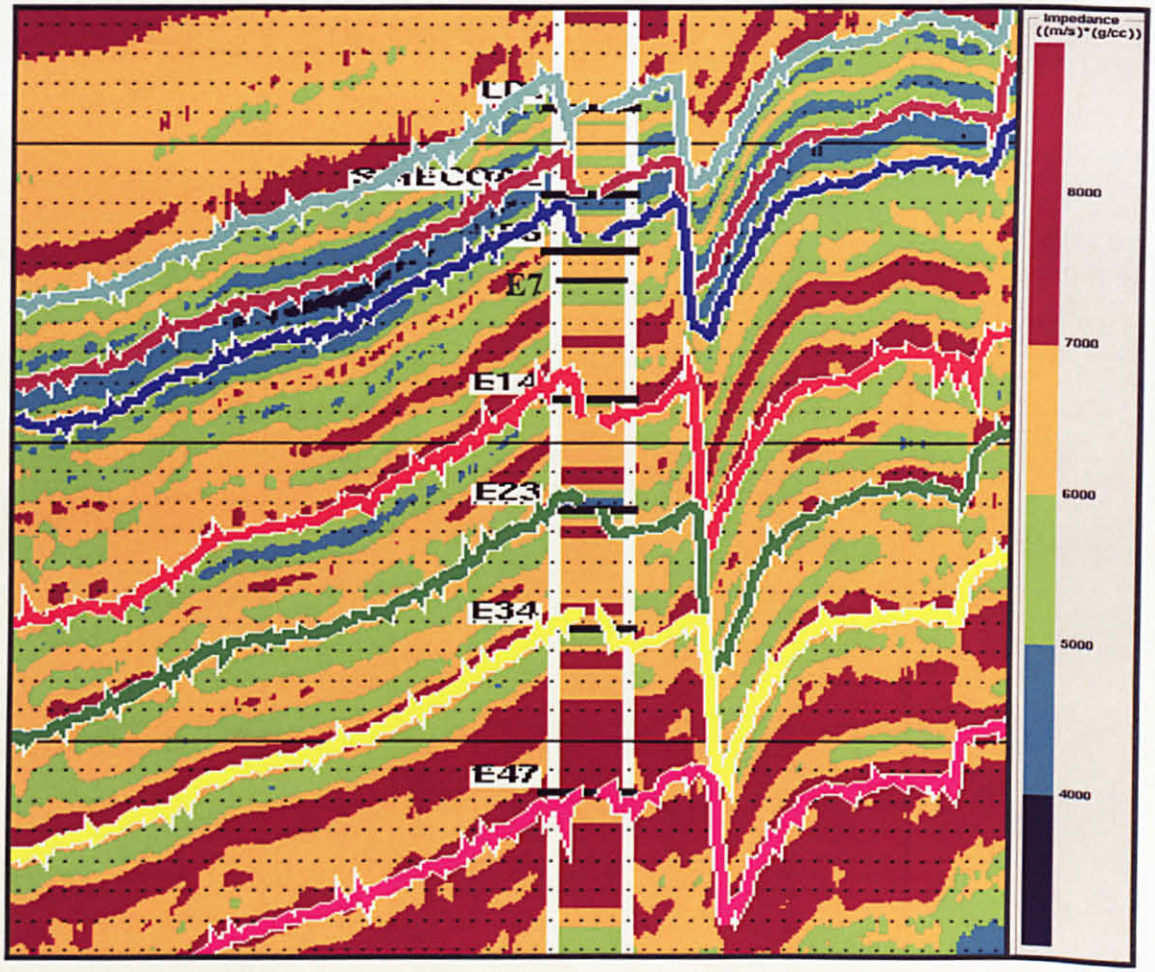

Depth (m)	Impedance ((m/s)*(g/cc)) at DLG01
1160	5700-6200 E7 – GAS SAND
1230	6000-6600 E14 – GAS SAND
1278	- E23 - water
1310	5400-6667 E34 – OIL SAND

Figure 5.7: Inversion result from Inline of 2082 (left) and the cross plot result (right) near DLG 01 well.

Now we look at the result, which in 2066 for inline and cross the DLG 02 well in Figure 5.8. Same color of impedance that is green and yellow is in sand class and shale is in red color. In DLG 02 inversion result, the well to seismic correlation is well tie. Generally, we can look the continuity of E sand reservoir at the log impedance and inversion result. Same thing as DLG 01 result, we have a massive sand bodies and shale as permeability barrier between the sand bodies. Then we will zoom in at the zone of interest that shows in Figure 5.9.

The same process has been done to the log data that is high cut filtered. By looking at the E7 gas sand in above figure, the value of impedance at cross plot is 4400 to 5700 impedance and it falls under light blue and green color. It is true for the inversion results; it was following the cross plot result. Next, we look at E14 gas sand reservoir, the cross plot impedance give a range between 5848 to 5882 impedance and for the inversion result, it falls under green color and it match each other.

For E23 gas sand reservoir, it has value of 5590 to 6790 impedance from the cross plot and it falls under green and yellow color for the inversion result. Therefore the inversion result the continuity of green color will break off with the yellow color and both are them still the sand class. Lastly, for E34 oil sand reservoir, it has impedance of 5110 to 6300 which is the impedance is mixing with the gas sand (E7, E14 and E23) and when we compare with the inversion result it falls under green color. The E34 sand is in a good quality of sand around 12.5% of volume of clay. (Refer to Appendix 6), therefore, E34 sand has low impedance and will falls under green color for the inversion result. We can make a conclusion if we have good correlation between well and seismic data; we have better interpretation on the inversion result. For example in E7 and E14 gas sand for the inversion result, it is clearly follow the cross plot and impedance log.

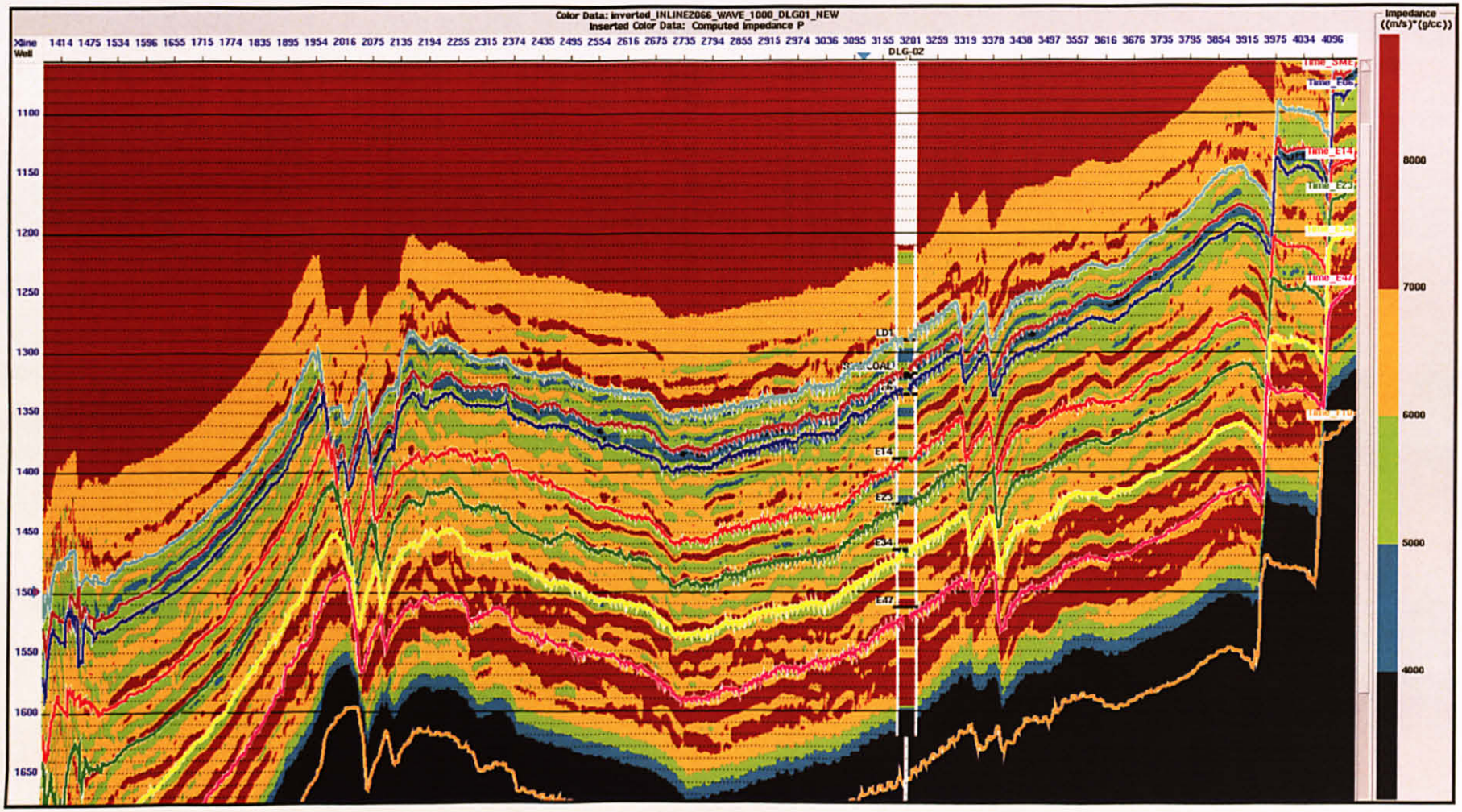

Figure 5.8: Inverted volume of P-impedance from the model-based inversion result through the impedance wells at DLG 02 using statistically estimated wavelet near the DLG 01 well.

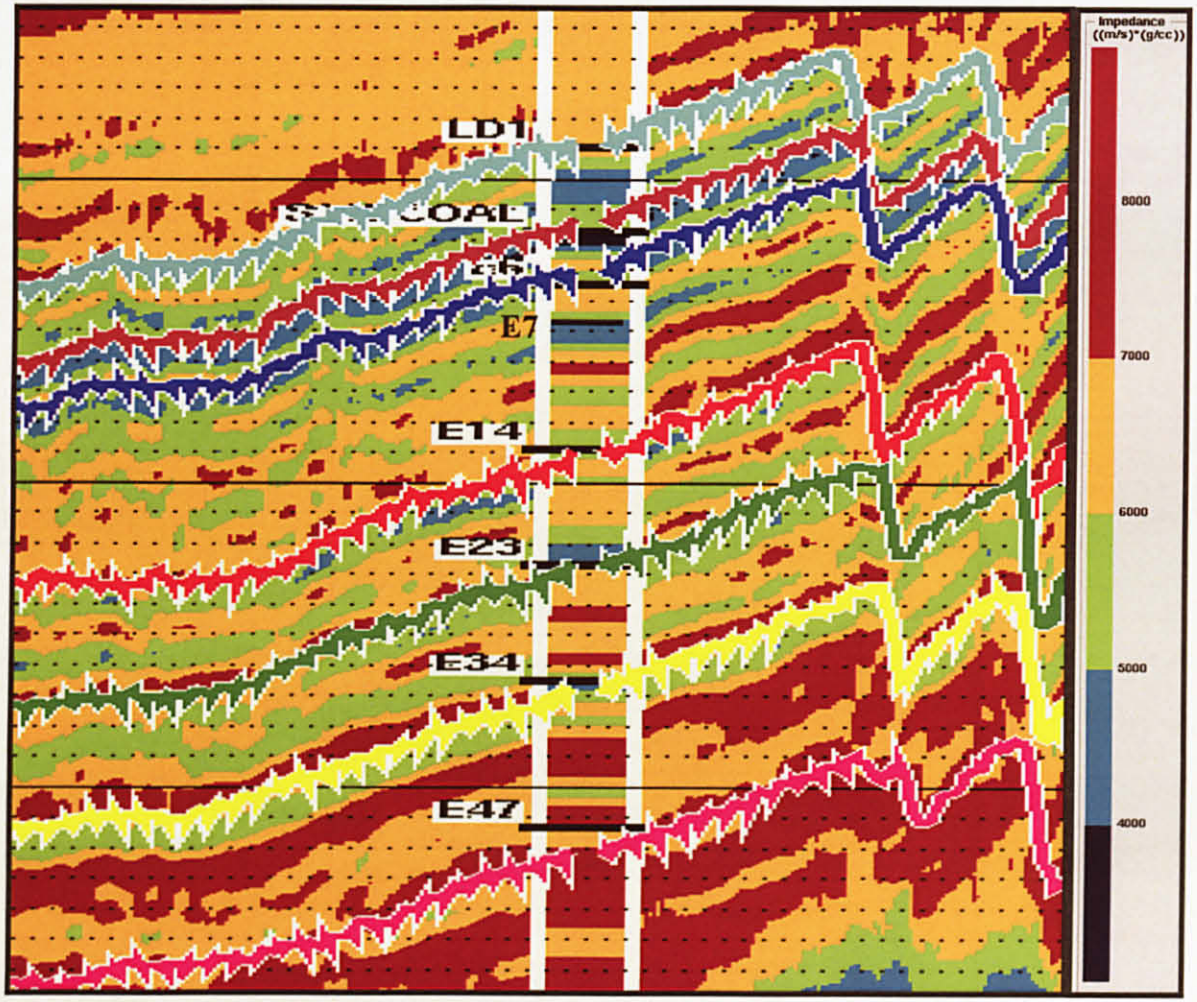

Depth (m)	Impedance ((m/s)*(g/cc)) at DLG02
1160	4400-5700 E7 – GAS SAND
1230	5848-5882 E14 – GAS SAND
1278	5590-6790 E23 –GAS SAND
1310	5110-6300 E34 – OIL SAND

Figure 5.9: Inversion result from Inline of 2066 (left) and the cross plot result (right) near DLG 02 well

Last line for the inversion result is on 2007 inline that is crossing the DLG 04 well that shown in Figure 5.10. Still using the same color for the impedance that is green and yellow represent sand class and red that is the highest impedance represent shale class. The well to seismic correlation is not too bad, because we can see a good tie in the bottom of the log with the inversion result. Same result from the previous two lines that are we just focus on the E-group reservoir, which has a massive sand bodies and shale act as a permeability barrier. Generally, we can have a look on the extension or continuity of each sand package in this 2D inversion line. Next figure, we will zoom in to the zone of interest and comparing with the cross plot results.

In figure 5.11, all the E-sand is in oil sand class. E7 oil sand with value of impedance 4700 to 5700 taken from cross plot was falls under green color in the inversion result. The impedance from log also in green color and we can look at the continuity of the sand. It goes to E14 oil sand, which has value of impedance that is from cross plot, is 5300 to 6000 and jives with the inversion result and the impedance from the log also in green color. Next, E23 and E34 oil sand, it falls under green and yellow color for the inversion result that has value of impedance from cross plot is 5100 to 6400 for E23 oil sand and 5900 to 6700 for E34 oil sand.

Generally, if we are looking at all the impedance at DLG 04 location, we can make a conclusion that is has low impedance compare to DLG 01 and DLG 02 results. We know that DLG 04 is away from DLG 01 and DLG 02 well and it is located in different block, so we can say that the depositional environment at DLG 04 is different with DLG 01 and DLG 02. In addition, if we are looking at the quality of sand in DLG 04, we can say that the sand is in clean sand because the value of volume of clay is below than 40% (Refer Appendix 7). Therefore, we can make a conclusion that DLG 01 and DLG 02, which is in the same block, have a different environment with DLG 04 due to the quality of sand. We can say that DLG 01 and DLG 02 it have marine influent and DLG 04 is clean sand due to the channel or delta features. However, we need to go back to the geology itself and some good knowledge in geology to prove it and it just my interpretation on the depositional environment for this field.

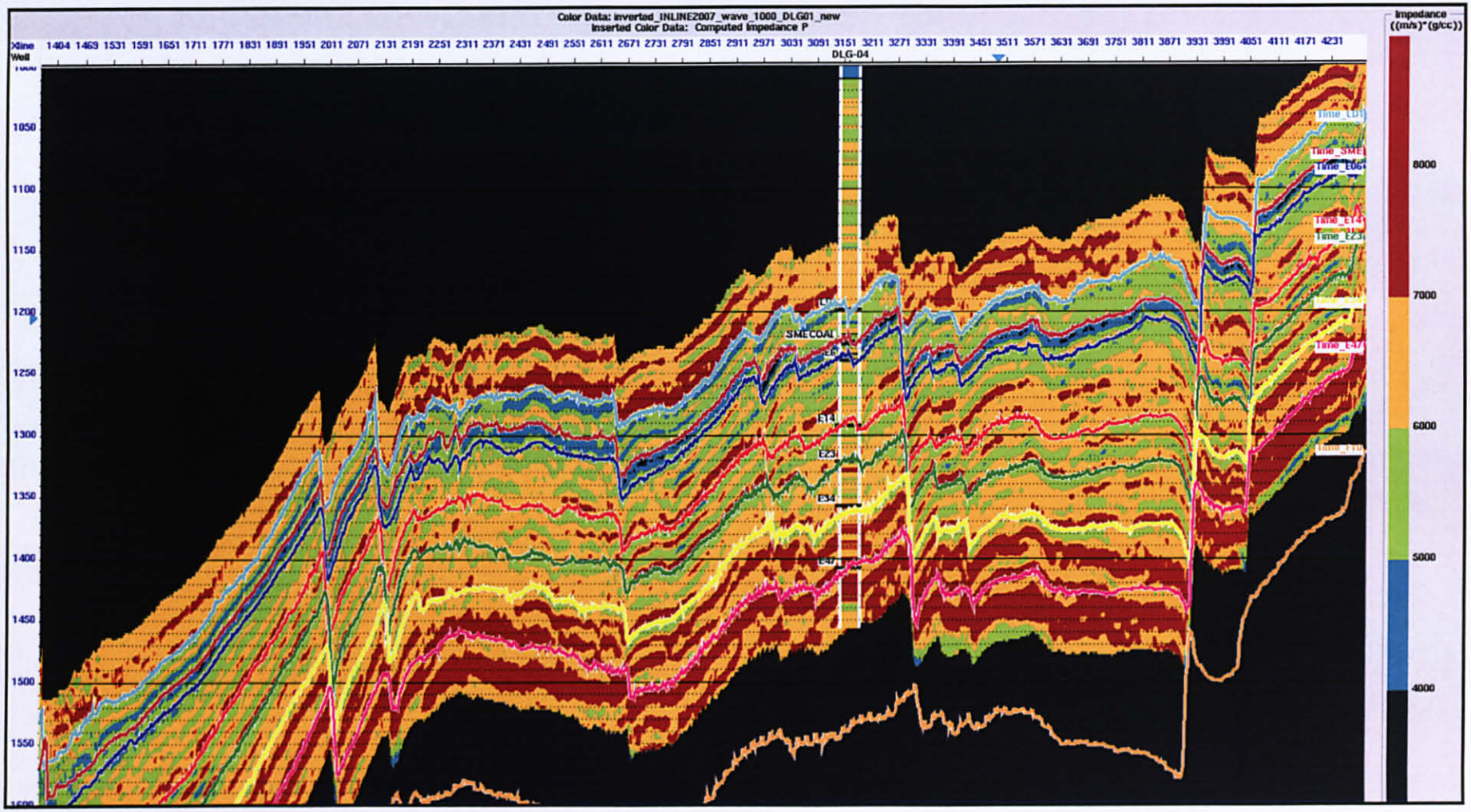

Figure 5.10: Inverted volume of P-impedance from the model-based inversion result through the impedance wells at DLG 04 using statistically estimated wavelet near the DLG 01 well.

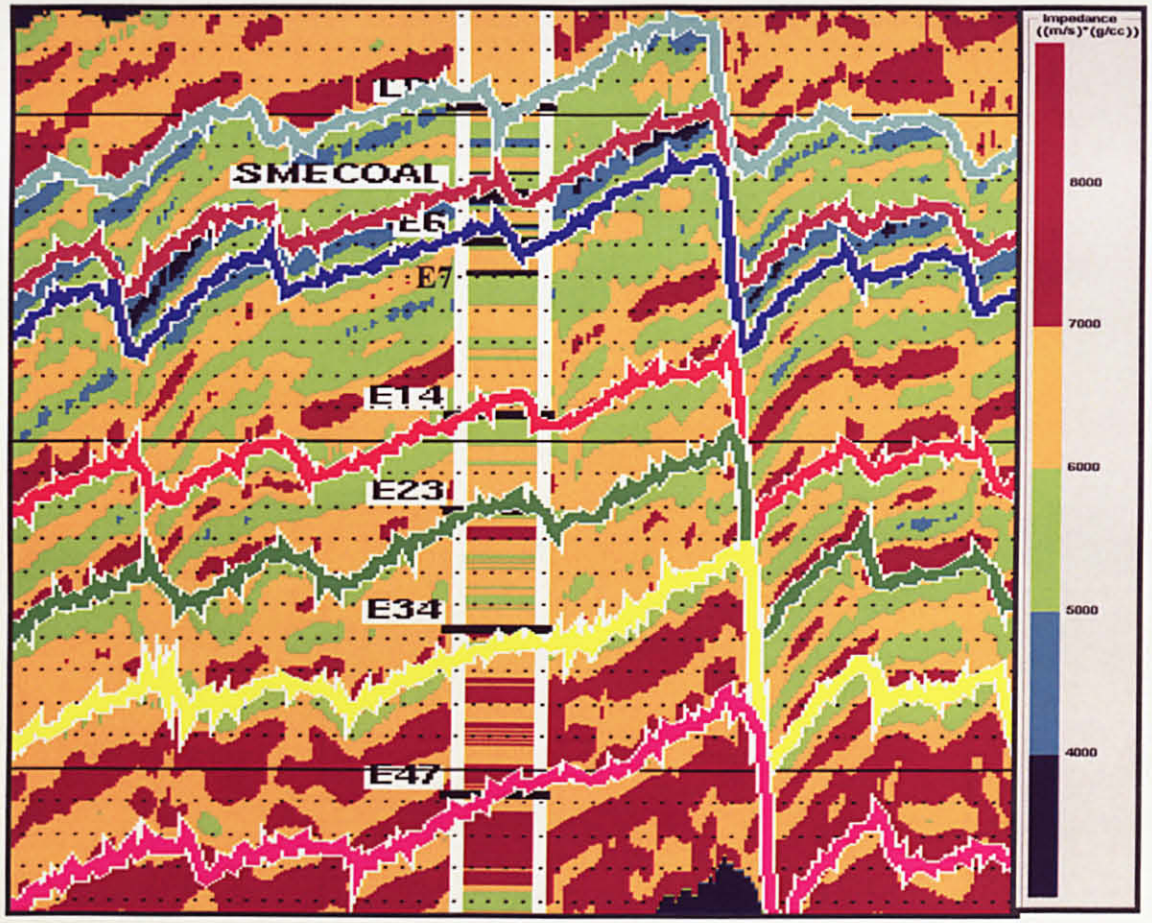

Depth (m)	Impedance ((m/s)*(g/cc)) at DLG04
1160	4700-5700 E7 – OIL SAND
1230	5300-6000 E14 – OIL SAND
1278	5100-6400 E23 – OIL SAND
1310	5900-6700 E34 – OIL SAND

Figure 5.11: Inversion result from Inline of 2007 (left) and the cross plot result (right) near DLG 04 well.

An inversion was performed through the arbitary line, which is consisting of DLG 01, DLG 02 and DLG 04 wells. It shown in Figure 5.12, it started from DLG 04 to DLG 02 and end at DLG 01 location. With this result, we can look at the extension of E-group sand reservoir through all the wells. First, we look at the SME Coal layer that is above E7 sand reservoir, which is having a continuous reflector through all the wells. The SME Coal layer can be detectable through all the wells and it is in low impedance but it falls under wrong color of impedance for the inversion. We will discuss after in the seismic resolution test.

Next, is E7 sand reservoir, which is in DLG 04 through DLG 02 and DLG 01 we can see the extension of that sand although there have an occurrence of fault at DLG 01. We also can see the extension of other E-sand that is E14, E23 and E34 through DLG 04, DLG 02 and DLG 01. Shale become as a permeability barrier between the sand packages. Unfortunately, gas sand cannot be separate between the oil sand because some of the gas sand has high impedance due to the impurities of shale and it will overlapping the impedance coming from oil sand. However, looking at Figure 5.12, generally we can look the extension of sand class in that reservoir.

After we get the inversion result, we need to look at the resolution. Figure 5.13 and 5.14, shows the test on the minimum thickness that can be detected or resolved from the seismic inversion results. By looking at the Figure 5.13, the thickness for the coal layer is 5meters and the seismic inversion result still can be mapped out the coal layer. We can see the coal impedance value is approximately 3000 ((m/s)*(g/cc)) shows as dark blue color in the well log (Acoustic Impedance). However, when we compare with the inversion result, the coal shows light blue color, that is higher than 4000 ((m/s)*(g/cc)). By looking at the inversion result, we can still separate with the other classes even though the value falls under the wrong impedance value. We may detect the coal layer with the right impedance that is approximately 3000, if we change the color scheme or number of samples of the impedance. However, this best impedance color bar is suitable for all classes. In Figure 5.14, which is the thickness for coal layer is 2meters; unfortunately, the inversion result could not map it.

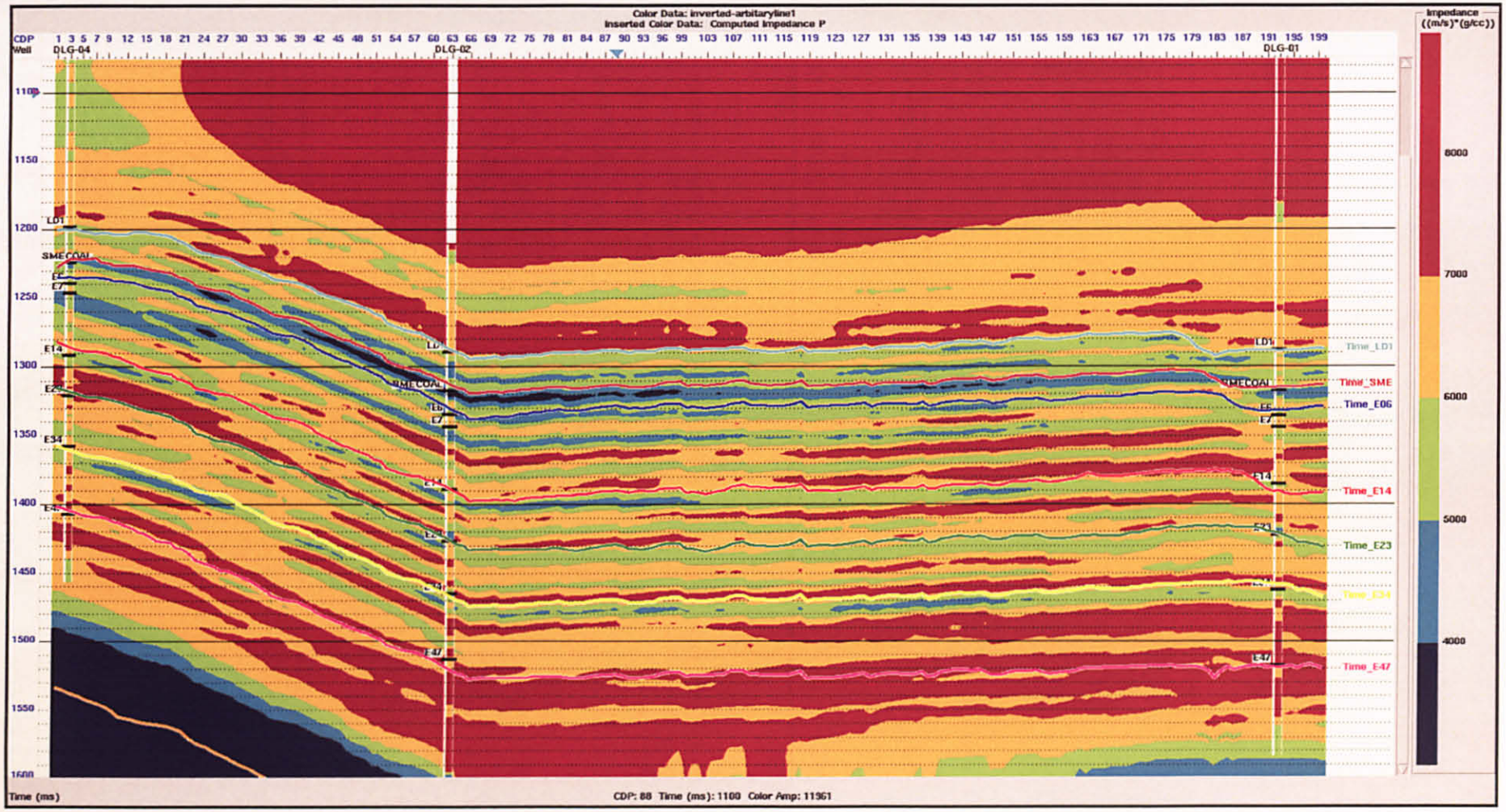

Figure 5.12: Inverted volume of P-impedance from the model-based inversion result through the impedance wells at DLG 01, DLG 02 and DLG 04 using statistically estimated wavelet near the DLG 01 well. This is taken from arbitary seismic line.

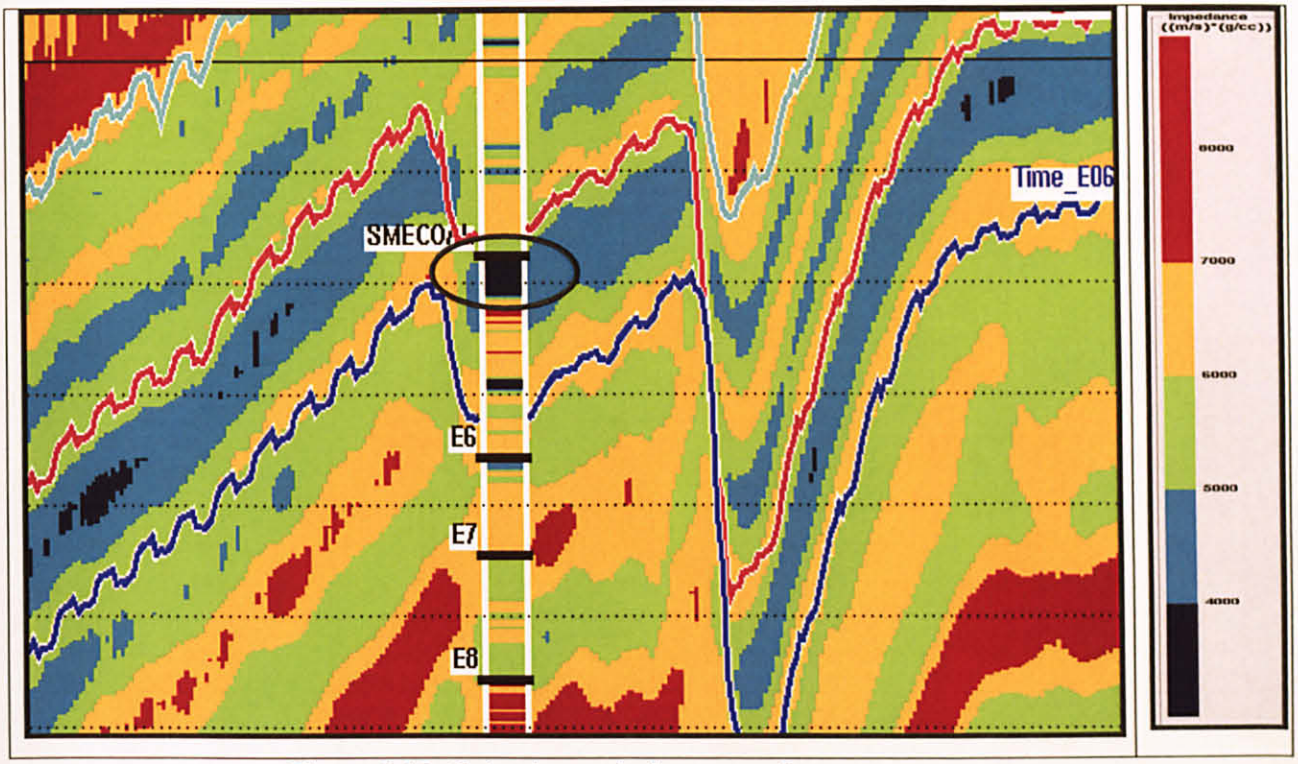

Figure 5.13: Seismic resolution test – 5meters

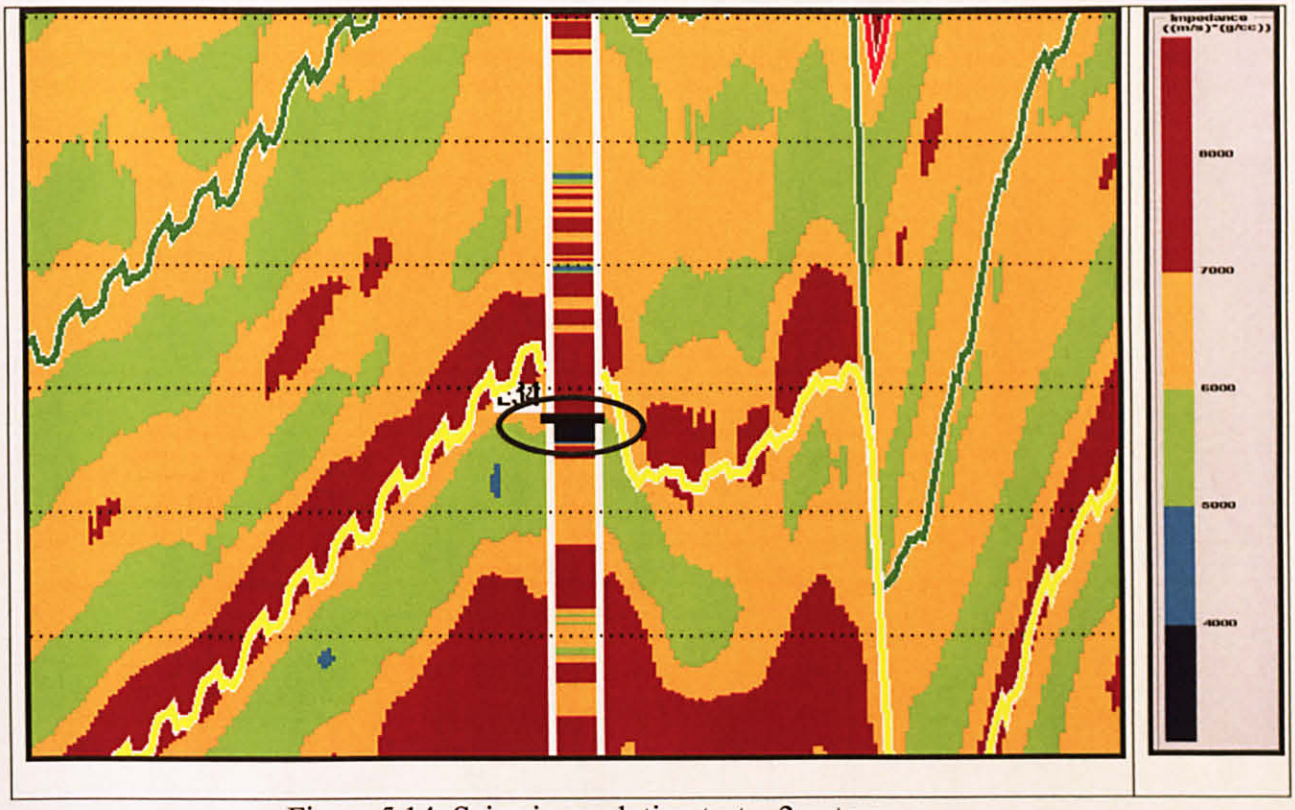

Figure 5.14: Seismic resolution test – 2meters

5.5 SUMMARY

The inverted impedance section through the impedance logs showed the continuity of E-sand reservoir in DLG 04 well to DLG 02 well and end at DLG 01 well which is in different block. The impedance log is in high-cut filtered (75-100Hz and it refer to the seismic data) to match the frequency of seismic data. The inverted impedance boundaries match with the filtered impedance logs boundaries and the inverted impedance values are close to the impedance logs. To get a better model we need to put in the correct parameter before the actual inversion is done such as number of iterations and scaler adjustment for the inverted logs to get a better match with the original log. In this study, number of iterations of 20 and scaler is at 1.00 (default) is being used to get the best inversion result. One more important thing is the color scheme for the impedance ((m/s)*(g/cc)) that is the third parameter is being used beside time (ms) in x-axis and cross line in y-axis. For the color scheme, We have classify into three that are light and dark blue is in low impedance, green and yellow is in middle impedance and it will represent sand. Finally yet importantly is the highest impedance that is shale is in red color.

CHAPTER 6
CONCLUSIONS

6.1 SUMMARY

- From the well data analysis and cross plotting technique, we observe that the P-impedance between coal, sand and shale are distinct from each other. The lithologies have distinct range of impedance for each class. Clean sand can be easily separated with shale but difficult if we have value of volume in clay more than 50%. This indicates the sand is a bad quality or dirty sand. For example, overlapping occurred between wet sand and shale class. Similarly, between gas sand and oil sand, the gas sand has higher impedance than oil sand due to the same problem of the volume of clay. Clean sand can be found mostly in DLG 04 as compared to DLG 01 and DLG 02. Possibly, due to the different fault block. This way indicate depositional environment where we can say that DLG 04 is in more a deltaic system as compared to DLG 01 and DLG 02 which are prone to marine influence.

- Wavelet extraction using statistical method was chosen for the well-to-seismic correlation and used in the inversion process. Besides statistical wavelet extraction, using well data was also tested. DLG 04 wavelet shows different result from DLG 01 and DLG 02 due to the different location or blocks since as we know that wavelet varies every trace to trace. Quality of logs is very important in the wavelet extraction, where editing need to be done due to invasion or mud cake in the original logs.

- One method used to invert seismic data is model-based inversion. Model-based inversion depends on the initial model generated using the impedance logs and geological model. Therefore, the log quality and well control is important to constrain the model. The model can be poorly defined laterally due to limited number of some log in this study area.

6.2 CONCLUSIONS

- Acoustic impedance inversion provides qualitative interpretation of the seismic data in the Dulang Unit area.

- We can also make a conclusion on the identification for coals. Impedance of coal is generally very low (below 3000 ((m/s)*(g/cc)), sand impedances range from 4000 to 6790 ((m/s)*(g/cc)), as found from E6, E14, E23 and E34 formations in all three wells. Shale impedances are the highest with values approximately 7000 to 8500((m/s)*(g/cc)).

- Impedance is the best way to separate sand from shale in this area. Gas sands can be identified from the impedance inversion results. However, some oil sands found in all the three wells could not be identified separately from the gas sand on impedance inversion results because of impurities of shales in the sand.

- Inversion provide additional information to evaluate prospect, however it does not provide exact answer but more of probabilities.

6.3 RECOMMENDATIONS

- Well log data

  The sparsity of well data may cause the initial model to be poorly defined because well data have been used to be as a control point in creating the model building. Beside that, the quality of the log data needs to be reviewed carefully and edited because it will make a wavelet difference. Further research need to be done at DLG 04 wavelet due to differences with other wells.

- Inversion methods

  Besides model-based inversion method, we need to use other inversion

methods such as colored inversion, band limited inversion, etc.

- Elastic Impedance

  We need to use shear wave (Vs) log to have better separation between sand and shale due to sand and shale class, which means same impedance. Therefore, we can use Vp and Vs logs to differentiate sand and shale.

REFERENCES

Alistair R. Brown, 1996, Seismic/Geology links critical: Geophysical Corner, AAPG Explorer.

Ashley M.Francis, Fakhar H. Syed, 2001, Application of Relative acoustic impedance inversion to constrain extent of E sand reservoir on Kadanwari field: SPE & PAPG Annual Technical Conference.

Brown, R.L., McElhattan, W., and Santiago, D., 1996, Wavelet estimation: An interpretive approach in Seismic signature estimation and measurement: Osman, O.M. and Robinson, E.A., eds., Society of Exploration Geophysics, 617-620.

Cooke,D., 1981, Generalized linear inversion of reflection seismic data: M.Sc. Thesis, Colorado School of Mines.

Cooke, D.A., and Schneider, W.A., 1983, Generalized linear inversion of reflection seismic data: Geophysics, 48, 665-676.

Francis, A., 1987, Acoustic impedance inversion pitfalls and some fuzzy analysis: The Leading Edge, 16, No. 3, 275-278.

G. Russell Young, 2006, Model-based inversion of multiple offset data for elastic parameter estimation: Exploration Geophysics Symposium.

Hampson, D. and Galbraith, M., 1981, Wavelet extraction by sonic log correlation: J. Can. Soc. Expl. Geophys., 17, no. 01, 24-42.

Hampson-Russell Ltd, 1999, The theory of strata program: Hampson-Russell Ltd.

Ida Herawati, 2002, The use of time lapse P-wave impedance inversion to monitor a CO_2 flood at Weyburn Field, Saskatchewan, Canada: M.Sc. Thesis, Colorado School of Mines.

Lancaster, P., Salkauskas, K., 1986, Curve and surface fitting –an introduction: Academic Press.

Nicolas W. Martin, 1995, Improving vertical resolution in the Penny field using 2D seismic inversion: CREWES Research Report – Volume 7, 17-1 – 17-15.

Oldenburg, D. W., Scheuer, T., and Levy, S., 1983, Recovery of the acoustic impedance from reflection seismograms: Geophysics, 48, 1318-1337.

Russell, B.H., Hampson, D., 2006, The old and the new seismic inversion, CSEG Recorder, 5-11.

Russell, B.H., 1988, Introduction to seismic inversion methods: SEG continuing education short course notes.

Sergio Sacani Sancevero, Armanda Zaupa Remacre and Rodrigo de Souza (2005). Comparing deterministic and stochastic seismic inversion for thin-bed reservoir characterization in a turbidite synthetic reference model of Campos Basin, Brazil. The Leading Edge, 1168-1172.

V.Dimri (1992), Deconvolution and Inverse Theory - Application to Gephysical Problems. Amsterdam: Elsevier Science Publisher B.V.

Yilmaz, O., 2001, Seismic data analysis: Vol I and II, Society of Exploration Geophysics.

Ziolkowski, A., Underhill, J.R., and Johnson, R. G. K., 1998, Wavelets, well ties, and the search for subtle stratigraphic traps: Geophysics, 63, 297-313.

Appendices

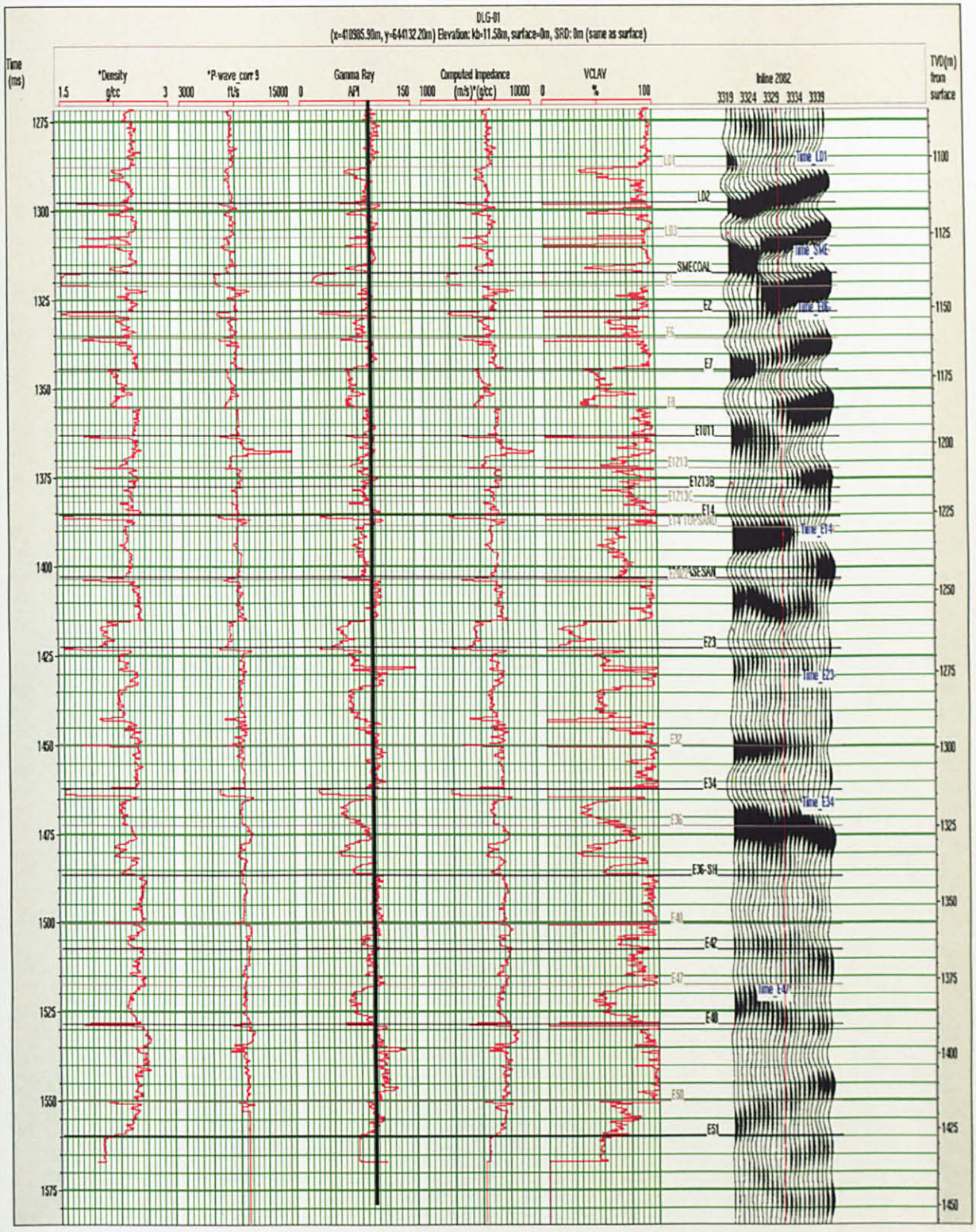

Appendix 1: The original logs from well DLG 01. Cut off of Gamma Ray is 75.00 API.

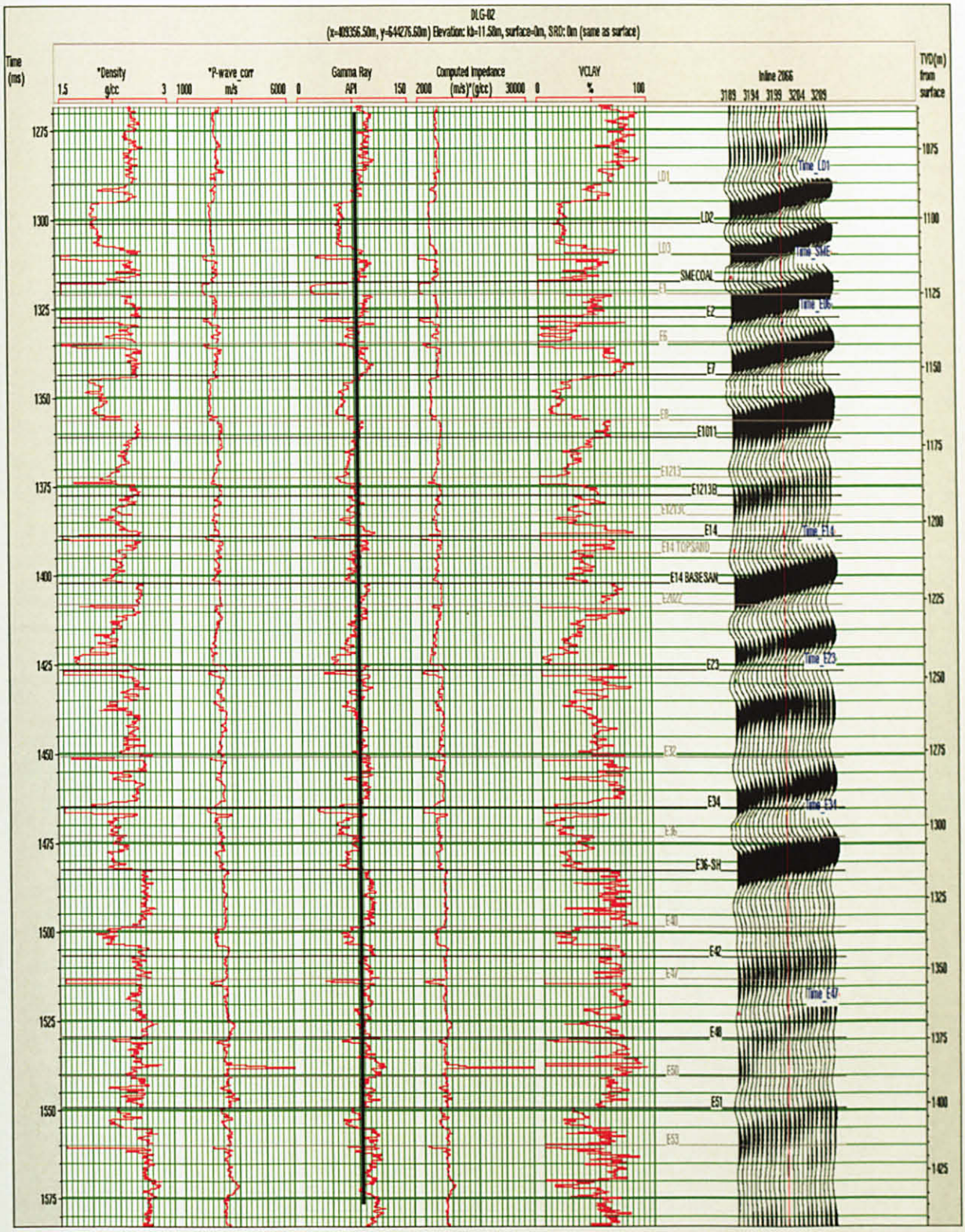

Appendix 2: The original logs from well DLG 02. Cut off of Gamma Ray is 75.00 API.

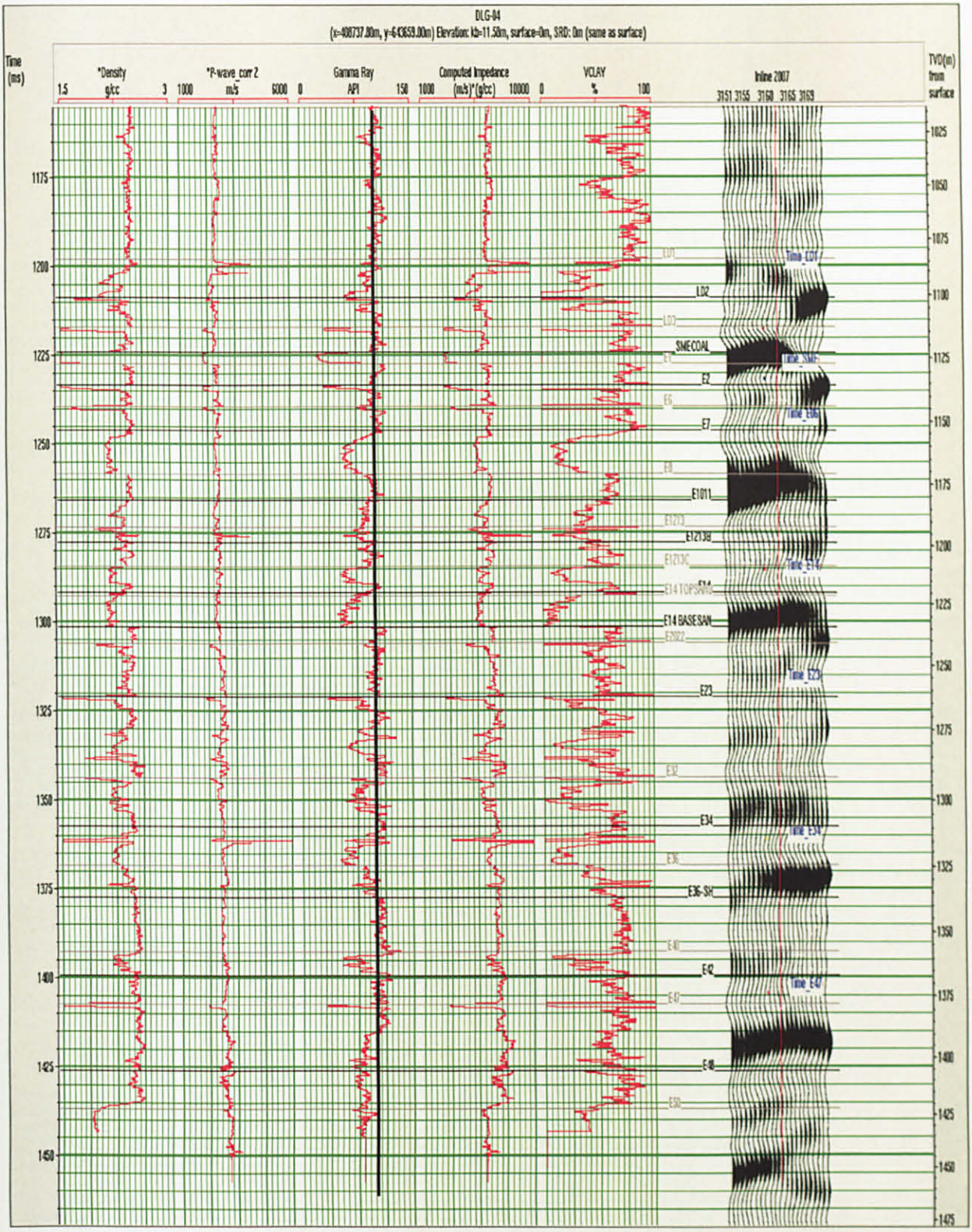

Appendix 3: The original logs from well DLG 04. Cut off of Gamma Ray is 90.00 API

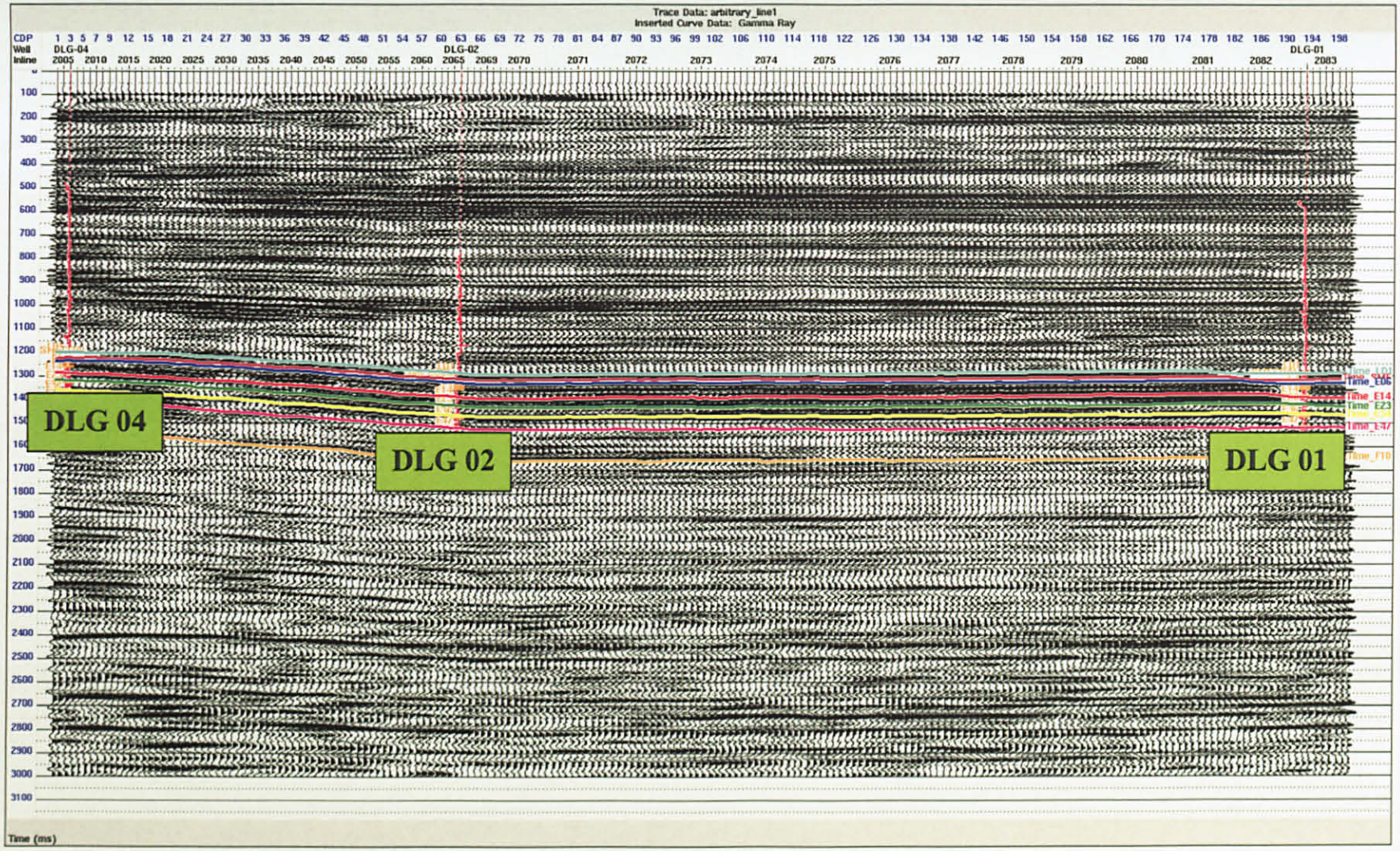

Appendix 4: Arbitary seismic line starting from DLG 04 to DLG 02 and end at DLG 01.

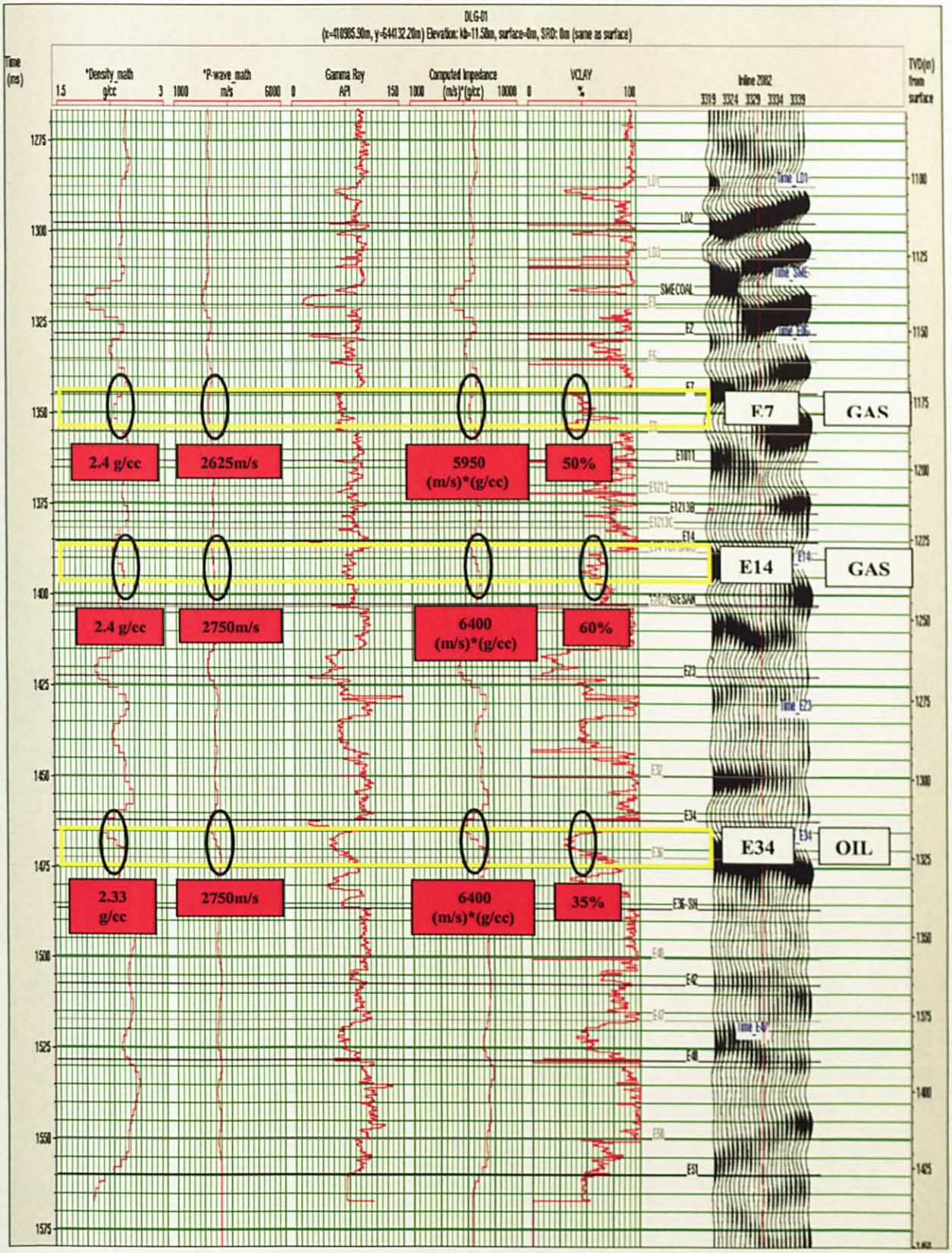

Appendix 5: Filtered logs from well DLG 01. All the value for Density, P-wave, Impedance and Volume of Clay are in average mode.